FUNCTIONAL HIPPOCAMPAL REDUNDANCY AS A MEASURE OF RESILIENCE TO PATHOLOGICAL AGING

Stephanie Langella

A dissertation submitted to the faculty at the University of North Carolina at Chapel Hill in partial fulfillment of the requirements for the degree of Doctor of Philosophy in the Department of Psychology and Neuroscience in the College of Arts and Sciences.

Chapel Hill
2021

Approved by:

Charlotte Boettiger

Eran Dayan

Jessica Cohen

Keely Muscatell

Kelly Giovanello

ABSTRACT

Stephanie Langella: Functional hippocampal redundancy as a measure of resilience to pathological aging
(Under the direction of Kelly Giovanello and Eran Dayan)

Aging is accompanied by declines in episodic memory and altered hippocampal function, each of which are exacerbated in response to the development of Alzheimer's disease. Therefore, it is critical to identify factors which support resilience to such pathological aging. One proposed factor is redundancy, the existence of duplicate elements within a system that offers protection against failure. Redundancy is hypothesized to operate within the brain as a neuroprotective mechanism, though this hypothesis has not been tested in the context of neurodegenerative diseases. This dissertation presents initial evidence that hippocampal redundancy, quantified from resting-state functional brain networks, operates as a neuroprotective mechanism in aging.

The role of hippocampal functional redundancy is examined in the context of clinical, cognitive, pathological, and experiential factors across three studies. The first study demonstrates that posterior hippocampal redundancy is lower in mild cognitive impairment, a precursor stage to Alzheimer's disease, than in healthy aging, though redundancy does not differ between early and late stages of mild cognitive impairment. Further, posterior hippocampal redundancy is related to better memory performance. The second study expands upon these results, relating hippocampal redundancy to pathological markers of Alzheimer's disease, showing that hippocampal redundancy mediates the relationship between hippocampal volume and memory performance. Additionally, the combination of low hippocampal redundancy, volume, and memory is associated with subsequent dementia conversion. The final study reveals that the

positive mnemonic benefit of redundancy weakens throughout healthy older adulthood and is specific to posterior rather than anterior hippocampus. However, this study finds no evidence that redundancy is influenced by either education or physical activity, two prominent protective factors for healthy aging.

Across these three studies, hippocampal redundancy, particularly in posterior regions, is shown to be associated with better clinical and cognitive outcomes. Future studies will benefit from longitudinal analysis of redundancy in relation to clinical progression and long-term measures of physical activity. Together, the results presented in this dissertation provide the initial evidence that hippocampal redundancy supports resilience to pathological aging.

ACKNOWLEDGEMENTS

Thank you to the Cognitive Neuroscience of Memory Lab, the Dayan Lab for Neuroinformatics, Dr. Peter Mucha, and the Cognitive area graduate students for the assistance and support to complete this project. Research reported in this publication was supported by the National Institute On Aging of the National Institutes of Health under Award Number R01AG062590. The content is solely the responsibility of the author and does not necessarily represent the official views of the National Institutes of Health.

Data used in preparation of this article, in part, were obtained from the Alzheimer's Disease Neuroimaging Initiative (ADNI) database (adni.loni.usc.edu). As such, the investigators within the ADNI contributed to the design and implementation of ADNI and/or provided data but did not participate in analysis or writing of this report. A complete listing of ADNI investigators can be found at: http://adni.loni.usc.edu/wp-content/uploads/how_to_apply/ADNI_Acknowledgement_List.pdf. Data collection and sharing for this project was in part funded by the Alzheimer's Disease Neuroimaging Initiative (ADNI) (National Institutes of Health Grant U01 AG024904) and DOD ADNI (Department of Defense award number W81XWH-12-2-0012). ADNI is funded by the National Institute on Aging, the National Institute of Biomedical Imaging and Bioengineering, and through generous contributions from the following: AbbVie, Alzheimer's Association; Alzheimer's Drug Discovery Foundation; Araclon Biotech; BioClinica, Inc.; Biogen; Bristol-Myers Squibb Company; CereSpir, Inc.; Cogstate; Eisai Inc.; Elan Pharmaceuticals, Inc.; Eli Lilly and Company; EuroImmun; F. Hoffmann-La Roche Ltd and its affiliated company Genentech, Inc.;

Fujirebio; GE Healthcare; IXICO Ltd.; Janssen Alzheimer Immunotherapy Research & Development, LLC.; Johnson & Johnson Pharmaceutical Research & Development LLC.; Lumosity; Lundbeck; Merck & Co., Inc.; Meso Scale Diagnostics, LLC.; NeuroRx Research; Neurotrack Technologies; Novartis Pharmaceuticals Corporation; Pfizer Inc.; Piramal Imaging; Servier; Takeda Pharmaceutical Company; and Transition Therapeutics. The Canadian Institutes of Health Research is providing funds to support ADNI clinical sites in Canada. Private sector contributions are facilitated by the Foundation for the National Institutes of Health (www.fnih.org). The grantee organization is the Northern California Institute for Research and Education, and the study is coordinated by the Alzheimer's Therapeutic Research Institute at the University of Southern California. ADNI data are disseminated by the Laboratory for Neuro Imaging at the University of Southern California.

Data were provided in part by the Human Connectome Project, WU-Minn Consortium (Principal Investigators: David Van Essen and Kamil Ugurbil; 1U54MH091657) funded by the 16 NIH Institutes and Centers that support the NIH Blueprint for Neuroscience Research; and by the McDonnell Center for Systems Neuroscience at Washington University.

TABLE OF CONTENTS

LIST OF TABLES

LIST OF FIGURES

LIST OF ABBREVIATIONS

Aß	Beta-amyloid
AD	Alzheimer's disease
CN	Cognitively normal
fMRI	Functional magnetic resonance imaging
MCI	Mild cognitive impairment
ROI	Region of interest

CHAPTER 1: INTEGRATIVE INTRODUCTION

Alzheimer's disease (AD), the sixth leading cause of death in the United States, is a neurodegenerative disease with a rapidly increasing prevalence ("2020 Alzheimer's disease facts and figures," 2020). AD is characterized by two hallmark pathologies: beta-amyloid (Aß) plaques and neurofibrillary tau tangles. The aggregation of AD neuropathology precedes the onset of clinical symptoms, beginning during healthy aging and continuing to aggregate throughout disease progression, affecting both brain structure and function (Jack et al., 2013; Nelson et al., 2012). AD progression can be roughly categorized into three phases: preclinical AD, mild cognitive impairment (MCI), and clinical dementia. Daily function is preserved in both preclinical and MCI stages despite an increasing neuropathological burden, but MCI, often regarded as a precursor stage to AD, is additionally characterized by cognitive impairment ("2020 Alzheimer's disease facts and figures," 2020; Jack et al., 2013; Jack Jr et al., 2018).

One of the earliest sites affected by AD pathology is the hippocampal formation of the medial temporal lobe (Braak & Braak, 1991; Harris et al., 2010; Jack et al., 2013; Schönheit, Zarski, & Ohm, 2004; Yankner, Lu, & Loerch, 2008). The hippocampus is the primary structure supporting episodic memory, the memory for distinct events defined by a specific context and time of occurrence (Eichenbaum, 2017), which is, in turn, the initial and primary cognitive deficit observed in MCI and early AD (Gallagher & Koh, 2011). In additional to pathological burden, the hippocampus experiences atrophy in both normal (or preclinical) and pathological aging, though higher rates are observed in MCI and AD (Apostolova et al., 2012; Barnes et al., 2009) and in individuals who show clinical progression rather than stability (Frankó & Joly,

2013; Jack et al., 2000). Such atrophy is related to deficits in episodic memory performance (Grundman et al., 2002; O'Shea, Cohen, Porges, Nissim, & Woods, 2016). As with structure, hippocampal function undergoes changes in normal aging, related to declines in episodic memory ability (Leal & Yassa, 2015; Yankner et al., 2008), though is further impaired in MCI and AD. As compared to healthy aging, there is hippocampal hyperactivity in MCI, followed by hypoactivity in AD (Dickerson et al., 2005), and this MCI-based hyperactivity predicts future cognitive decline (Miller et al., 2008). Further, individuals with some level of cognitive impairment show decreased hippocampal activity overtime (O'Brien et al., 2010).

Studies of pathology, structure, and function have long demonstrated that the hippocampus is a critically affected region across clinical AD stages. However, a high proportion of cognitively healthy individuals harbor AD pathology without ever displaying clinical symptoms (Bennett et al., 2006; Katzman et al., 1988; Price et al., 2009; Price & Morris, 1999). Mechanisms which support continued hippocampal function across preclinical and MCI stages are critical to research to further understand why some individuals can harbor AD pathology without displaying clinical impairment. In other words, certain functional properties of the hippocampus may be neuroprotective against AD pathology.

The notion of reserve developed from these findings of discrepant pathological and clinical status (Katzman et al., 1988; Stern, 2006). Reserve refers to the difference between the extent of brain damage and its outward clinical or cognitive presentation, such that individuals with more reserve exhibit resilience to physical brain damage (Cabeza et al., 2018; Montine et al., 2019; Stern, Barnes, Grady, Jones, & Raz, 2019). Functional connectivity has been posited as a reserve mechanism and has garnered extensive support in the cognitive aging community in recent years. Functional connectivity describes how brain regions interact across time. In the

context of cognitive aging, functional connectivity is typically derived from functional magnetic resonance imaging (fMRI), which estimates the blood-oxygen-level-dependent (BOLD) signal as a proxy of brain activity. Functional connectivity derived from fMRI, then, represents the correlated time series of the BOLD response between two regions. Resting-state functional connectivity is calculated during a session in which the participant remains awake in the scanner but does not complete any task, representing an intrinsic state of functional networks. Resting-state scans are more commonly used in patient populations than are task-based designs, due to the relative ease of acquisition and ability to compare results widely across research groups. As such, resting-state functional connectivity has been examined extensively in MCI populations.

As is observed in activation studies, hippocampal functional connectivity patterns are impaired in MCI and AD as compared to healthy aging (Binnewijzend et al., 2012; Sohn, Yoo, Na, & Jeong, 2014; Z. Wang et al., 2011). Despite hippocampal functional impairments between healthy and pathological aging, greater hippocampal resting-state functional connectivity within individuals with MCI is related to better memory performance. Mnemonic benefits of hippocampal connectivity have been found broadly, including via connections to the default mode network and associated regions (Dunn et al., 2014; Su et al., 2017; Y. Wang et al., 2013; Yan, Zhang, Chen, Wang, & Liu, 2013), to the cerebellum (Delli Pizzi, Punzi, & Sensi, 2019), and to the brain globally (i.e., hippocampal whole-brain connectivity) (Sheng et al., 2017). These results indicate that higher connectivity (i.e., stronger correlations) between the hippocampus and other brain regions are supportive of memory function.

However, what remains unclear are the mechanisms through which certain individuals exhibit a resilience to AD pathology and demonstrate preserved clinical and cognitive functioning. In addition to characterizing the strength of correlations between timeseries',

functional connectivity between brain regions can further be characterized as a network, in which the correlation between the timeseries' of two brain regions are represented as edges in a matrix representing all pairs of brain regions (Rubinov & Sporns, 2010). Properties derived from such graph-based networks may provide additional insight as to how hippocampal connectivity is beneficial in preclinical aging and MCI. Despite a relative emphasis on properties defined by shortest or direct paths within a network, longer-range connections are likely to exist in complex brain networks and contribute to resilience (Avena-Koenigsberger, Misic, & Sporns, 2018). One such property is redundancy, conceptually referring to the existence of duplicate elements within a system that, in case of failure of a specific element, provide alternate means of functionality (Tononi, Sporns, & Edelman, 1999). Redundancy, a prominent principle in engineering fields (Billinton & Allan, 1992), exists in a variety of biological systems, offering preserved functionality, for example, in the event of gene deletions (Navlakha, He, Faloutsos, & Bar-Joseph, 2014) or organ failure (Glassman, 1987), and contributes to robustness of neural networks (Pitkow & Angelaki, 2017).

As a graph measure specifically, redundancy is quantified as the sum of direct and indirect paths between two nodes. In this sense, redundancy was introduced using resting-state electroencephalogram (EEG) timeseries' in healthy young adults, providing evidence that redundancy exists in brain network organization (De Vico Fallani et al., 2012). These results were supported when redundancy was applied to magnetoencephalography (MEG) data, again showing evidence of redundancy in brain networks, and further showing a difference between redundancy and other common graph properties, namely shortest path (a direct contrast to redundancy's emphasis on longer paths), and communicability (a walk-based metric that incorporates indirect paths) (Di Lanzo, Marzetti, Zappasodi, De Vico Fallani, & Pizzella, 2012).

In an extension to psychiatric group comparisons, individuals with depression were shown to have lessened modulation of EEG-based functional redundancy during painful stimulation (Leistritz et al., 2013). However, despite prior hypotheses that redundancy is neuroprotective in neurodegenerative diseases (Arkadir, Bergman, & Fahn, 2014; Creasey & Rapoport, 1985; Glassman, 1987), it has not been applied to healthy and pathological aging populations.

This dissertation examines the potentially protective role of functional hippocampal redundancy derived from resting-state fMRI networks in healthy and early pathological aging, with an emphasis on its relation to cognitive and biological markers of AD. As the hippocampus is affected in early disease stages, redundancy of the hippocampus in particular is a probable mechanism for resilience to AD pathology. In healthy brains, communication should be similar between low and high redundancy networks. However, upon neurodegeneration, networks with low redundancy may lose critical connections between brain regions. Conversely, networks with high redundancy have alternative channels for communication, thereby supporting connections that may be lost in a low redundancy network. To that end, high hippocampal redundancy may support clinical and cognitive function in aging. Therefore, Study 1 characterizes hippocampal functional redundancy across various stages of healthy and pathological aging, along with its associations with cognitive performance. This study is the first to examine redundancy as a graph property in the context of neurodegenerative disease, providing a basis with which to further study its involvement in resilience.

Expanding upon the clinically-defined group approach in Study 1, Study 2 incorporates known biological markers of AD. A recently introduced biologically-oriented research framework, ATN (amyloid, tau, neurodegeneration), advocates the use of biomarkers that reflect the buildup of AD pathologies to stage AD progression (Jack Jr et al., 2018). Indeed,

hippocampal neurodegeneration is related to clinical progression (Apostolova et al., 2012; Barnes et al., 2009; Frankó & Joly, 2013; Jack et al., 2000) and poor memory performance (Golomb et al., 1993; Huang et al., 2019; Nathan et al., 2017; O'Shea et al., 2016; Peng et al., 2015). Therefore, it is imperative to understand the relationships between hippocampal redundancy and AD biomarkers. Study 2 examines how hippocampal redundancy relates to two such markers: hippocampal atrophy and cortical Aß. Specifically, hippocampal redundancy was examined as a potential underlying mechanism through which hippocampal atrophy relates to memory impairment, a relationship which may be moderated by Aß burden. This study puts functional redundancy in the context of known pathological markers and suggests a mechanistic role in cognitive aging.

Findings from initial investigations of functional redundancy in aging suggest that changes in redundancy likely occur before the onset of MCI. Specifically, upon diagnosis of MCI, hippocampal redundancy has already declined substantially compared to healthy aging (Langella, Sadiq, Mucha, Giovanello, & Dayan, 2021; Study 1), hippocampal atrophy is accompanied by low hippocampal redundancy (Study 2), and whole-brain redundancy declines during healthy aging (Sadiq, Langella, Giovanello, Mucha, & Dayan, 2021). Healthy older adults, however, are not a homogenous group. Despite a general tendency for clinically healthy older adults to experience brain changes and episodic memory decline, some older adults are able to better retain memory function due to various factors, including high reserve (Stern, 2006; Stern et al., 2019). Two prominent protective factors are education and physical activity, each related to better clinical outcomes in aging (Meng & D'Arcy, 2012; Norton, Matthews, Barnes, Yaffe, & Brayne, 2014; Rashid, Zahid, Zain, Kabir, & Hassan, 2020). However, further research is needed on the functional mechanisms which may support preserved memory ability in older

adulthood. Therefore, Study 3 examines hippocampal redundancy across healthy older adulthood, characterizing the contributions of hippocampal redundancy to preserved cognition in healthy aging. Hippocampal redundancy is treated as a mechanism through which education and physical activity may relate to cognition. In contrast to Studies 1 and 2, Study 3 examines hippocampal redundancy as a neuroprotective mechanism in healthy rather than impaired populations, particularly in the context of factors that influence reserve.

Together, this research aims to present hippocampal redundancy as a neuroprotective mechanism through which certain individuals exhibit resilience to AD-related clinical and cognitive decline. Resting-state fMRI, widely collected in healthy and patient populations, provides insights into intrinsic brain organization. Current knowledge from resting-state fMRI data have illuminated many functional changes associated with aging and AD; however, functional redundancy as a graph measure has not been widely adopted despite strong theoretical support for its beneficial role. These studies leverage existing knowledge of the course of AD, focusing analyses on the hippocampus and known biomarkers, while introducing a novel measure to understand resilience in aging.

CHAPTER 2: LOWER FUNCTIONAL HIPPOCAMPAL REDUNDANCY IN MILD COGNITIVE IMPAIRMENT[1]

Alzheimer's disease (AD) is a neurodegenerative disease that poses a significant public health concern, with dementia constituting the fifth leading cause of death worldwide (Nichols et al., 2019). AD is characterized by the accumulation of amyloid beta plaques and neurofibrillary tau tangles, which disrupt neural communication and contribute to functional and structural changes across the brain (Nelson et al., 2012). These pathologies aggregate during healthy aging and continue into mild cognitive impairment (MCI), regarded as a precursor stage to AD (Aisen et al., 2010). Although individuals diagnosed with MCI are more likely to later progress to AD, there is considerable variability in individual trajectories, with conversion estimates ranging from 8% to 25% (Petersen et al., 2018). In addition, the prevalence of biologically-defined AD (diagnosed post-mortem) is up to three times higher than clinically-defined AD, illustrating that a high proportion of older adults are presenting normal cognitive function despite extensive neural pathology (Jack et al., 2013). This suggests that in certain individuals, neuroprotective mechanisms allow the brain to cope with early neurodegeneration and retain normal cognitive function. With an increasing aging population, it is critical to identify the mechanisms that mitigate cognitive decline, yet these mechanisms are currently not well understood.

The general notion of reserve has been introduced to refer to the difference between the extent of brain damage and its outward presentation (clinically or cognitively) (Cabeza et al.,

[1]This chapter previously appeared as an article in Translational Psychiatry. The original citation is as follows: Langella, S., Sadiq, M. U., Mucha, P. J., Giovanello, K. S., & Dayan, E. (2021). Lower functional hippocampal redundancy in mild cognitive impairment. *Translational Psychiatry, 11*(61). https://doi.org/10.1038/s41398-020-01166-w

2018; Montine et al., 2019; Stern et al., 2019).Thus, individuals with more reserve exhibit a resilience to or temperance of physical brain damage (Cabeza et al., 2018; Montine et al., 2019; Stern et al., 2019). Reserve mechanisms in the brain are difficult to quantify. One potential quantifiable reserve mechanism is redundancy: the existence of duplicate elements within a system that provide alternative functionality in case of failure (Navlakha et al., 2014; Tononi et al., 1999). This design principle is abundant in engineering fields, where redundant elements protect a design from total failure in the event of malfunction of a specific element (Billinton & Allan, 1992). Redundancy exists in biological systems as well, with examples in genetic structures and cells, up to the level of whole organs (Glassman, 1987; Navlakha et al., 2014; Pitkow & Angelaki, 2017). For example, recent work has demonstrated that redundant elements are effective at preserving functioning in the event of gene deletions (Navlakha et al., 2014) and providing robustness in neural networks (Pitkow & Angelaki, 2017). Since physical redundancy is not a requirement to support informational or functional redundancy (Nguyen, Xu, Luu, Zhao, & Yang, 2019), functional redundancy can be calculated from a graph-based representation of functional brain networks (Di Lanzo et al., 2012; Leistritz et al., 2013). Numerous studies have derived graph-based measures and topological properties from resting-state functional magnetic resonance imaging (rs-fMRI) data, in which systems are represented as a collection of nodes (brain regions) and edges (correlated timeseries data) (Bassett & Sporns, 2017; Bullmore & Sporns, 2009; Rubinov & Sporns, 2010). This approach has recently been employed to analyze functional redundancy in young adults, quantified as the sum of direct and indirect paths between any pair of nodes (Di Lanzo et al., 2012; Leistritz et al., 2013). Similar approaches have been used to quantify redundancy in other biological networks, leading to the consideration that path redundancy (the presence of multiple paths between a pair of nodes) is an important contributor

to robustness of cellular networks (Aittokallio & Schwikowski, 2006). However, while the role of redundancy in neuroprotection has been postulated before (Arkadir et al., 2014; Glassman, 1987), it has not yet been formally quantified to date for studying neuroprotection in neurodegenerative diseases.

It remains unknown, therefore, if redundancy is neuroprotective against age-related cognitive decline. A plausible site where neuroprotective functional redundancy may be detected is the hippocampus. This medial temporal lobe structure, critical for memory processes, is among the earliest sites affected by AD pathology (Harris et al., 2010). Functional and structural alterations in the hippocampus are early and precede the onset of AD (Jack et al., 2013), and MCI is characterized by declines in memory and hippocampal functioning (Gallagher & Koh, 2011). We thus reasoned that hippocampal functional redundancy may serve as a neuroprotective mechanism to outward clinical presentation of MCI, such that in a redundant network, communication could continue even in the presence of neurodegeneration of a node (e.g., hippocampus) (Fig. 2.1A). Conversely, communication within a less redundant network should be severely disrupted in the presence of neurodegeneration (Navlakha et al., 2014) (Fig. 2.1A).

The current study investigates functional redundancy in 130 cognitively normal (CN), early MCI (eMCI), and late MCI (lMCI) older adults (Fig. 2.1B) across four anterior and posterior hippocampal nodes (Fig. 2.1C) to elucidate how functional redundancy is associated with healthy (or asymptomatic) and pathological aging. Three potential relationships between redundancy and cognitive status were considered: (a) no relationship between redundancy and cognitive status (i.e., redundancy is not a neuroprotective mechanism), (b) redundancy declines linearly with cognitive status (i.e., redundancy is protective in both healthy and pathological aging), or (c) redundancy declines from healthy to pathological aging, but plateaus upon

reaching MCI (i.e., redundancy is neuroprotective in healthy or asymptomatic aging, but ceases to offer functional benefits upon appearance of neurodegeneration) (Fig. 2.1D). We hypothesize that functional redundancy will be related to diagnosis, such that CN individuals will have greater redundancy than those with MCI. Further, if redundancy acts as a neuroprotective mechanism, then we hypothesize that higher redundancy will be related to better cognitive performance.

Figure 2.1 | Study design and hypotheses

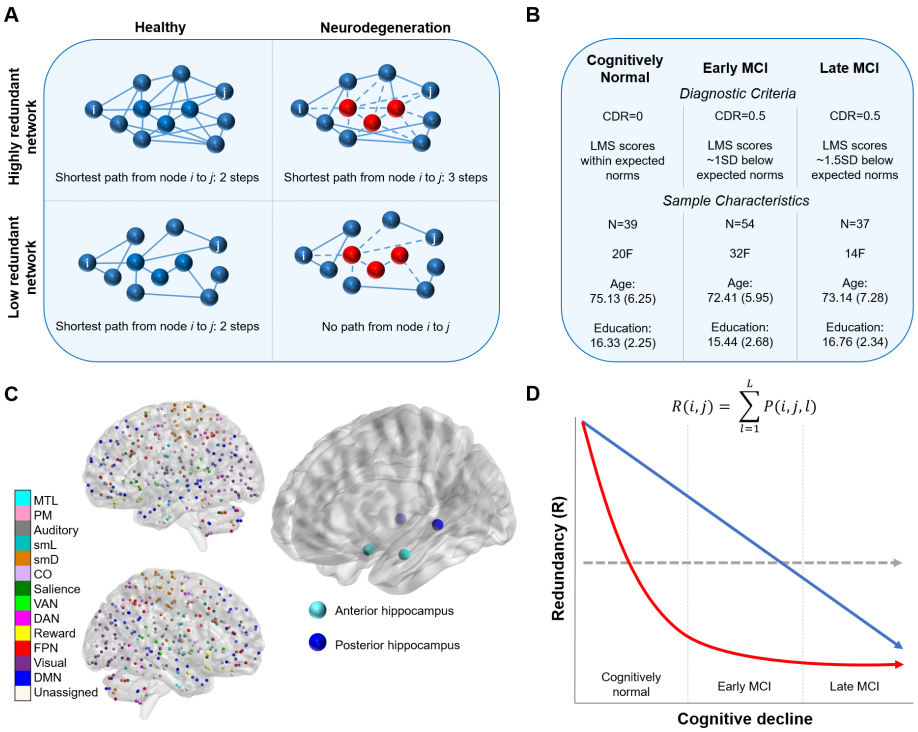

A. Examples of networks with high and low redundancy. The shortest path between nodes *i, j* do not differ between high and low redundancy in a healthy state. In the case of neurodegeneration (red nodes), a highly redundant network retains a path between nodes *i, j*, whereas there are no paths between nodes *i, j* in a low redundancy network. **B.** Sample characteristics of the included subjects. **C.** Representation of the functional parcellation used in the current study made up of 300 nodes representing cortical, subcortical, and cerebellar regions (Seitzman et al., 2020). The four hippocampal nodes are shown next to the full atlas parcellation, representing anterior (cyan) and posterior (blue) hippocampus. **D.** Three hypothesized relationships between redundancy and cognitive decline. There could be no relationship between redundancy and cognitive decline (gray line), a linear relationship such that redundancy declines linearly across healthy aging, early MCI, and late MCI states (blue line), or a nonlinear relationship, such that redundancy declines between healthy aging and MCI, but plateaus in MCI (red line). Redundancy equation presented above hypothesized relationships, in which redundancy, *R*, of node pair *i,j* is represented by the sum of all paths between *i,j* at length *l*, up to a maximum path length, *L*.

Materials and Methods

Dataset

Data were obtained from the Alzheimer's Disease Neuroimaging Initiative (ADNI) database (adni.loni.usc.edu), a longitudinal multi-site study launched in 2003 and led by Principal Investigator Michael W. Weiner, MD. For up to date information, see www.adni-info.org. Subjects were participants of the ADNIGO/2 protocol, which distinguishes between a diagnosis of early and late MCI and includes rs-fMRI data. Study visits were approved by each site's local IRB. All participants provided informed consent. The following inclusion criteria were established by ADNI:

MCI subjects: subjective memory concern, clinical dementia rating (CDR) of 0.5, Mini-Mental State Exam (MMSE) score between 24 and 30, an abnormally low score on the Wechsler Memory Logical Memory II subscale (LM-II), no significant levels of impairment in other cognitive domains, preserved activities of daily living, non-demented.

Early MCI (eMCI): LM-II score between 9-11 for ≥ 16 years of education, 5-9 for 8-15 years of education, 3-6 for 0-7 years of education

Late MCI (lMCI): LM-II score ≤ 8 for ≥ 16 years of education, ≤ 4 for 8-15 years of education, ≤ 2 for 0-7 years of education

Cognitive normal (CN) subjects: no subjective memory concern, CDR of 0, MMSE scores between 24 and 30, scores on LM-II within the expected range (≥ 9 for 16 or more years of education, ≥ 5 for 8-15 years of education, ≥ 3 for 0-7 years of education), no reported memory complaints, non-depressed, non-MCI, non-demented.

The distinction between early and late MCI was determined by ADNI via the extent of low performance on the LM-II subscale, such that an eMCI diagnosis was made for scores about

1 SD below the education adjusted norm, and a lMCI diagnosis for scores about 1.5 SD below the education adjusted norm, in addition to meeting the above MCI criteria (Aisen, Petersen, Donohue, & Weiner, 2015). In an independent sample, participants classified as eMCI displayed less severe cognitive impairment and a slower rate of progression than those classified as lMCI (Aisen et al., 2010). Participants were included in the current study if (1) they had a diagnosis of either CN, eMCI, or lMCI, (2) they were between 60 and 90 years old, (3) they had rs-fMRI and anatomical MRI collected on the same day, and (4) the images were collected using a 3 Tesla scanner. The first available scan that met these criteria was used for each subject. All participants that met these criteria were included in the study (n = 143).

Image acquisition and preprocessing

Structural magnetization-prepared rapid gradient echo and rs-fMRI images were collected on a Philips Intera 3 Tesla scanner. Functional images were collected using a GR pulse sequence (flip angle = 80 degrees, slice thickness = 3.31mm, TE = 30ms, TR = 3000ms). Participants were instructed to keep their eyes open during resting-state scans.

Preprocessing steps were implemented in the MATLAB (R2017b) Conn toolbox (conn18b) (Whitfield-Gabrieli & Nieto-Castanon, 2012). Structural images underwent segmentation of gray matter, white matter, and cerebrospinal fluid. Functional images were preprocessed by realignment and unwarping, slice-timing correction, co-registration to structural images, spatial normalization, and motion outlier identification. White matter, cerebrospinal fluid, and 12 subject-motion parameters were included as nuisance regressors. Temporal band-pass filtering was employed to remove BOLD signal frequencies below 0.008 Hz or above 0.09 Hz. Outlier volumes were defined as having greater movement than 1.5mm or a Z threshold of 7.

Subjects with greater than 50% of volumes removed were excluded from subsequent analyses (n = 13), resulting in a final sample of 130 subjects.

Matrix construction and calculations of network measures

Functional timeseries were obtained using a functionally defined parcellation of 300 non-overlapping spherical regions of interest (ROIs) (Seitzman et al., 2020), including substantial cortical, subcortical, and cerebellar coverage (Fig. 2.1C; coordinates available at https://wustl.app.box.com/s/twpyb1pflj6vrlxgh3rohyqanxbdpelw). Unweighted functional connectivity matrices were constructed for each subject with edges representing correlations between each ROI, by Fisher Z transformation and binarizing at thresholds selected for densities ranging from the top 2.5% to 25% of edges retained in each individual network.

Redundancy. A redundancy matrix (R) was calculated for each node pair from each subject's connectivity matrix, defined as the sum of the direct and indirect edges between any two nodes (i, j), where l represents the total allowed path length and L represents the maximum path length (set to 4, in line with previous work and computational demands):

$$R(i,j) = \sum_{l=1}^{L} P(i,j,l)$$

The four hippocampal nodes of the parcellation were *a priori* defined as the main ROIs in this study: left and right anterior, along with left and right posterior hippocampus. Redundancy was calculated between each hippocampal ROI and all other nodes (i.e., the average R value for the 299 ROI-node pairs). Five additional regions were identified for secondary analysis, focused on nodes within two functional networks affected in early AD: the default mode and frontoparietal networks (Badhwar et al., 2017) (see Appendix A, Supplementary Methods).

Degree. Unweighted degree was calculated for each hippocampal ROI, *i*, defined as the sum of all its binarized edges, where $d_{i,j}$ represents the edge between nodes *i* and *j*.

$$k_i = \sum_{j=1}^{n} d_{i,j}$$

Global efficiency. Global efficiency, E_{global}, was calculated from each subject's binarized connectivity matrix, defined as the inverse of the shortest path length between two nodes (*i, j*), where *n* is the total number of nodes in the graph, and $L_{i,j}$ is the length of the shortest path between *i* and *j*:

$$E_{global} = \frac{1}{n(n-1)} \sum_{i,j,j \neq i} \frac{1}{L_{i,j}}$$

Cognition

We selected two cognitive domains that vary in the strength of their association with pathological aging: memory, the earliest reported cognitive deficit in MCI, and executive function, in which deficits are observed in later disease stages (Arnaiz & Almkvist, 2003). These were represented by composite measures MEM and EF respectively (Crane et al., 2012; Gibbons et al., 2012) (see Appendix A, Supplementary Methods).

Participant characteristics

The final sample included 130 subjects in rs-fMRI analyses (39 CN, 54 eMCI, 37 lMCI; Fig. 2.1B). The groups did not differ in age, $F(2,127) = 2.07$, $p = .130$, or sex, $X^2(2) = 4.04$, $p = .133$. The groups differed in education, $F(2,127) = 3.41$, $p = .036$, such that the lMCI group had more years of education than the eMCI group, $p = .036$ (CN-eMCI $p = .202$, CN-lMCI: $p = .734$). Of this sample, 118 (37 CN, 50 eMCI, 31 lMCI) had cognitive data within three months of their scan date and were included in the cognition analyses. Within this subset, the groups did not differ in age, $F(2,115) = 2.66$, $p = .074$, education, $F(2, 115) = 2.47$, $p = .089$, or sex, $X^2(2) =$

1.52, p = .468. The early and late MCI groups did not differ in percentage of amyloid-positive subjects, $X^2(1) = 0.16$, p = .686, 95% CI [-0.17, 0.31] (see Appendix A, Supplementary Methods).

Statistical analysis

Analyses were performed at all matrix densities (2.5% to 25%) and on the values averaged across densities. For brevity, results are reported in-text and in figures using the average across densities; results for each individual density are reported in the Supplementary Materials in Appendix A. Statistical analyses were run using R and MATLAB using raw data. Data were normalized for visualization.

Group comparisons. Permutation tests were used for group comparisons of graph measures as they do not make assumptions about the distribution of the data and are more robust to non-normality than are parametric tests. Group comparisons were tested using the aovperm function from the permuco R package, which conducts analysis of covariance (ANCOVA) using permutation testing (Frossard & Renaud, 2019). Three-group omnibus tests were first computed using redundancy or degree as the dependent variable, group as the independent variable, and education as a covariate. Each test was run using 10,000 permutations and a significance level of $p < .05$. Significant tests were followed by post hoc tests using the permutation ANOVA for each pairwise group comparison with 10,000 permutations. Education was only included as covariate in eMCI-lMCI comparisons, as the other groups did not differ in years of education. Multiple comparisons in post hoc testing were corrected for using the Benjamini & Hochberg procedure to reduce false discovery rate (FDR) using the p.adjust R function. Cohen's d and 95% confidence intervals (CI) were calculated using the effsize R function for pairwise comparisons (Torchiano, 2020).

Group differences in overall functional connectivity, white matter hyperintensities, and cognition were analyzed separately using a one-way ANOVA implemented with the aov R function, with a significance level of $p < .05$. Significant omnibus tests were probed using Tukey's post-hoc Honest Significant Difference test using the TukeyHSD R function, which adjusts the *p*-values for multiple comparison testing at a significance level of $p < .05$. Education was included as a covariate in overall functional connectivity analyses, and age and education were included as covariates in white matter hyperintensity analyses, due to group demographic differences in the respective samples.

Nodal ratios. To quantify the magnitude of differences in redundancy between each group, pairwise nodal ratios were computed by dividing the average redundancy, *R*, of node *i* in one group by the average *R* of *i* in a second group. Redundancy of node *i* is the sum of its row in the redundancy matrix. This value was averaged to create a group-mean nodal redundancy value for each of the groups, which was then used to compute the ratio. This was done for all 300 nodes for each pairwise group comparison. For example, the average redundancy of each node for the CN subjects was divided by the redundancy of each node for the eMCI subjects, resulting in a CN:eMCI ratio for each of the 300 atlas nodes, such that a ratio of 1 indicates equivalent redundancies and a ratio greater than 1 indicates higher redundancy in CN than in eMCI. This process was repeated for CN:lMCI and eMCI:lMCI comparisons. To test the significance of the posterior hippocampal nodal ranks, left and right posterior hippocampal ratios were averaged to create one posterior hippocampal ratio for each group ratio set and compared to the average ratio of a null distribution of random node pairs in each set, excluding posterior hippocampus (total: 10,000 random node pairs).

Redundancy regressions. Linear regressions were implemented using the lm R function, with redundancy as the independent variable and either cognition or global efficiency as the dependent variable, first collapsing across group, followed by within-group regressions. MEM and EF were regressed separately on hippocampal redundancy. Global efficiency was regressed on hippocampal redundancy, with education included as a covariate in the full sample regression. Hippocampal redundancy was regressed on MMSE within the MCI subjects to provide an alternate measure of MCI progression. Standardized betas are reported for all regression output. Due to the non-normality of the redundancy data, analyses were repeated using robust regression using Huber weights with the rlm function from the MASS R package (Ripley, 2020), with a Wald test of significance using the f.robftest function from the sfsmisc R package (Maechler, 2020).

Data and code availability. Neuroimaging and cognitive data are available at http://adni.loni.usc.edu/. The processed datasets generated in the current study are available from the corresponding author upon reasonable request.

Results

Lower hippocampal redundancy in MCI

We first compared hippocampal redundancy across healthy and pathological aging using an omnibus ANCOVA permutation test (Fig. 2.2A; Fig. S2.1; Tables S2.1-2.3). Neither left nor right anterior hippocampal nodes significantly differed by group [left: $F(2,126) = 1.43$, $p = .250$; right: $F(2, 126) = 2.15$, $p = .125$]. Conversely, both posterior hippocampal nodes significantly differed by group [left: $F(2,126) = 4.84$, $p = .009$; right: $F(2, 126) = 5.22$, $p = .004$]. Post hoc tests revealed greater redundancy in the CN group as compared to either MCI group in both left [eMCI: $F(1,91) = 7.76$, $p = .014$, Cohen's $d = 0.59$, 95% CI(0.16, 1.01); lMCI: $F(1,74) = 4.67$, p

= .048, d = 0.50, 95% CI(0.03, 0.96)] and right [eMCI: $F(1,91) = 9.00$, p = .011, d = 0.63, 95% CI(0.20, 1.06); lMCI: $F(1,74) = 6.21$, p = .021, d = 0.57, 95% CI(0.11, 1.04)] posterior hippocampus. The MCI groups, on the other hand, did not differ in posterior hippocampal redundancy [left: $F(1,88) = 0.09$, p = .771, d = 0.05, 95% CI(-0.48, 0.37); right: $F(1,88) = 0.02$, p = .893, d = 0.03, 95% CI(-0.45, 0.39)].

To probe the relative importance of the observed group differences in hippocampal redundancy, we calculated between-group nodal redundancy ratio sets (CN:eMCI, CN:lMCI, eMCI:lMCI), thereby identifying the nodes with the greatest magnitude of group differences (top 20 presented in Fig. 2.2B). Posterior hippocampal nodes consistently appeared in the top 5% of nodes in the CN:eMCI and CN:lMCI sets across network densities (Figs. S2.2-2.4). Left posterior hippocampus had the second highest ratio in the CN:eMCI set and the sixth highest ratio in the CN:lMCI set, indicating that not only does posterior hippocampal redundancy significantly differ between CN and MCI groups, but that posterior hippocampus has some of the largest differences across all nodes between CN and MCI groups. Indeed, posterior hippocampal ratios were significantly higher than the random node ratios in both the CN:eMCI set ($M_{\text{posteriorHC}}$ = 1.76, M_{random} = 1.15, SE_{random} = 0.002, p = .001; Fig. 2.2C; Table S2.4) and the CN:lMCI set ($M_{\text{posteriorHC}}$ = 1.66, M_{random} = 1.20, SE_{random} = 0.002, p = .017). The posterior hippocampus ratio did not differ from the random nodes in the eMCI:lMCI set ($M_{\text{posteriorHC}}$ = 0.95, M_{random} = 1.06, SE_{random} = 0.001, p = .831), supporting the finding that posterior hippocampal redundancy was less central for comparisons across MCI stages.

Although our analysis divided MCI into two groups based on LM-II scores, other ways exist to formalize MCI progression. Therefore, we additionally assessed the association between hippocampal redundancy and MMSE scores within the MCI participants. MMSE was not related

to hippocampal redundancy in any of the four hippocampal nodes (lowest p = .204; Fig. S2.5; Tables S2.5-2.6), consistent with the absence of group differences between early and late MCI.

Figure 2.2 | Hippocampal whole-brain functional redundancy differs in CN and MCI groups

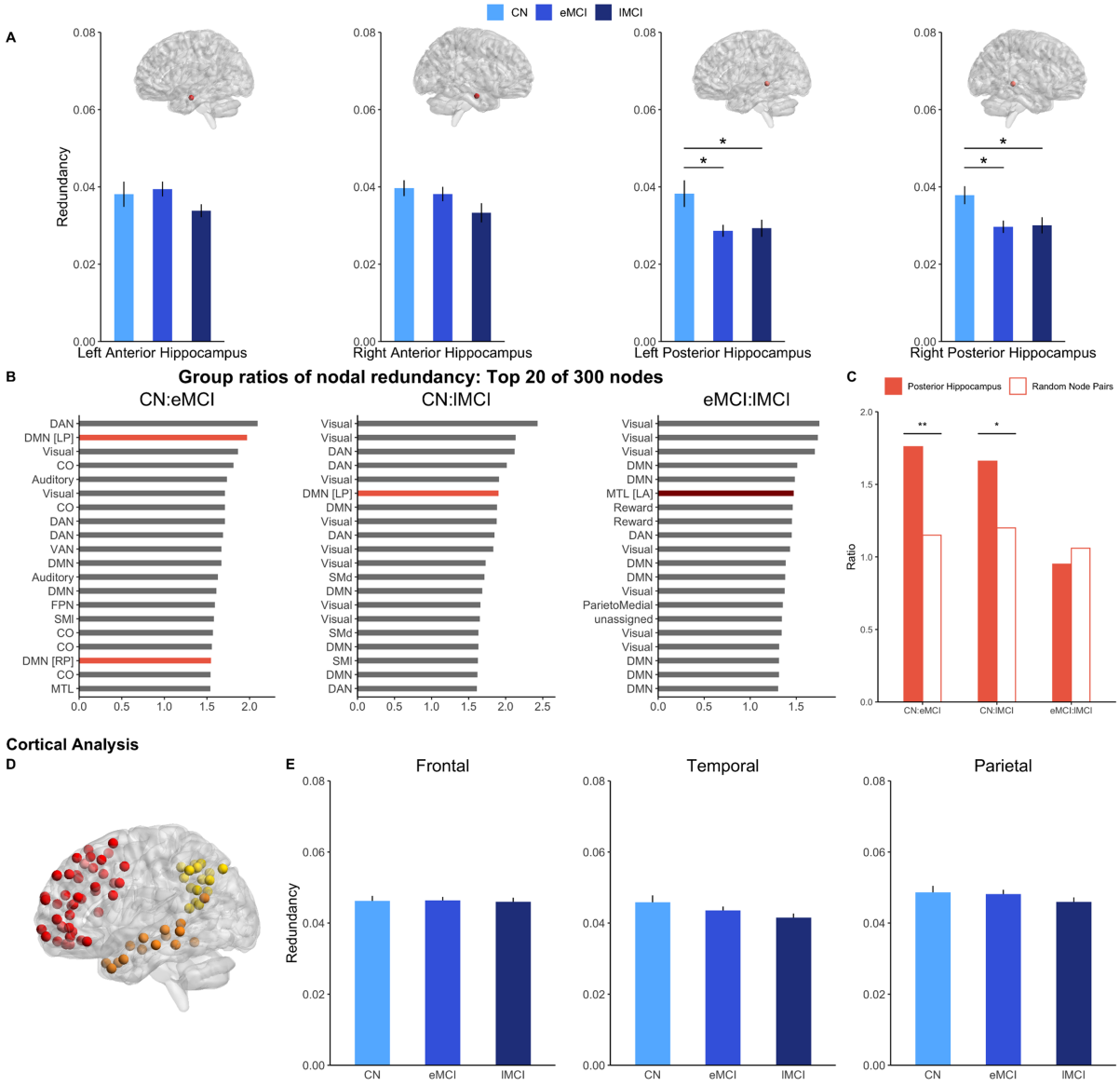

A. Group comparisons for the four hippocampal nodes. Error bars represent one standard error of the mean. **B.** The top 20 of 300 nodal ratios in each ratio set. Posterior hippocampal nodes (peach) and anterior hippocampal nodes (dark red) are highlighted. Bar labels denote the node's Seitzman et al. 2020 network affiliation. Hippocampal nodes are further labeled with "LP", "RP", "LA", or "RA" to represent left posterior, right posterior, left anterior, and right anterior respectively. **C.** Statistical comparison of the average posterior hippocampal ratio to random node pairs in each ratio set. **D.** Nodes included in the frontal (red), parietal (yellow), and temporal (orange) cortical analysis. **E.** Group comparisons for the cortical nodes. Error bars represent one standard error of the mean. *p < .05, **p < .01

To further validate the specific role of hippocampal redundancy in cognitive aging, we analyzed a set of frontal, temporal, and parietal nodes to determine whether the observed effects were widespread across cortical regions affected in early AD (Badhwar et al., 2017) (Fig. 2.2D). Redundancy did not differ by group in any of the selected regions (lowest $p = .097$), suggesting this effect was, for the most part, unique to the hippocampus (Figs. 2.2E, S2.6; Tables S2.7-2.8).

Hippocampal redundancy is related to memory but not executive function

We sought additional evidence of a protective role of redundancy in aging from the relationship between cognitive performance and redundancy, hypothesizing that functional redundancy would be associated with a cognitive benefit. The groups significantly differed in MEM scores [$F(2, 115) = 24.60$, $p < .001$, (Fig. 2.3A)], such that the CN group ($M = 1.01$, $SD = 0.55$) had higher scores than the eMCI group ($M = 0.47$, $SD = 0.58$, $p < .001$, 95% CI[-0.83, -0.25]) and the lMCI group ($M = 0.07$, $SD = 0.53$, $p < .001$, 95% CI[-1.26, -0.62]), and the eMCI group had higher scores than the lMCI group ($p = .006$, 95% CI[-0.70, -0.10]). We initially collapsed our sample into a single group to examine the overall relationship between cognition and redundancy, focusing on posterior hippocampal redundancy due to its consistency in group difference analyses and prominence in nodal rankings. Both left and right posterior hippocampal redundancy were related to higher MEM scores (Figs. 2.3B-C; Tables 2.1, S2.9-2.10). Although the results reveal an overall effect of higher redundancy relating to better memory performance, we performed separate regressions by group as this relationship could differ based on cognitive status. The positive relationship between MEM and left hippocampal redundancy was retained in the CN group but not in either MCI group (Figs. 2.3B-C insets, S2.7; Tables 2.1, S2.9). In right hippocampus, only the eMCI group showed a positive relationship, but significance was inconsistent across densities (Fig. S2.7; Tables 2.1, S2.10).

This analysis process was repeated for EF. The groups differed in EF scores [$F(2, 115) = 3.69$, $p = .028$, (Fig. 2.3D)], such that the CN group ($M = 0.78$, $SD = 0.77$) had higher scores than the lMCI group ($M = 0.22$, $SD = 0.97$, $p = .021$, 95% CI[-1.06, -0.07]), but did not differ from the eMCI group ($M = 0.49$, $SD = 0.84$, $p = .245$, 95% CI[-0.74, 0.14]). The two MCI groups did not differ from each other ($p = .370$, 95% CI[-0.73, 0.20]). Posterior hippocampal redundancy was not related to EF scores in our full sample, nor in any group (Figs. 2.2,2.3E-F, S2.7; Tables 2.1, S2.11-2.12). Results for both MEM and EF were consistent when using robust regression methods (Table S2.13), suggesting the results were not driven by outliers.

Table 2.1 | Posterior hippocampal redundancy-cognition regressions for averaged density

	Left posterior			Right Posterior		
	ß	***p*-value**	**Adjusted R^2**	**ß**	***p*-value**	**Adjusted R^2**
Memory						
Whole group	0.187	.001	0.076	0.135	.022	0.036
CN	0.206	.023	0.115	0.014	.877	0.028
eMCI	0.119	.152	0.022	0.186	.021	0.087
lMCI	-0.075	.427	0.012	-0.058	.530	0.020
Executive Function						
Whole group	0.067	.403	0.003	0.033	.680	0.007
CN	0.143	.274	0.007	0.073	.571	0.019
eMCI	0.077	.529	0.012	0.043	.718	0.018
lMCI	-0.280	.099	0.060	-0.198	.237	0.015

Figure 2.3 | Relationship between redundancy and cognitive performance

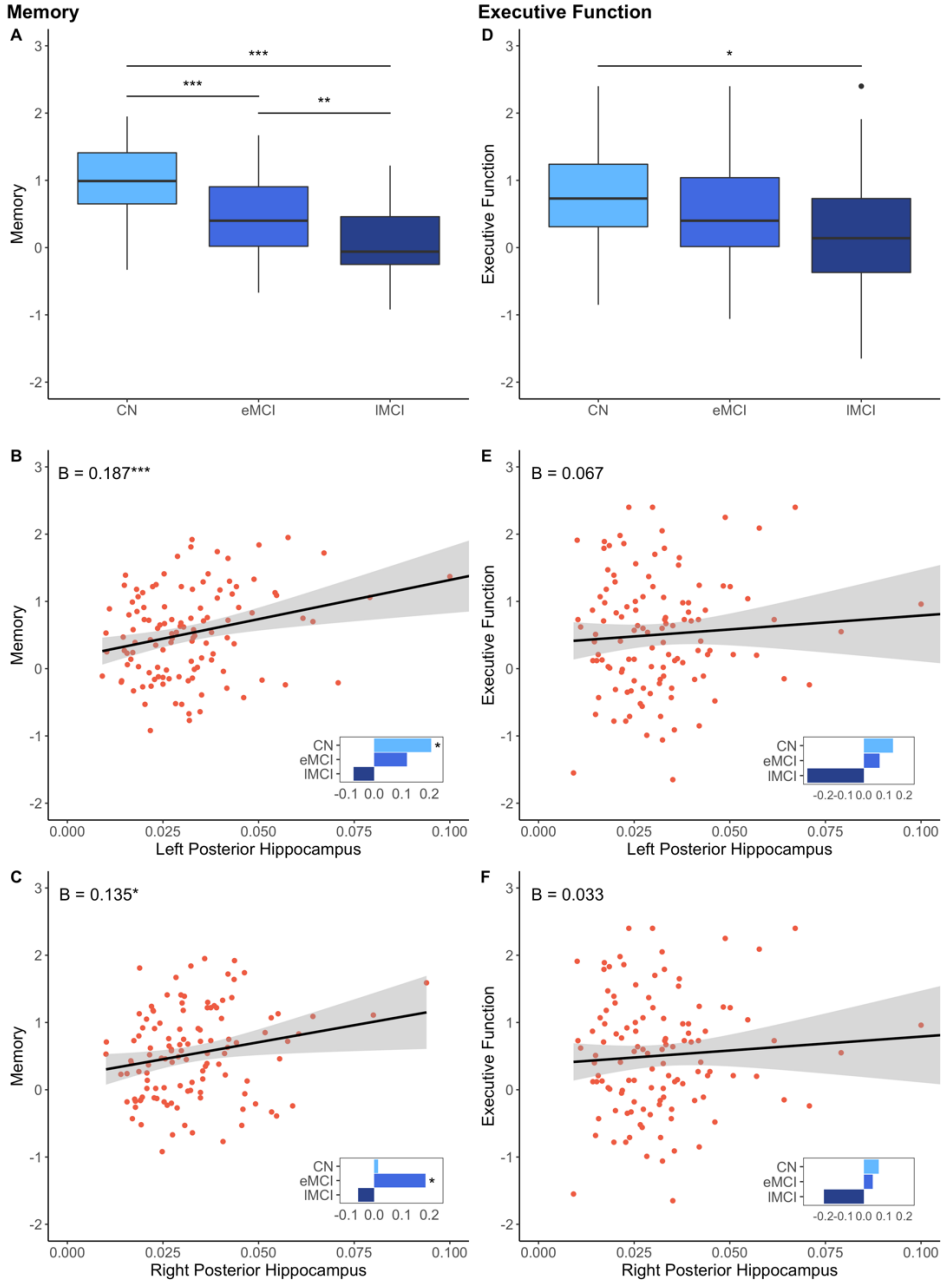

A. Memory composite scores across groups. Boxplot denotes the median (bold bar), first and third quartiles (box limits), and +/- 1.5 times the inter-quartile range (whiskers). **B.** Whole sample regression of left posterior hippocampal redundancy on memory composite score. Inset shows within-group regression beta-weights. **C.** Whole sample regression of right posterior hippocampal redundancy on memory composite score. Inset shows within-group regression beta-weights. **D.** Executive function composite scores across cognitive groups. Boxplot denotes the median (bold bar), first and third quartiles (box limits), and +/- 1.5 times the inter-quartile range (whiskers). **E.** Whole sample regression of left posterior hippocampal redundancy on executive function composite score. Inset shows within-group regression beta-weights. **F.** Whole sample regression of right posterior hippocampal redundancy on executive function composite score. Inset shows within-group regression beta-weights. *$p < .05$, **$p < .01$, ***$p < .001$

Specificity of redundancy as a topological property

Because the redundancy measure includes paths of length 1 (i.e., direct connections), we next examined whether similar group differences would be observed using only these length-1 paths by way of node degrees (e.g., whether the inclusion of indirect paths is informative). No significant group differences were observed for any of the hippocampal nodes [left anterior: $F(2, 126) = 0.94$, $p = .390$; right anterior: $F(2, 126) = 0.80$, $p = .455$; left posterior: $F(2, 126) = 2.74$, $p = .071$; right posterior: $F(2, 126) = 0.90$, $p = .413$; Fig. 2.4A; Table S2.14].

Groups were compared on overall functional connectivity for each of the hippocampal nodes to ensure graph measures were not biased due to underlying functional connectivity differences (van den Heuvel et al., 2017) (see Supplementary Methods in Appendix A). No group differences were found when retaining only positive correlations [left anterior: $F(2, 126) = 1.15$, $p = .319$; right anterior: $F(2, 126) = 1.68$, $p = .191$; left posterior: $F(2, 126) = 2.58$, $p = .080$; right posterior: $F(2, 126) = 1.31$, $p = .274$], or when taking the absolute value of all correlations, [left anterior: $F(2, 126) = 0.55$, $p = .580$; right anterior: $F(2, 126) = 0.72$, $p = .489$; left posterior: $F(2, 126) = 0.39$, $p = .679$; right posterior: $F(2, 126) = 0.05$, $p = .954$].

Additionally, there were no group differences in total volume of white matter hyperintensities, $F(2, 109) = 0.31$, $p = .737$, nor did volume of white matter hyperintensities relate to hippocampal redundancy in any of the four ROIs (Table S2.15). Together, these results suggest that the redundancy measure provides valuable and specific information differentiating CN and MCI individuals.

Redundancy does not come at the cost of efficiency

Our final analysis examined whether the existence of redundant edges in brain networks is associated with compromised communication efficiency within the network, measured by

global efficiency. There was no significant relationship between global efficiency and redundancy in any of the hippocampal nodes when collapsing across group [left anterior: β = -0.17, p = .061, adjusted R^2 = 0.02; right anterior: β = -0.03, p = .766, adjusted R^2 = 0.01; left posterior: β = 0.07, p = .411, adjusted R^2 = 0.003; right posterior: β = 0.05, p = .573, adjusted R^2 = 0.01] (Fig. 2.4B; Table S2.16), suggesting that efficient network communication is not compromised by having high functional redundancy. We further probed redundancy-efficiency relationships within each group, finding no significant relationships in either the CN or lMCI groups (Fig. 2.4B; Tables S2.17-S2.19). There was a positive relationship between global efficiency and left posterior hippocampal redundancy in the eMCI group, β = 0.32, p = .017, adjusted R^2 = 0.09. Results were consistent using robust regression methods (Table S2.20).

Figure 2.4 | Degree and global efficiency

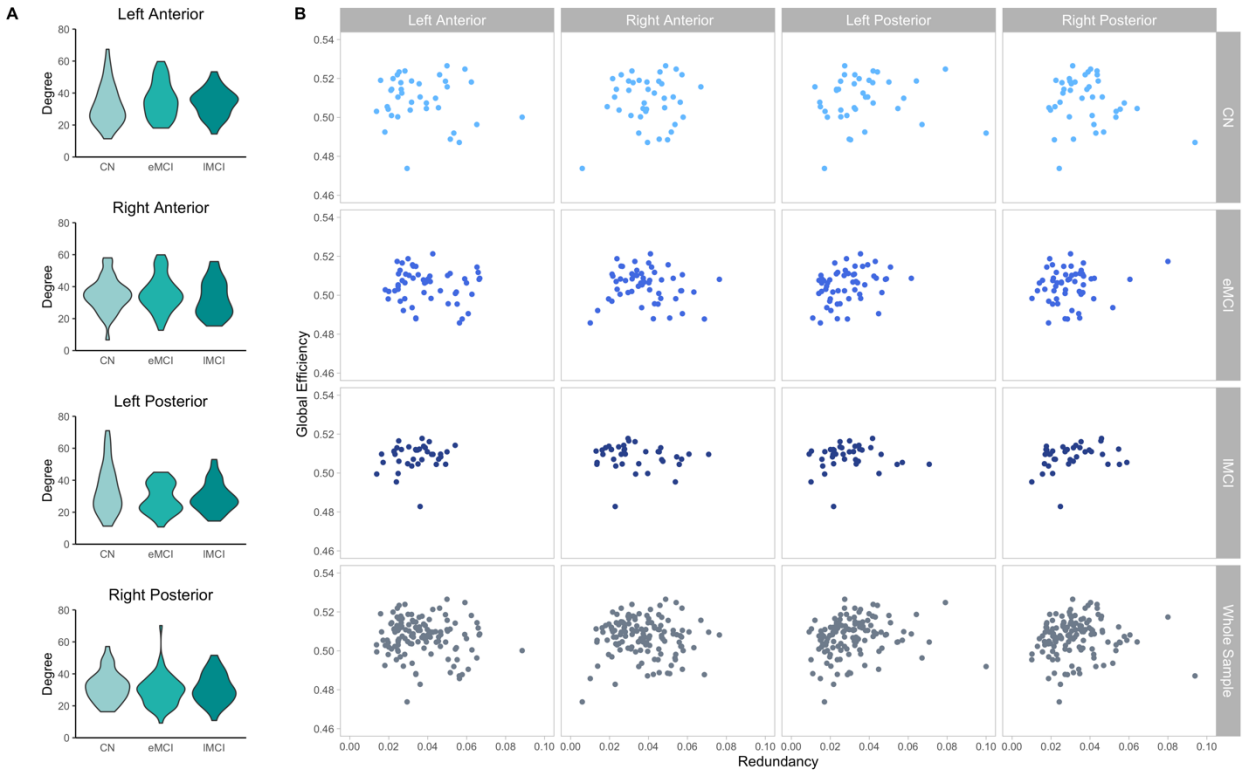

A. Group comparisons of degree in each hippocampal ROI. **B.** Global efficiency regressed on hippocampal redundancy in each ROI within each group and collapsing across groups.

Discussion

Certain individuals exhibit normal cognition despite harboring the characteristic pathology of AD and other dementias (Driscoll et al., 2006; Driscoll & Troncoso, 2011; Jack et al., 2013), yet mechanisms of neuroprotection in the human brain remain elusive and difficult to quantify. Early work postulated that redundancy may exist in the brain, but it could not be quantified with the contemporary methods (Glassman, 1987). In the current study we quantified functional redundancy in healthy older adults and those with either early or late stage MCI to test whether redundancy acts as a neuroprotective mechanism against pathological aging. Consistent with previous reports of beneficial redundancy in biological systems (Nguyen et al., 2019; Pitkow & Angelaki, 2017), we found evidence that redundancy serves a neuroprotective role in cognitive aging. Specifically, healthy older adults showed higher posterior hippocampal redundancy than individuals with MCI, and posterior hippocampal redundancy was positively related to memory performance, with this association primarily driven by the cognitively intact group. The MCI groups did not differ in levels of hippocampal redundancy nor did they exhibit relationships between redundancy and cognition, thereby supporting the conclusion that redundancy incurs a neuroprotective benefit in healthy (and possibly asymptomatic) aging, which plateaus in symptomatic pathological aging (Fig. 2.1D, red line). Further, we found no group differences in temporal, parietal or frontal cortical nodes, suggesting these results are mostly specific to the hippocampus.

We found a clear distinction between anterior and posterior hippocampus, such that only posterior hippocampus consistently differentiated healthy aging from MCI. This distinction may be explained by the functional specialization along the long-axis of the hippocampus. As established in the rodent literature, dorsal (posterior in primates) hippocampus underlies memory

processes, and ventral (anterior in primates) hippocampus is involved in emotional processing. The anatomical connectivity of these regions supports this functional segregation, with ventral hippocampus connecting to the amygdala and dorsal hippocampus connecting to retrosplenial and anterior cingulate cortices (Fanselow & Dong, 2010). This distinction is further supported by a prominent memory theory (Ranganath & Ritchey, 2012), differentiating between a posterior medial and an anterior temporal functional network in humans, which largely overlap with the previously described structural connections (Fanselow & Dong, 2010). Relatedly, posterior, but not anterior, hippocampal nodes clustered with the default mode network (DMN) in the parcellation employed in the current study (Seitzman et al., 2020). The DMN has considerable overlap with the proposed posterior medial network (Ranganath & Ritchey, 2012), and exhibits functional deficits in the context of aging and AD (Buckner, Andrews-Hanna, & Schacter, 2008; Koch et al., 2012; Mohan et al., 2016), thereby supporting our primary findings in posterior rather than anterior hippocampus.

In addition to group differences in redundancy, we found that posterior hippocampal redundancy is related to memory performance. This relationship held in both our full sample and in healthy older adults but not in either MCI group. It is possible that the MCI groups, since they on average have lower redundancy than the CN group, may not exhibit enough hippocampal redundancy to benefit performance. Another interpretation is that the relationship between redundancy and cognition differs across groups. Though neither reached significance, the eMCI group had a positive memory-redundancy relationship, unlike the lMCI group which exhibited a negative relationship. Future work should probe whether there is an amount of redundancy that is necessary to benefit cognition, or if redundancy rather becomes a hindrance in later disease stages. We did not find any relationship between hippocampal redundancy and executive

function. Although hippocampal function has been associated with a range of cognitive processes (Shohamy & Turk-Browne, 2013), its role is particularly critical to mnemonic processes (R. E. Clark & Squire, 2013; Eichenbaum, 2017). This dissociation, then, indicates a selective cognitive benefit of nodal functional redundancy which can be further explored in other brain regions (e.g., prefrontal cortex and executive function).

Taken together, these results provide support for redundancy as a quantifiable neuroprotective mechanism, but further research is needed to satisfactorily describe its role as either a reserve or compensatory mechanism (Cabeza et al., 2018; Montine et al., 2019). Reserve encompasses both structural and functional properties of the brain accumulated over time that support cognitive or clinical function in the event of damage, as opposed to a compensatory mechanism that reacts in response to damage (Cabeza et al., 2018; Montine et al., 2019; Stern et al., 2019). We would expect increased redundancy in MCI if it acted as compensatory response; rather, we observed a benefit in healthy aging, suggesting it serves as a reserve mechanism. AD-type pathology is already present in healthy aging and MCI stages, particularly in the hippocampus (Jack et al., 2013); aging individuals with more reserve (e.g., redundancy) are likely to show better cognitive outcomes, and therefore exhibit resilience to that damage. However, it is possible that redundancy increases for some individuals in healthy aging as a compensatory response to the accumulation of early pathology, that does not occur in individuals who are subsequently diagnosed with MCI or AD. Lifespan or longitudinal studies can provide additional evidence to elucidate its exact role.

Several limitations exist in this study. Although our results suggest a cognitive benefit of functional redundancy, our data were cross-sectional, limiting our claims about the progression of redundancy during the course of aging. Future studies should investigate longitudinally and

probe the potential difference in anterior and posterior hippocampal redundancy in differentiating stages of healthy and pathological aging, as later stages of MCI and AD may be expected to differ from healthy controls in anterior-based mnemonic processes (Koen & Yonelinas, 2014; Poppenk, Evensmoen, Moscovitch, & Nadel, 2013). In fact, our results demonstrated anterior hippocampal nodes are consistently among the highest 5% of nodal ratios between MCI groups. However, we did not observe significant group differences. The definition of early and late MCI used here, adopted from the ADNI protocol, may have precluded our ability to observe differences between MCI stages. The early versus late distinction is determined solely on performance on the LM-II, which could be affected by factors other than later stage cognitive decline (e.g., fatigue, concentration, practice effects) (Escandon, Al-Hammadi, & Galvin, 2010; Salthouse, 2010). However, we have no reason to believe these factors would differentially affect the groups, and we did not find a relationship between hippocampal redundancy and MMSE scores in MCI. Recently, it was proposed that an accurate staging of MCI and AD progression can be achieved through a combination of amyloid-beta, tau, and neurodegenerative markers (Jack Jr et al., 2018). The shift from staging MCI based on symptomatic markers to biological markers should be considered in future investigations.

In conclusion, we found that posterior hippocampal redundancy is greater in healthy or asymptomatic older adults than in individuals with MCI. Our data suggest a decrease in redundancy between healthy aging and MCI, upon which the amount of redundancy plateaus and no longer provides a functional advantage. Further, higher amounts of hippocampal redundancy are related to better memory performance. Although previous discussions of redundancy have been wary of a trade-off with efficiency (Glassman, 1987), we did not observe any reduction in

efficiency as a result of hippocampal redundancy. These data provide novel and promising quantitative support that redundancy acts as a neuroprotective mechanism in cognitive aging.

CHAPTER 3: THE ASSOCIATION BETWEEN HIPPOCAMPAL VOLUME AND MEMORY IN PATHOLOGICAL AGING IS MEDIATED BY FUNCTIONAL REDUNDANCY

Alzheimer's disease (AD) characteristic neuropathology, extracellular plaque deposits of ß-amyloid (Aß) and neurofibrillary tangles of hyperphosphorylated tau, accumulates during both healthy aging and mild cognitive impairment (MCI), and is accompanied by neurodegeneration and cognitive decline (Jack et al., 2013). Neurodegeneration, though not specific to AD (Jack Jr et al., 2018), has critical effects on cognition (Apostolova et al., 2012; Barnes et al., 2009; Frankó & Joly, 2013; Jack et al., 2000; Morra et al., 2009). Hippocampal atrophy in particular has been consistently associated with worse memory performance in cognitively normal (CN) individuals and in pathological aging (Golomb et al., 1993; Grundman et al., 2002; Huang et al., 2019; Nathan et al., 2017; O'Shea et al., 2016; Peng et al., 2015). Higher rates of atrophy are observed in later AD stages and in individuals with progressive cognitive decline as compared to those who remain stable (Apostolova et al., 2012; Barnes et al., 2009; Frankó & Joly, 2013; Jack et al., 2000; Morra et al., 2009). However, the functional mechanisms through which atrophy relates to impaired cognition remain uncertain.

Our primary objective was to determine whether topological properties of functional brain networks underlie the relationship between atrophy and cognition in older adulthood. Focusing on the hippocampus as one of the earliest sites of AD pathology (Harris et al., 2010), we considered two theoretically opposing functional properties through which hippocampal volume may relate to memory function: redundancy versus efficiency (Fig. 3.1). Redundancy, present in numerous biological systems, provides robustness to the system in the event of failure

of a specific element through the existence of alternative channels of communication (Billinton & Allan, 1992; Glassman, 1987; Navlakha et al., 2014; Tononi et al., 1999). On the other hand, local efficiency, an important property in small-world networks, refers to the efficiency of local information exchange, with higher local efficiency contributing to a lower cost of information flow (Achard & Bullmore, 2007; Latora & Marchiori, 2001; Rubinov & Sporns, 2010).

Figure 3.1 | Study hypotheses

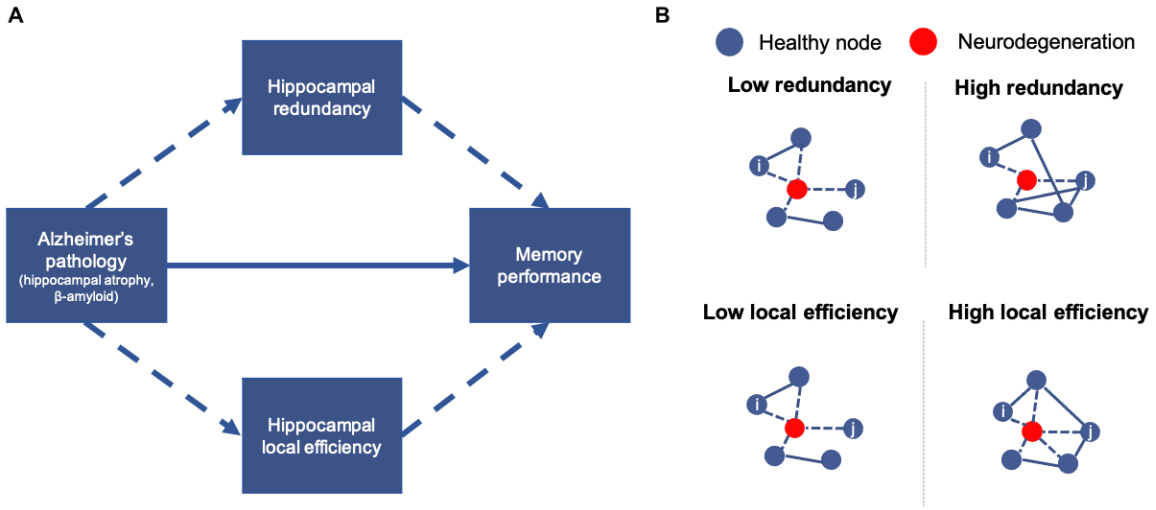

A. Hypothesized mechanism through which hippocampal atrophy relates to memory impairment. **B**. Depiction of topological properties considered. In low redundancy or low local efficiency networks, degeneration of a node results in no paths between nodes *i,j*. In high redundancy and high local efficiency networks, alternate paths exist between nodes *i,j*.

As a network property, redundancy is computed as the sum of direct and indirect paths (edges) between nodes in a network (Di Lanzo et al., 2012; Langella et al., 2021; Leistritz et al., 2013; Sadiq et al., 2021). Whole-brain redundancy declines in aging (Sadiq et al., 2021), whereas hippocampal redundancy specifically benefits memory in aging and is reduced in MCI (Langella et al., 2021). In contrast to redundancy's emphasis on indirect connections, local efficiency refers to the efficiency of communication between neighboring nodes (i.e., those with direct paths). Local efficiency is lower in older adults as an averaged whole-brain property, in specific

functional networks (e.g., default mode network), and regionally (e.g., hippocampus) (Achard & Bullmore, 2007; Cao et al., 2014; Geerligs, Renken, Saliasi, Maurits, & Lorist, 2015). Therefore, we hypothesized that reduced redundancy or loss of local efficiency may underlie the relationship between hippocampal atrophy and cognitive impairment.

Secondly, we examined the moderating effects of Aß burden on these relationships. Higher Aß burden, a more specific AD biomarker (Jack Jr et al., 2018), is also related to memory impairment in healthy aging and MCI (Huang et al., 2019; Nathan et al., 2017). Therefore, individuals with greater pathological burden may show differential relationships between volume, function, and cognition. Finally, neurodegeneration itself is a poor predictor of conversion to AD, but we reasoned that the combination of structural, functional and cognitive measures may aid in predicting clinical outcomes. To that end, we assessed whether such a combination relates to subsequent dementia conversion. In sum, we aimed to elucidate whether topological network measures, either via robustness and redundancy or through efficiency of communication, are mechanisms through which atrophy impacts cognitive function.

Materials and Methods

Dataset

Data were obtained from the Alzheimer's Disease Neuroimaging Initiative (ADNI) database (adni.loni.usc.edu), a longitudinal multi-site study launched in 2003 and led by Principal Investigator Michael W. Weiner, MD. For up to date information, see www.adni-info.org. Study visits were approved by each site's local IRB. All participants provided informed consent. The following diagnostic inclusion criteria were established by ADNI: CN participants have no subjective memory concern or objective impairment, clinical dementia rating (CDR) = 0, Mini-Mental State Exam (MMSE) $\geq$ 24, non-depressed, non-MCI, non-demented; MCI

participants have a subjective memory concern and objective memory impairment, CDR = 0.5, MMSE ≥ 24, no significant impairment in other cognitive domains, preserved activities of daily living, non-demented. CN and MCI participants from the ADNIGO/2 protocol between 60 and 90 years old with available resting-state fMRI (rs-fMRI), structural MRI, florbetapir PET, and cognitive composite scores were included in this study. Functional and structural MRI images were collected on the same day, and PET images and cognitive measures were collected within three months of the MRI scan. The first available timepoint meeting these criteria was used for each participant (initial n = 116 participants).

MRI data acquisition and processing

MRI scans were acquired on a 3 Tesla Philips Intera scanner (structural magnetization-prepared rapid gradient echo: flip angle = 9 degrees, slice thickness = 1.2 mm, TE = 3.1ms, TR = 6.8ms, sagittal plane; functional gradient echo: flip angle = 80 degrees, slice thickness = 3.31mm, TE = 30ms, TR = 3000ms, eyes open). Image preprocessing was completed using the Conn toolbox, version 18b (Whitfield-Gabrieli & Nieto-Castanon, 2012), running on MATLAB (R2017b). Preprocessing included realignment and unwarping, correction of slice-timing, co-registration of functional to structural images, spatial normalization to MNI space, and segmentation of gray matter, white matter, and CSF. Motion outlier identification was used to identify and remove volumes with movement greater than 1.5mm or a global signal Z threshold of 7. Noise components from white matter and CSF along with six participant-motion parameters and their first order derivatives were included as nuisance variables. Signal frequencies below 0.008 Hz and above 0.09 Hz were removed using temporal band-pass filtering. Participants with greater than 50% of volumes removed due to excessive motion were excluded from subsequent analyses (n = 12).

Functional network construction and calculation of topological measures

Functional timeseries were extracted based on a functionally defined parcellation template composed of 300 distinct spherical regions of interest (ROIs), or nodes, encompassing cortical, subcortical, and cerebellar regions (Seitzman et al., 2020). Participant-level correlation matrices were constructed, in which edges represent Fisher Z transformed correlations between each node. Individual matrices were binarized at a range of densities retaining the top 2.5–25% of edges in each network, representing each participant's unweighted functional connectivity matrix. As we considered whole hippocampal volume as our variable of interest, network measures were calculated for each of the four hippocampal nodes included in the parcellation (encompassing bilateral anterior and posterior regions), then averaged to create one hippocampal ROI. To examine the specificity of any hippocampal effects, analyses were also conducted for the insula (comprised of eight nodes), a deep cortical structure which can be reliably segmented with T1 images, yet has slower rates of atrophy than do medial temporal lobe regions (Sluimer et al., 2009). Network measures were not related to total volume of white matter hyperintensities, nor did groups differ in underlying functional connectivity (see Appendix B, Supplemental Methods).

Redundancy: The path array, P, was calculated as the number of indirect and direct paths between each node pair (i, j) with path length l from each connectivity matrix. The redundancy matrix, R, was calculated as the sum of the paths between nodes i and j, up to maximum path length L, set to 4 (Langella et al., 2021; Sadiq et al., 2021). The average of each hippocampal nodal sum over j of R (hippocampal node, j) yielded the whole hippocampal ROI redundancy.

$$R(i,j) = \sum_{l=1}^{L} P(i,j,l)$$

Local Efficiency: Local efficiency, E_{local}, of the hippocampal ROI, i, was calculated as the average nodal efficiency among the neighboring nodes (where $L = 1$, and $L_{j,k}$ denotes the shortest path between nodes j,k) of node i, excluding itself, where N is the number of nodes in graph G_i, and G_i is the subgraph of G that includes all neighboring nodes of i: (Rubinov & Sporns, 2010)

$$E_{local} = \frac{1}{N_{G_i}(N_{G_i} - 1)} \sum_{j,k \in G_i} \frac{1}{L_{j,k}}$$

Regional brain volume

Regional volume was available through ADNI. FreeSurfer v. 5.1 (Fischl, 2012) was used to segment anatomical MRI scans using the Desikan-Killany atlas and were manually checked for accuracy (full methods are available through ADNI). All structural MRI scans were taken on the same day as the rs-fMRI. Scans that failed the quality check were excluded from this analysis, as that indicates failed segmentation of the hippocampus ($n = 2$). Hippocampal volume was averaged across hemispheres as there were no hemispheric differences in either the whole sample, $t(101) = 0.16$, $p = .875$, or in MCI participants only, $t(74) = 0.18$, $p = .861$. The resulting average volume was normalized by dividing hippocampal volume by total intracranial volume and multiplied by 10^6 to retain the original scaling. All participant scans passed the insula quality control check. As with the hippocampus, left and right hemisphere volumes were averaged, and resulting values were normalized using total intracranial volume.

Florbetapir PET

Florbetapir PET imaging was available through ADNI for participants within three months of their MRI scan dates. Mean florbetapir uptake was calculated for cortical gray matter regions, averaged to create a single cortical value, and normalized using a cerebellar reference region. Participants with normalized florbetapir uptake ≤1.11 were classified as Aß positive

(Aß+), and those below 1.11 were classified as Aß negative (Aß-) (C. M. Clark et al., 2011; Joshi et al., 2012). Full methods are available through ADNI.

Cognitive measures

We chose two cognitive processes as our outcome measures, in which deficits are observed throughout AD progression: memory, the earliest and primary cognitive deficit, and executive function (EF), which declines later in the disease (Arnaiz & Almkvist, 2003). Memory (primarily reflecting verbal recall and recognition) and EF were evaluated using composite measures calculated using an IRT framework (mean = 0, standard deviation = 1) (Crane et al., 2012; Gibbons et al., 2012) (see Appendix B, Supplementary Methods).

Statistical analysis

Raw data were used for statistical analyses and were normalized for visualization. For brevity, statistical results and figures in the main text are reported using values averaged across densities, and results from each individual density are included in the supplemental materials (Appendix B). Analyses were completed in both the whole-sample and in the MCI participants only. Across analyses, a significance level of $p < .05$ was used.

Group differences were analyzed in R using an independent samples *t*-test with equal variance assumed for two group comparisons, an ANOVA for comparisons involving more than two groups or when including covariates, and a chi-square test for dichotomous variables. Permutation ANCOVA was used for group comparisons of network measures because it is more robust to non-normality, implemented using the aovperm function from the permuco R package (Frossard & Renaud, 2019) (10,000 permutations, and with age, sex, and years of education as covariates). Linear regressions were estimated in R using the lm R function, with age, sex, and years of education included as covariates of no interest: (1) volume on cognition (memory, EF),

(2) volume on network measure (redundancy, local efficiency), and (3) network measure on cognition. Resulting beta-weights were standardized using the lm.beta R function.

Mediation models were estimated using the mediation R package (Tingley, Yamamoto, Hirose, Keele, & Imai, 2014) with volume as the predictor, cognition as the outcome, network measure as the mediator, and age, sex, and education as covariates of no interest. Effects were estimated using bootstrapping (10,000 simulations). In significant mediation models, Aß was included as a dichotomous moderator of the mediation, included in the path between the predictor and mediator. Indirect and direct effects of the model were conditionalized on Aß- and Aß+ separately. Indirect effects at each level were compared using bootstrapping (10,000 simulations).

K-means clustering was implemented in MATLAB. Values of *k* ranging from 2 to 8 were considered. The optimal *k* was determined using the silhouette method with 10,000 iterations and 10 simulations. Distance was measured using city block (Manhattan) distance, as it is less sensitive to outliers. Since different densities may result in different cluster solutions, rendering comparison across densities difficult, only the average density was used. Variables were normalized for clustering. Three-dimensional clustering was computed using hippocampal volume, memory, and redundancy. To assess the specific contribution of redundancy, we also completed two-dimensional clustering using memory and volume. Because redundancy was positively related to hippocampal volume and memory, the residuals from regressing volume on redundancy and from regressing memory on redundancy were used in the cluster analysis, thereby removing the effect of redundancy on each variable.

Groups resulting from the clustering procedure described above were compared with a survival analysis, testing the extent to which the groups differ in rates of conversion to dementia,

using the survival (Therneau, 2020) and survminer (Kassambara, Kosinski, Biecek, & Fabian, 2020) R packages, based on the Kaplan-Meier method to estimate survival probability. Groups were compared using a log-rank test. Participants were examined up to three years following the MRI visit to determine their conversion status. The earliest time point was selected if a participant did convert to dementia. If the participant did not convert, the latest available time point, up to three years post scan, was used (average follow-up time: 23.58 months for the whole sample and 23.94 months for MCI only). In total, 12 participants converted to dementia.

Results

Association between hippocampal volume, memory, and topological network properties

The final sample consisted of 102 participants (Table 3.1). Diagnostic groups did not differ in hippocampal volume [$F(1,97) = 0.25$, $p = .621$]. The CN group had higher hippocampal redundancy than the MCI group [$F(1,97) = 7.48$, $p = .008$], but the groups did not differ in hippocampal local efficiency [$F(1, 97) = 0.12$, $p = .743$] (Table S3.1). Additionally, there was a positive relationship between redundancy and local efficiency, indicating that one does not come at the expense of the other (whole-sample: ß = 0.40, $p < .001$, $R^2_{adjusted} = .135$; MCI: ß = 0.38, $p = .001$, $R^2_{adjusted} = .127$; Table S3.2).

Table 3.1 | Participant characteristics by diagnosis

	CN (*n* = 27)	MCI (*n* = 75)	Test Statistic	*p*
Age	75.26 (6.51)	71.85 (6.51)	$t(100) = 2.33$	**.022**
Sex	15F/12M	36F/39M	$X^2(1) = 0.20$	.654
Education	16.19 (1.98)	16.15 (2.68)	$t(100) = 0.07$	.946
Aß burden	8+/19-	43+/32-	$X^2(1) = 5.04$	**.025**
MMSE	28.74 (1.10)	27.99 (1.75)	$t(100) = 2.09$	**.039**
Memory	0.99 (0.57)	0.34 (0.59)	$t(100) = 4.93$	**< .001**
EF	0.87 (0.74)	0.43 (0.92)	$t(100) = 2.24$	**.027**

Note: Standard deviation given in parentheses; age and education given in years

We first tested whether hippocampal volume was associated with our two cognitive measures. Lower hippocampal volume was associated with lower memory (whole-sample: ß = 0.38, $p < .001$, $R^2_{adjusted} = .230$; MCI: ß = 0.43, $p = .001$, $R^2_{adjusted} = .303$; Fig. 3.2A) but not to EF (whole-sample: ß = 0.17, $p = .102$, $R^2_{adjusted} = .218$; MCI: ß = 0.14, $p = .276$, $R^2_{adjusted} = .249$). Next, we examined the relationships of the topological network measures with volume and cognition (Tables 3.2, S3.3-S3.8). Lower hippocampal volume was related to lower redundancy, and in turn, lower hippocampal redundancy was related to worse memory performance (but not EF) (Fig. 3.2B). As with redundancy, lower hippocampal volume was related to lower local efficiency (Fig. 3.2C). However, local efficiency was not related to memory or EF.

Table 3.2 | Linear regression output between hippocampal topological measures, volume, and cognition at the averaged density

	Redundancy-Volume			**Redundancy-Memory**			**Redundancy-EF**		
	ß	*p*	R^2	ß	*p*	R^2	ß	*p*	R^2
All	0.27	.022	.025	0.34	<.001	.242	0.17	.052	.227
MCI	0.29	.039	.032	0.32	.002	.277	0.11	.280	.249

	Efficiency-Volume			**Efficiency-Memory**			**Efficiency-EF**		
	ß	*p*	R^2	ß	*p*	R^2	ß	*p*	R^2
All	0.24	.043	.009	0.12	.209	.138	0.05	.608	.198
MCI	0.34	.019	.026	.096	.362	.184	-0.01	.893	.237

Note: Output from analyses using all participants (CN and MCI) and MCI only. ß = standardized beta, R^2 = adjusted R^2

Hippocampal redundancy underlies the hippocampal volume-memory relationship

We then estimated models to determine whether the topological properties mediated volume-cognition relationships (Tables 3.3, S3.9-S3.12). Hippocampal volume exerted a significant effect on memory through redundancy (whole-sample proportion mediated = 0.20, *p*

= .013; MCI only proportion mediated = 0.17, p = .039; Fig. 3.2D). Conversely, local efficiency did not mediate the hippocampal volume-memory relationship (Fig. 3.2E). Neither redundancy nor local efficiency mediated the relationship between volume and EF in either the whole group or in MCI only, suggesting a specific role for hippocampal redundancy in memory ability.

The prior results suggest that participants with more risk for AD (i.e., low hippocampal volume), have accompanying low functional redundancy, which contributes to memory impairment. To test the hypothesis that individuals with higher rates of AD pathology would show different relationships between structural and functional measures, we included Aß as a moderator in the volume-redundancy-memory mediation model (Tables S3.13, S3.14). In the whole group, neither the Aß+ (indirect effect: ß = 1.44×10^{-4}, 95% CI[-9.16×10^{-7}, 3.44×10^{-4}], p = .051; direct effect: ß = 7.92×10^{-4}, 95% CI[3.85×10^{-4}, 1.26×10^{-3}], p < .001) nor Aß- (indirect effect: ß = 1.21×10^{-4}, 95% CI[-2.25×10^{-6}, 2.96×10^{-4}], p = .054; direct effect: ß = 1.25×10^{-4}, 95% CI[-3.65×10^{-4}, 6.82×10^{-4}], p = .654) effects reached significance, and the indirect effects were not significantly different from each other (p = .870). When limiting to MCI participants, however, redundancy was a partial mediator of the volume-memory relationship for Aß+ participants (indirect effect: ß = 1.47×10^{-4}, 95% CI[4.28×10^{-6}, 4.00×10^{-4}], p = .040; direct effect: ß = 8.12×10^{-4}, 95% CI[4.08×10^{-4}, 1.24×10^{-3}], p < .001; proportion mediated: 0.15). Conversely, redundancy was not a significant mediator when estimating for Aß- participants (indirect effect: ß = 4.15×10^{-5}, 95% CI[-5.78×10^{-5}, 1.64×10^{-4}], p = .351; direct effect: ß = 8.85×10^{-5}, 95% CI[-4.53×10^{-4}, 6.97×10^{-4}], p = .746), suggesting that the functional redundancy mediation is specific to individuals harboring AD pathology. However, the indirect effects for Aß+ and Aß- did not differ from one another (p = .288).

Figure 3.2 | Relationships between hippocampal volume, topological network measures, and memory

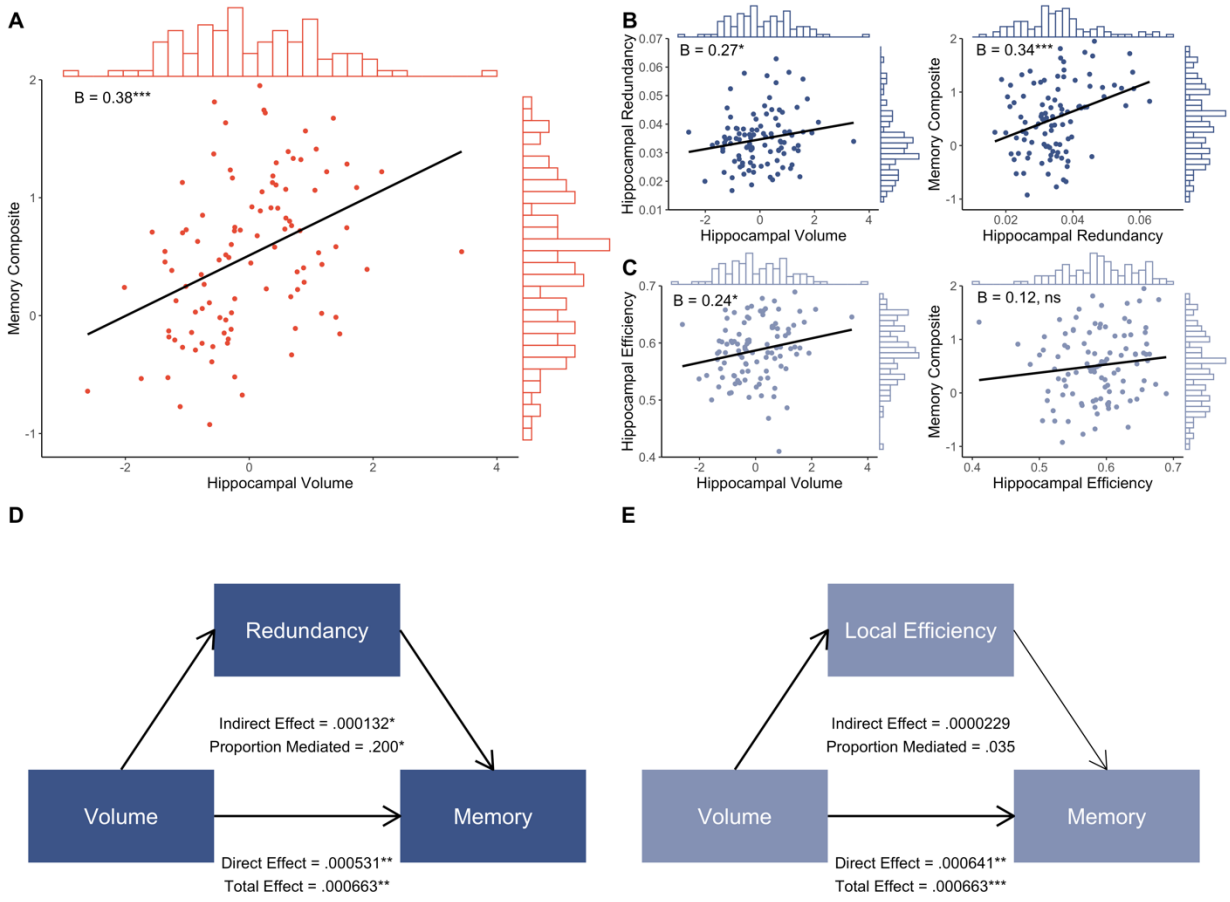

A. Whole-sample regression of hippocampal volume on memory composite score, with histograms showing distribution of variable values and inset standardized beta coefficients. **B.** Whole-sample regression of hippocampal volume on hippocampal redundancy, and of hippocampal redundancy on memory composite score, with histograms showing distribution of variable values and inset standardized beta coefficients. **C.** Whole-sample regression of hippocampal volume on hippocampal local efficiency, and of hippocampal local efficiency on memory composite score, with histograms showing distribution of variable values and inset standardized beta coefficients. **D.** Mediation results from hippocampal volume-redundancy-memory model. Bold lines denote significant paths. **E.** Mediation results from volume-local efficiency-memory model. Bold lines denote significant paths. *$p < .05$, **$p < .01$, ***$p < .001$

Table 3.3 | Mediation output at the averaged density

Volume – Redundancy – Memory						
	Indirect Effect			**Direct Effect**		
	ß	**95% CI**	***p***	**ß**	**95% CI**	***p***
All	$1.32x10^{-4}$	$2.40x10^{-5}$, $2.81x10^{-4}$	.013	$5.31x10^{-4}$	$1.83x10^{-4}$, $9.25x10^{-4}$	.004
MCI	$1.08x10^{-4}$	$2.74x10^{-6}$, $3.00x10^{-4}$	.038	$5.34x10^{-4}$	$1.64x10^{-4}$, $9.20x10^{-4}$	.006
Volume – Local Efficiency – Memory						
	Indirect Effect			**Direct Effect**		
	ß	**95% CI**	***p***	**ß**	**95% CI**	***p***
All	$2.29x10^{-5}$	-6.06×10^{-5}, 1.31×10^{-4}	.562	$6.40x10^{-4}$	$2.87x10^{-4}$, $1.02x10^{-3}$	.001
MCI	$-2.58x10^{-8}$	$-1.38x10^{-4}$, $1.07x10^{-4}$	.968	$6.42x10^{-4}$	$3.11x10^{-4}$, $1.04x10^{-3}$	<.001
Volume – Redundancy – Executive Function						
	Indirect Effect			**Direct Effect**		
	ß	**95% CI**	***p***	**ß**	**95% CI**	***p***
All	$9.63x10^{-5}$	$-2.27x10^{-5}$, $2.79x10^{-4}$	.122	$3.18x10^{-4}$	$-1.56x10^{-4}$, $7.86x10^{-4}$	.184
MCI	$6.11x10^{-5}$	$-7.29x10^{-5}$, $3.02x10^{-4}$	.417	$2.54x10^{-4}$	$-3.04x10^{-4}$, $7.62x10^{-4}$	.373
Volume – Local Efficiency – Executive Function						
	Indirect Effect			**Direct Effect**		
	ß	**95% CI**	***p***	**ß**	**95% CI**	***p***
All	$9.90x10^{-6}$	$-1.10x10^{-4}$, $1.61x10^{-4}$	.841	$4.05x10^{-4}$	$-8.57x10^{-5}$, $8.88x10^{-4}$	.099
MCI	$-3.76x10^{-5}$	$-2.28x10^{-4}$, $1.68x10^{-4}$	.664	$3.53x10^{-4}$	$-2.12x10^{-4}$, $8.99x10^{-4}$	.207

Note: Output from analyses using all participants (CN and MCI) and MCI only. ß = unstandardized beta

Low volume, redundancy, and memory predict subsequent dementia conversion

We sought to further explore the relationship between these variables using a data-driven approach, more specifically clustering participants based on hippocampal volume, redundancy,

and memory. In our whole group, a two cluster solution emerged, in which one cluster had low redundancy, volume, and memory (low RVM, $n = 50$), and the other had high values on all three variables (high RVM, $n = 52$). Each cluster was comprised of both CN and MCI participants, along with Aß- and Aß+ participants (Fig. 3.3A-B). The low RVM cluster had more MCI participants than the high RVM cluster [$X^2(1) = 6.63$, $p = .010$], but the clusters had similar proportions of Aß+ participants [$X^2(1) = 3.18$, $p = .075$]. Additionally, the low RVM group was older [$t(100) = 3.74$, $p < .001$] and had fewer years of education [$t(100) = 1.99$, $p = .049$].

The mediation results and cluster characteristics suggest that the combination of low hippocampal volume and low hippocampal redundancy is a risk factor for pathological aging. We sought additional evidence of this notion by examining rates of conversion to dementia in each of the clusters. Strikingly, no participants in the high RVM group converted to dementia, whereas all dementia conversions ($n = 12$) occurred in the low RVM group. The survival probability was thus lower in the low RVM cluster than in the high RVM cluster ($p < .001$) (Fig. 3.3D). Critically, the two clusters did not differ in average follow-up time [$t(100) = 1.47$, $p = .145$].

Clustering just the MCI participants resulted in similar results, again finding a low RVM ($n = 35$) and a high RVM ($n = 40$) group. The clusters had similar proportions of Aß+ participants [$X^2(1) = 2.58$, $p = .108$]. The low RVM group was older than the high group [$t(73) = 3.43$, $p < .001$], but they had similar levels of education [$t(73) = 1.49$, $p = .141$]. Finally, individuals in the low RVM group were more likely to convert to dementia than those in the high RVM group ($p = .007$), with 10 of the 12 participants who converted to dementia clustering with low RVM. The two clusters did not differ in average follow-up time [$t(73) = 1.09$, $p = .281$].

To test the specific contribution of redundancy to the clustering approach reported above, we repeated the analysis using only volume and memory. The removal of redundancy changed the results considerably, yielding four groups, between which survival probability did not differ (whole-sample: $p = .160$; MCI: $p = .120$). Further, the low VM group contained only four of the 12 converters in the whole group and seven of the 12 in the MCI only participants, compared to the respective 12 and 10 converters in the analogous low RVM group.

Figure 3.3 | Characteristics of three-dimensional *k*-means clustering solution groups

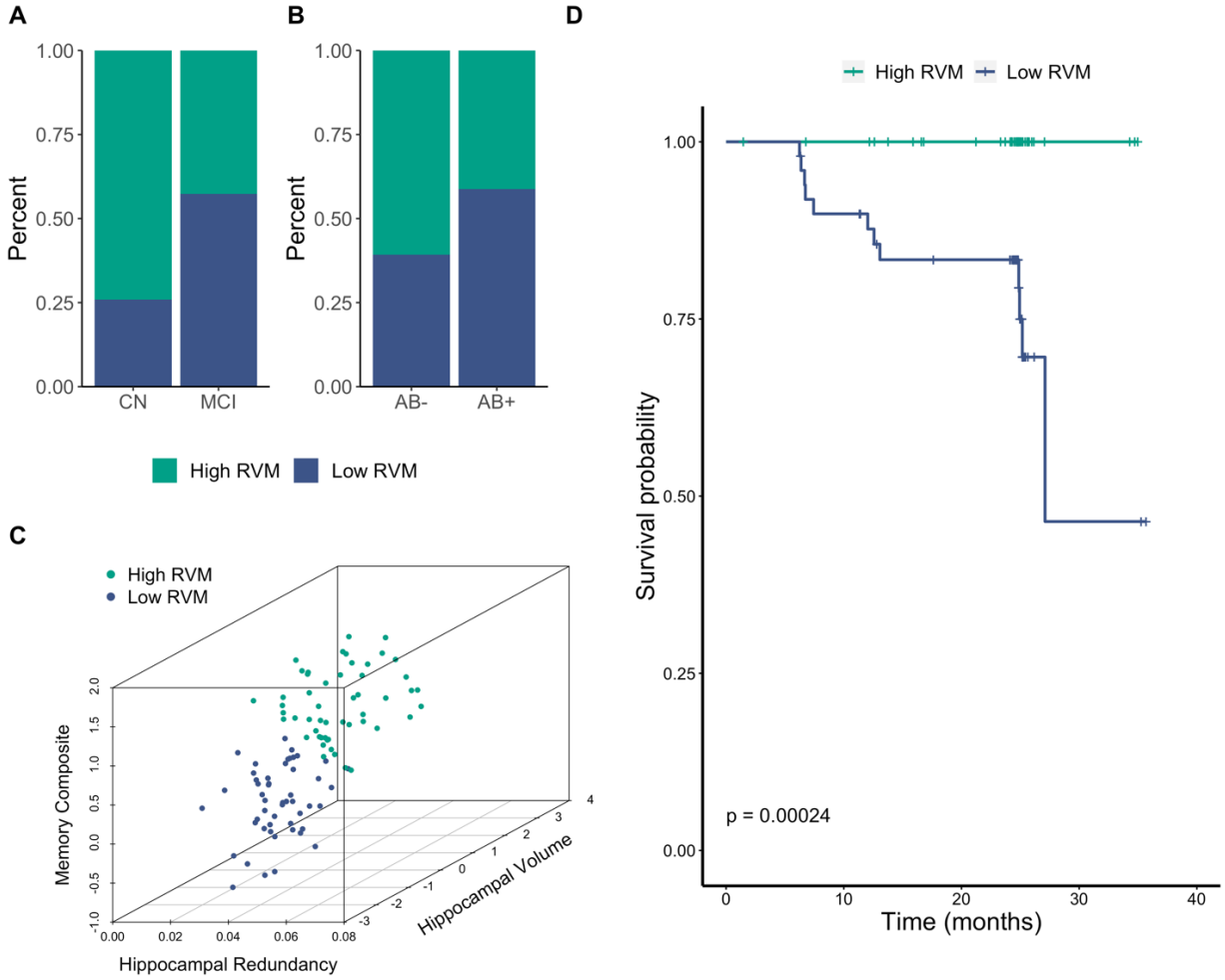

A. Percent of CN and MCI participants within each cluster. **B.** Percent of Aß- and Aß+ participants within each cluster. **C.** Scatterplot showing the relationship between hippocampal redundancy, hippocampal volume, and memory in each cluster. **D.** Survival probability for each cluster over time. Vertical drop in curve indicates a conversion to dementia. Tick marks represent censoring of a participant (i.e., final timepoint). RVM = redundancy, volume, memory

Specificity of hippocampal atrophy

Finally, we examined the relationships between volume, redundancy, and memory in the insula, a deep cortical structure exhibiting a slower rate of atrophy in preclinical stages (Sluimer et al., 2009), to determine the specificity of hippocampal atrophy and function (Fig. 3.4; Tables S3.15-S3.17). Insular volume was not related to memory (whole-sample: ß = 0.14, p = .140, $R^2_{adjusted}$ = .144; MCI: ß = 0.10, p = .368, $R^2_{adjusted}$ = .184), nor to insular redundancy (whole-sample: ß = 0.11, p = .315, $R^2_{adjusted}$ = .010; MCI: ß = 0.10, p = .428, $R^2_{adjusted}$ = .025). Insular redundancy was not related to memory (whole-sample: ß = 0.08, p = .396, $R^2_{adjusted}$ = .131; MCI: ß = 0.02, p = .847, $R^2_{adjusted}$ = .175). Further, insular redundancy did not mediate the relationship between insular volume and memory in either the whole sample or MCI only (ps > .628).

Figure 3.4 | Relationships between insular volume, redundancy, and memory

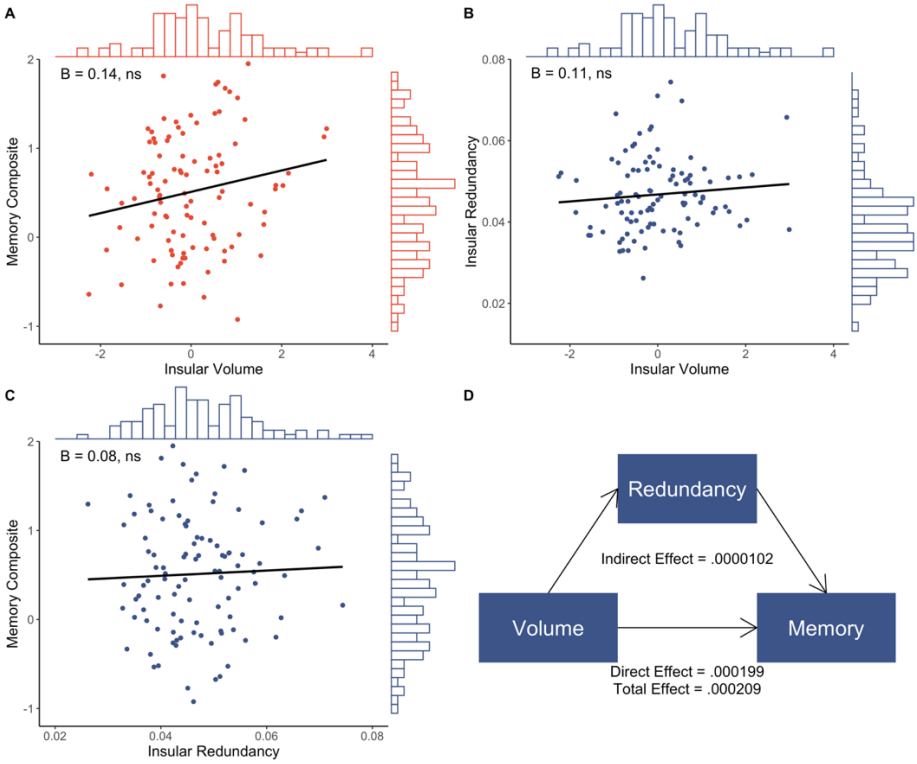

Whole sample regression of insular volume on memory composite score **(A)**, insular volume on insular redundancy **(B)**, and insular redundancy on memory composite score **(C)**, with histograms showing distribution of variable values and inset standardized beta coefficients. **D.** Mediation results from insular volume-redundancy-memory model.

Discussion

Despite widespread findings of hippocampal atrophy across healthy and pathological aging (Apostolova et al., 2012; Barnes et al., 2009; Frankó & Joly, 2013; Jack et al., 2000; Morra et al., 2009), the functional mechanisms through which hippocampal atrophy relates to impaired cognition remain uncertain. Our data suggest that hippocampal redundancy is one such mechanism. In CN and MCI older adults, we found that low hippocampal volume was related to low memory performance, which was mediated by low redundancy but not local efficiency. Data-driven clustering methods supported these findings, such that participants with low volume, redundancy, and memory clustered together and separately from those with high values on all three measures. Further, the low RVM cluster included all of the participants who subsequently converted to dementia. Overall, these results provide evidence that low hippocampal redundancy underlies the relationship between hippocampal atrophy and memory impairment, and that this presentation of low structure, function, and cognition is a risk factor for conversion to dementia.

Our analysis focused on two topological network measures, redundancy and local efficiency, but only redundancy mediated the relationship between hippocampal volume and memory. Redundancy supports robustness in cellular and neural networks (Aittokallio & Schwikowski, 2006; Pitkow & Angelaki, 2017), and hippocampal functional redundancy is beneficial for memory and is reduced in pathological aging (Langella et al., 2021). Retaining hippocampal redundancy, then, may be neuroprotective in early stages of AD. Significant mediation effects were observed in both our combined sample as well as in just MCI participants. However, only in MCI was there evidence that the role of redundancy may differ as a result of Aß burden. Although the difference between Aß+ and Aß- effects did not reach significance, mediation was significant only for Aß+ participants, providing initial evidence that

redundancy contributes to low memory in individuals with greater risk for developing AD (e.g., individuals with MCI who are Aß+), but exerts no effect in less impaired groups. The loss of hippocampal redundancy may accompany the accumulation of disease pathology. Future work should further probe potential differences as a function of pathological burden.

Our results also demonstrate a specificity to the role of hippocampal redundancy. Significant mediation by redundancy was only observed for the association of memory with hippocampal atrophy, not for EF. Whole-brain redundancy, on the other hand, supports EF in healthy adults (Sadiq et al., 2021). Though hippocampal function is implicated widely in cognition (Shohamy & Turk-Browne, 2013), given its primary involvement in mnemonic processes (R. E. Clark & Squire, 2013; Eichenbaum, 2017), our findings show that regional measures of redundancy appear to be selective in their effects. Additionally, insular redundancy did not mediate a relationship between insular volume and cognition, suggesting a relatively specific effect of the hippocampus in healthy and early pathological aging.

The finding of low and high RVM clusters in our dataset support our mediation findings that low structure, function, and cognition accompany each other. Further, the combination of low values on all three variables represents a risk state, with a higher proportion of individuals subsequently converting to dementia. However, when clustering on volume and memory, and equating redundancy, a more complex four-cluster solution emerged with ill-defined risk groups. The low VM cluster did not capture the high proportion of conversions that was achieved when including functional redundancy. Indeed, hippocampal neurodegeneration itself is not specific to AD (Jack Jr et al., 2018), and atrophy is common in healthy aging (Daugherty, Bender, Raz, & Ofen, 2016). In our sample, low hippocampal volume was a poor predictor of subsequent

dementia conversion, but when accompanied by hippocampal redundancy, prediction substantially improves.

This study has several limitations. Our sample consisted of disproportionately more participants with MCI than CN individuals. To address this limitation, analyses were repeated using just MCI participants, with results supporting the same conclusions. However, we did not have a large enough CN sample to repeat the analyses in just CN participants. Additionally, the markers of interest were examined cross-sectionally, precluding longitudinal assessment of hippocampal atrophy or Aß accumulation. Future work should also employ longitudinal assessment of functional hippocampal redundancy to elucidate whether redundancy is malleable across healthy and pathology aging, such as in response to neuropathology.

In sum, we find that hippocampal redundancy underlies the relationship between low hippocampal volume and poor memory performance. Although neurodegeneration is a non-specific risk factor for AD (Jack Jr et al., 2018), by including this functional correlate of hippocampal atrophy, the ability to differentiate between stable and converter participants is improved. Topological network properties are thus critical in understanding the link between atrophy and cognitive impairment in preclinical older adults.

CHAPTER 4: POSTERIOR HIPPOCAMPAL REDUNDANCY IS RELATED TO MEMORY BUT NOT TO EDUCATION OR PHYSICAL ACTIVITY IN HEALTHY AGING

Aging is characterized by normative and pathological changes to the brain, accompanied by declines in cognitive function. One of the primary regions affected in aging is the hippocampus, a medial temporal lobe structure which supports memory processes. Although the hippocampus is severely affected in pathological aging (e.g., Alzheimer's disease, AD), hippocampal functional deficits, atrophy, and episodic memory declines are also observed in normative aging (Fjell, McEvoy, Holland, Dale, & Walhovd, 2014; O'Shea et al., 2016; Raz et al., 2005; Yankner et al., 2008). However, periods of normative aging are marked by significant variability, and some older adults maintain high levels of cognition throughout older adulthood (de Godoy et al., 2020; Wilson, Wang, Yu, Bennett, & Boyle, 2020). Given the detrimental effects of cognitive decline, it is imperative to understand the factors that support such preserved cognition in aging.

Individual differences in accumulated reserve may explain some of this variability: reserve mechanisms build throughout an individual's life which support resilience to physical brain damage (e.g., pathological build-up, neurodegeneration), thereby delaying the onset of observable clinical or cognitive decline (Cabeza et al., 2018; Montine et al., 2019; Stern, 2006; Stern et al., 2019). Recent evidence suggests that functional redundancy derived from resting-state fMRI networks relates to reserve and resilience in aging. Whole-brain redundancy increases throughout the adolescent and adult lifespan, then begins to decline in older adulthood, though redundancy diminishes age-related declines in cognition (Sadiq et al., 2021). Hippocampal

redundancy, in particular, is related to higher memory performance in healthy aging and is lower in individuals with mild cognitive impairment (Langella et al., 2021). These findings indicate that redundancy serves as a neuroprotective mechanism in cognitive aging, through which cognition is preserved. However, no study to date has comprehensively examined the relationship between hippocampal redundancy and memory in healthy cognitive aging. Because the hippocampus exhibits long-axis functional specialization, also reflected in its functional connections, (Blessing, Beissner, Schumann, Brünner, & Bär, 2016; Fanselow & Dong, 2010; Strange, Witter, Lein, & Moser, 2014), it is critical to examine potential differences in anterior and posterior hippocampal redundancy as it relates to various aspects of memory. Further, it is unknown how protective factors commonly studied in the context of reserve may influence hippocampal redundancy.

Education and physical activity have been identified as two important potentially modifiable, protective factors that impact AD risk (Norton et al., 2014). Although higher reserve as a general construct is related to better cognition (Cabral et al., 2016; Giogkaraki, Michaelides, & Constantinidou, 2013), a meta-analysis comparing proxies of cognitive reserve identified consistent support that high levels of education is independently related to reduced risk of AD and higher clinical functioning in older adulthood (Meng & D'Arcy, 2012). Higher levels of education also relate to slower rates of cognitive decline in aging (Butler, Ashford, & Snowdon, 1996; Christensen et al., 1997). Strikingly, education was identified as the best predictor of cognitive change in older adults over a two-year period aside from baseline cognition (Albert, Jones, Savage, Berkman, & et al, 1995). These positive outcomes may arise from education-facilitated synaptic density (Piras, Cherubini, Caltagirone, & Spalletta, 2011) and volumetric increases (see Wenger & Lövdén, 2016 for a review) in the hippocampus.

Physical activity is similarly deemed a protective factor for healthy aging. Higher physical activity has been related to both delayed onset and slowed progression of AD (see Rashid, Zahid, Zain, Kabir, & Hassan, 2020 for a review). In healthy aging, physical activity moderates age-related atrophy of the medial temporal lobe, such that older adults with high levels of activity do not show signs of atrophy which are evident in older adults with low activity levels (Bugg & Head, 2011). Further, implementation of exercise programs increases hippocampal volume (Erickson et al., 2011) and memory performance (Ji et al., 2018) in healthy older adults. Higher self-reported physical activity in older adults is associated with better global cognition and episodic memory performance, regardless of the intensity of activity (Reas et al., 2019). Mechanistically, exercise induces neurogenesis in the hippocampus, including cellular proliferation and promoting synaptic plasticity, thereby supporting learning and memory and deterring cognitive decline (Ma et al., 2017; Olson, Eadie, Ernst, & Christie, 2006).

Based on the ability of both education and physical activity to impact hippocampal structure and function, it is plausible that they similarly positively influence hippocampal redundancy. Therefore, the current study utilizes a large sample of healthy older adults between the ages 60 and 90 years to probe the relationship between hippocampal redundancy and cognition and assess whether hippocampal redundancy serves as an underlying mechanism through which education and physical activity support preserved cognition in older adulthood (Fig. 4.1). We hypothesize that hippocampal redundancy will be positively associated with memory performance, and will explore potential differences between anterior and posterior hippocampal regions, as well as differences between item-level and contextual episodic memory. We hypothesize that higher education and higher physical activity will be related to higher hippocampal redundancy, which, in turn, will relate to better memory performance.

Figure 4.1 | Study design and hypotheses

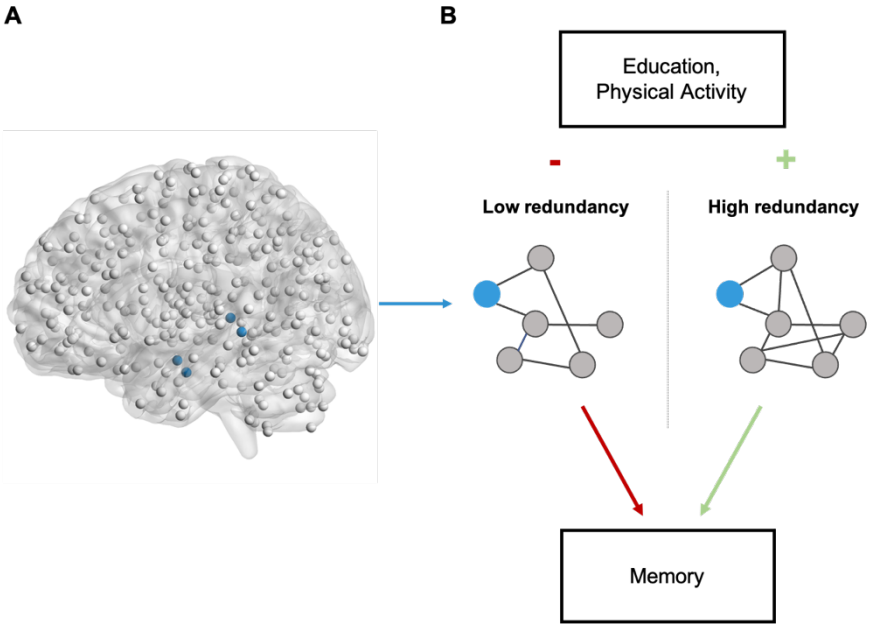

A. Cortical-subcortical-cerebellar parcellation used to define functional networks. Hippocampal nodes shown in blue, representing left and right anterior and posterior hippocampus. Non-hippocampal nodes shown in gray. **B.** Hypothesized relationships between protective factors, redundancy, and memory, such that high education or physical activity relate to higher redundancy, which in turn promotes memory performance. Alternatively, low education or physical activity relate to lower hippocampal redundancy, which in turn relates to low memory performance.

Materials and Methods

Dataset and participants

Data were obtained from the Human Connectome Project – Aging (HCP-Aging) database (Harms et al., 2018) for older adults between 60 and 90 years old who demonstrated normal cognitive functioning as assessed by the Montreal Cognitive Assessment (MoCA) [60-69 years: score equal to or above 26; 70 years and above: score within one standard deviation of their age and education adjusted norm (Malek-Ahmadi et al., 2015)] and preserved activities of daily living as assessed by the Lawton-Brody Instrumental Activities of Daily Living (IADL) scale (score at or above 7, maximum score of 8). All participants who met the above criteria and had available resting-state fMRI, structural MRI, and cognitive data were included in this study.

Participant characteristics and final sample sizes per measure of interest are included in Table 4.1.

Image processing and redundancy calculation

Structural and functional images were collected on a 3 Tesla Siemens Prisma scanner (Harms et al., 2018). Structural images were collected using a multi-echo magnetization prepared rapid gradient echo sequence (voxel size: 0.8x0.8x0.8mm, TR = 2500ms, TE = 1.8/3.6/5.4/7.2ms, flip angle = 8 degrees). Functional images were collected using a 2D multiband gradient-recalled echo echo-planar imaging sequence (voxel size: 2x2x2mm, TR = 800ms, TE = 37ms, flip angle = 52 degrees). Participants had two functional scans with opposite phase encoding direction (posterior-anterior and anterior-posterior). A fixation cross was displayed during the functional scans, and participants were instructed to keep their eyes open. Images which had undergone minimal preprocessing using the HCP-Pipelines were obtained for this study (described in Glasser et al., 2013). Each functional run was processed separately. Additional processing steps and timeseries extraction were implemented in the MATLAB (R2017b) Conn toolbox (conn18b) (Whitfield-Gabrieli & Nieto-Castanon, 2012), including outlier identification, nuisance regression (white matter, cerebrospinal fluid, and 12 motion parameters), and temporal band-pass filtering (0.01 – 0.1Hz). Outlier volumes were identified from the functional images, defined as movement greater than 0.9mm or global blood-oxygen-level-dependent signal changes above 5SD, and were removed. Outlier volumes per participant ranged from 0 to 94 of 956 total frames.

Functional timeseries were obtained from 300 regions of interest (ROIs) for each functional run. ROIs were defined using a functionally-defined parcellation of spherical, non-overlapping cortical, subcortical, and cerebellar nodes (Seitzman et al., 2020). Fisher Z

transformed correlation matrices (300 x 300) were constructed for each session for each participant, and resulting correlation matrices for each session were averaged to create a single correlation matrix per participant. Individual matrices were binarized to retain the top 2.5 – 25% of edges in 2.5% increments. A redundancy matrix (R) was calculated from each participant's unweighted functional connectivity matrix, represented as the sum of direct and indirect paths between nodes i and j with path length l (up to maximum path length L, set to 4):

$$R(i,j) = \sum_{l=1}^{L} P(i,j,l)$$

Four nodes representing left and right anterior and posterior hippocampus were considered as the primary study ROIs. Hippocampal redundancy was calculated separately for each hippocampal ROI as the summed redundancy between the hippocampal ROI and all other matrix ROIs (i.e., across row j). Hippocampal redundancy was not related to number of volumes removed nor to mean motion at any density (all ps > .176; Table S4.1).

Cognitive measures

Due to its strong relation to the hippocampus and age-related cognitive decline (Leal & Yassa, 2015), memory was the primary cognitive domain of interest and was assessed using two tasks: the Ray Auditory Verbal Learning Task (RAVLT) and Picture Sequence Memory (PSM). The RAVLT is a neuropsychological task for evaluating item-level episodic memory. The experimenter reads a list of 15 unrelated words, and the participant repeats the words back that they remember. This process is repeated five times. Participants' total scores on these five learning trials represent a measure of encoding and recall ability ("Learning", possible scores range from 0-75). After hearing a distractor list, participants are asked to recall the original word list ("Immediate Recall", possible scores range from 0-15). PSM is a task in which participants are shown a series of pictures depicting activities while a story is read aloud, and participants are

asked to recall the sequence of the pictures (trials include one 15-item sequence and one 18-item sequence). Scores are determined using item response theory (IRT) methodology, then normalized to have a mean of 100 and standard deviation of 15.

To assess whether any observed effects are specific to memory or extend to other cognitive domains, executive function was also examined, quantified as completion time for the Trails Making Test Part B (TMT-B). During the TMT-B, participants must connect a set of 25 dots as quickly and accurately as possible. Each dot is labeled with a letter or number, and the participant must alternate between consecutive letters and numbers until reaching the end.

Education and physical activity

Education and physical activity were chosen as two protective factors that may influence hippocampal redundancy. Education was represented as self-reported years of education completed and was treated as a continuous variable. Physical activity was quantified using the Short International Physical Activity Questionnaire (IPAQ), a 4-item report addressing the number of days and minutes engaged in various levels of activity over the last week. Time spent on walking, moderate, and vigorous activity per week was expressed as a single variable of MET-minutes per week (MET = metabolic equivalent of task) consistent with IPAQ guidelines. Due to non-normality of the responses, scores were log-transformed for analyses.

Statistical analysis

Analyses were performed at each density and on the values averaged across densities. The average values are reported in the main text, and individual density information is reported in the Supplemental Materials in Appendix C. Statistical analyses were run using R. Age and sex were included as covariates in all analyses. An alpha level of .05 was used to determine statistical significance for all tests.

Linear regression. Linear regressions were estimated using the lm R function. Standardized betas are reported using the lm.beta R function. Because of the non-normality of functional redundancy values, analyses were repeated using robust regression using Huber weights with the rlm function from the MASS R package (Ripley, 2020), with a Wald test of significance using the f.robftest function from the sfsmisc Rpackage (Maechler, 2020). Interactions between predictors were probed using the interactions R package (Long, 2019).

Mediation. Multiple mediation models were estimated using the mma R package (Yu & Li, 2020) with education and physical activity as predictors, cognition as the outcome, and redundancy as the mediator. In each model, hippocampal ROIs were simultaneously tested as mediators, and separate models were run for each predictor and outcome variable. Effects were estimated using bootstrapping (10,000 simulations).

Table 4.1 | Participant characteristics and sample sizes per measure of interest

	N	Mean (SD)
Sex	122F	-
MoCA	214	27.29 (1.72)
IADL	214	7.97 (0.17)
Age	214	73.36 (8.41)
Education (years)	214	17.79 (2.28)
MET-min per week	214	2669.64 (2488.06)
RAVLT Immediate Recall	211	9.19 (3.08)
RAVLT Learning	208	44.64 (9.54)
Picture Sequence Memory	181	98.82 (13.22)
TMT-B (seconds)	213	77.88 (42.10)

Note: F = female; RAVLT = Rey Auditory Learning Test; TMT-B = Trails Making Test Part B

Results

Left posterior hippocampal redundancy is related to better memory performance

The first aim of this study was to assess whether hippocampal redundancy was related to memory in healthy older adulthood and whether any differences existed due to mnemonic task or

hippocampal subregion. Therefore, performance on three memory tasks were regressed on each of the four hippocampal nodes, controlling for age and sex (Fig. 4.2). Higher left posterior hippocampal redundancy was related to better performance on the PSM (ß = 0.18, p = .011, adjusted R^2 = 0.14), demonstrating a positive relationship between redundancy and contextual episodic memory retrieval. Hippocampal redundancy was not related to learning or immediate recall, which tax verbal item-level encoding and retrieval (Tables 4.2, S4.2-4.4). Results were consistent using robust regression (Table S4.6).

Figure 4.2 | Redundancy-memory relationships across hippocampal ROIs and tasks

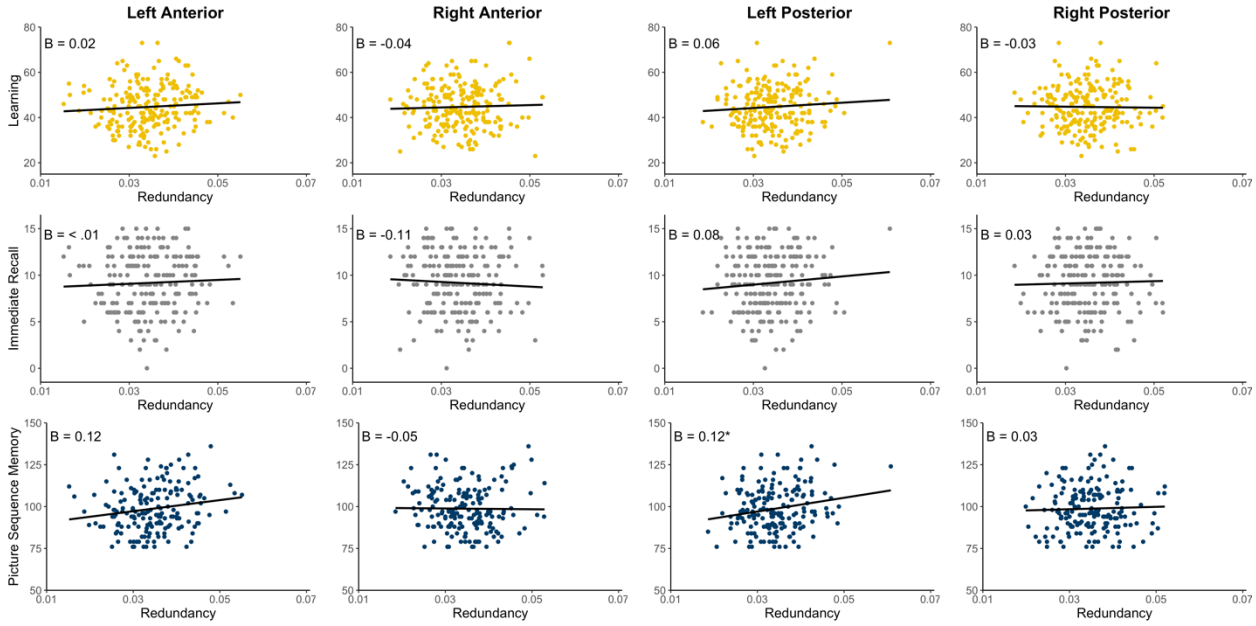

Scatterplot of hippocampal redundancy and RAVLT Learning (top row), RAVLT Immediate Recall (middle row), and PSM (bottom row), with standardized beta weights. * p < .05

To assess whether hippocampal redundancy effects are specific to memory, regressions were repeated using TMT-B completion time as the cognitive outcome measure. Redundancy was not related to TMT-B completion time in any hippocampal node (left anterior: ß = -0.06, p = .336, adjusted R^2 = 0.08; right anterior: ß = 0.01, p = .938, adjusted R^2 = 0.08; left posterior: ß = -0.04, p = .552, adjusted R^2 = 0.08; right posterior: ß = -0.04, p = .526, adjusted R^2 = 0.08; Table S4.5). These results suggest a specific effect on contextual episodic memory performance.

Table 4.2 | Linear regression output between hippocampal redundancy and memory at the averaged density

	Left Anterior		Right Anterior		Left Posterior		Right Posterior	
	ß	*p*	ß	*p*	ß	*p*	ß	*p*
Learning	0.02	.788	-0.04	.564	0.06	.311	-0.03	.680
Recall	-0.004	.955	-0.11	.098	0.08	.220	0.02	.751
PSM	0.12	.091	-0.05	.507	0.18	.011	0.03	.684

Note: Analyses included age and sex as covariates. ß = standardized beta

Redundancy-memory relationship weakens in later older adulthood

To determine whether redundancy relates to cognition similarly throughout older adulthood, we further explored the redundancy-cognition relationship by testing for interactions between redundancy and age (Table S4.7). Given the relationship between left posterior hippocampus and memory in the prior analysis and its prominent role in healthy aging reported in Langella et al. (2021), this analysis was limited to left posterior hippocampal redundancy. Age significantly interacted with left posterior hippocampal redundancy in predicting two of the three memory tasks, immediate recall and PSM, such that with increasing age, the effect of redundancy on memory lessens. For immediate recall performance, there was a negative main effect of age (ß = -0.30, $p < .001$), no main effect of redundancy (ß = 0.07, $p = .312$), and a significant negative age-redundancy interaction (ß = -0.14, $p = .035$). Redundancy-memory slopes were probed at three ages spanning the decades included in this study, representing early older adulthood (65 years), middle older adulthood (75 years), and later older adulthood (85 years). These results indicated that redundancy predicted recall performance only in earlier older adulthood ($p = .022$), but not in middle ($p = .518$) or later older adulthood ($p = .305$). Similar results were observed for PSM (Fig. 4.3). There were significant main effects of age (ß = -0.32, $p < .001$) and redundancy (ß = 0.15, $p = .028$) and a negative interaction (ß = -0.19, $p = .010$).

Redundancy predicted PSM performance in early older adulthood ($p < .001$), but not for middle ($p = .282$) or later older adulthood ($p = .301$). There were no age-redundancy interactions for learning (ß = -0.06, $p = .362$) or for TMT-B performance (ß = -0.01, $p = .934$). Together, these results suggest a specific positive relationship between left posterior hippocampal redundancy and memory performance that weakens across older adulthood.

Figure 4.3 | Redundancy-memory relationships weakens in later older adulthood

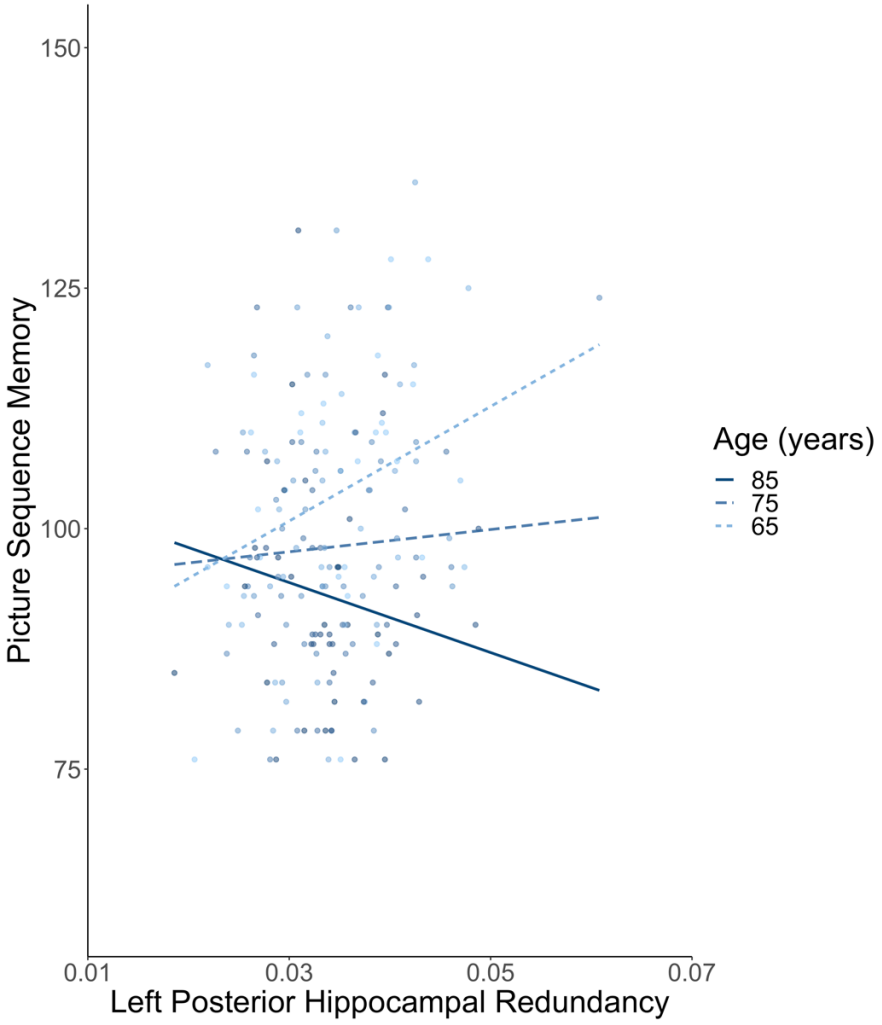

Scatterplot showing Picture Sequence Memory performance as a function of left posterior hippocampal redundancy. Regression lines represent the slope at three ages, chosen to represent early older adulthood (65 years, light blue short dash), middle older adulthood (75 years, medium blue long dash), and later older adulthood (85 years, dark blue solid line).

No relationship between hippocampal redundancy and education or physical activity

Because hippocampal redundancy demonstrates a beneficial effect on memory in aging, we next sought to determine whether certain protective factors may influence hippocampal redundancy. To that end, hippocampal redundancy was regressed on education and recent physical activity. Neither education (left anterior: ß = -0.03, p = .645, adjusted R^2 = 0.01; right anterior: ß = -0.03, p = .678, adjusted R^2 = 0.02; left posterior: ß = 0.09, p = .221, adjusted R^2 = 0.01; right posterior: ß = 0.05, p = .474, adjusted R^2 = 0.01) nor physical activity (left anterior: ß = 0.001, p = .980, adjusted R^2 = 0.01; right anterior: ß = -0.09, p = .210, adjusted R^2 = 0.03; left posterior: ß = -0.02, p = .757, adjusted R^2 = 0.01; right posterior: ß = -0.05, p = .486, adjusted R^2 = 0.01) were related to hippocampal redundancy (Fig. 4.4; Table S4.8-S4.10).

Figure 4.4 | Relationships between hippocampal redundancy and education, physical activity

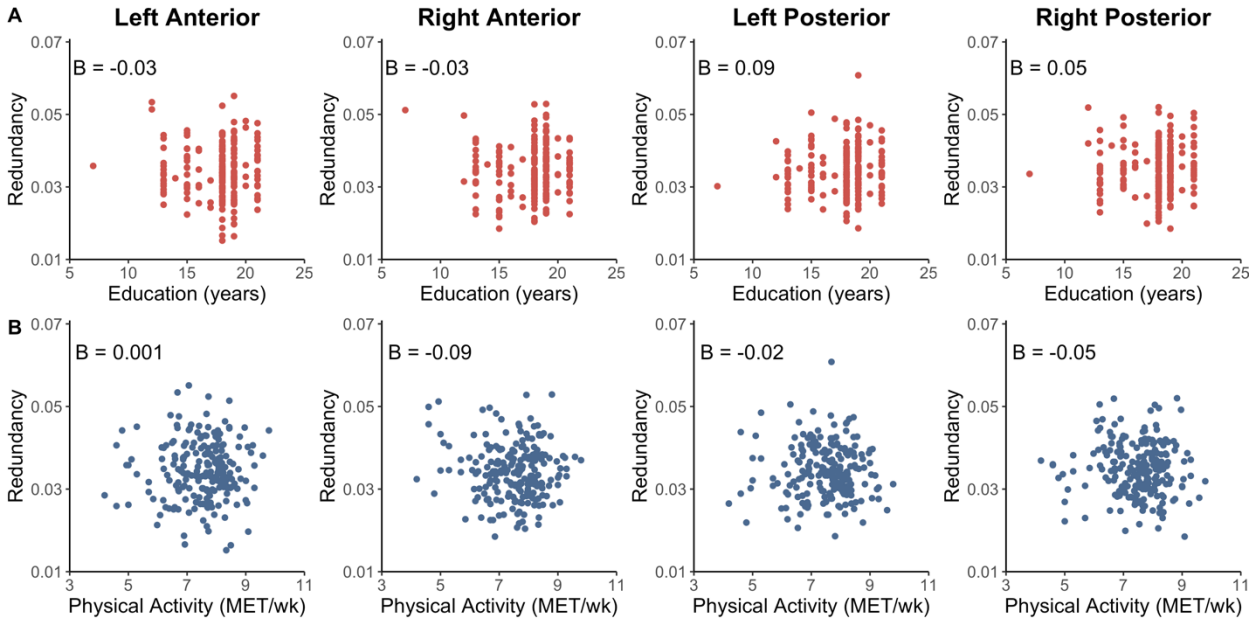

Scatterplots of redundancy for each hippocampal ROI and years of education **(A)** and physical activity **(B)** with standardized beta weights.

Indirect effects between education and physical activity and cognition, through hippocampal redundancy, were tested using multiple mediation. The four hippocampal nodes were tested as joint mediators, and age and sex were included as covariates of no interest. There was no significant mediation effect, by the hippocampal nodes jointly or individually, for any predictor and outcome variable combination (Tables 4.3, 4.4, S4.11-S4.19). Taken together with the regression analyses, we did not find evidence that education or recent physical activity relates to hippocampal redundancy in healthy aging.

Table 4.3 | Multiple mediation indirect effects of education on cognition through redundancy at the averaged density

	Learning		**Recall**		**PSM**		**TMT-B**	
	ß	*p*	ß	*p*	ß	*p*	ß	*p*
Left Anterior	<-0.01	.974	<0.01	.973	<0.01	.963	0.02	.917
Right Anterior	<0.01	.987	<-0.01	.975	<-0.01	.972	0.01	.918
Left Posterior	0.02	.620	0.01	.494	0.07	.466	-0.02	.832
Right Posterior	-0.01	.792	<0.01	.955	0.01	.934	-0.01	.947
Joint	0.01	.850	0.01	.724	0.07	.654	-0.01	.985

Note: Analyses included age and sex as covariates.

Table 4.4 | Multiple mediation indirect effects of physical activity on cognition through redundancy at the averaged density

	Learning		**Recall**		**PSM**		**TMT-B**	
	ß	*p*	ß	*p*	ß	*p*	ß	*p*
Left Anterior	0.01	.878	<0.01	.871	-0.04	.740	-0.01	.980
Right Anterior	0.04	.623	0.03	.551	0.09	.566	-0.09	.758
Left Posterior	-0.01	.890	<-0.01	.902	<-0.01	.985	0.05	.828
Right Posterior	0.02	.792	-0.01	.750	<0.01	.998	0.06	.865
Joint	0.06	.682	0.02	.772	0.05	.877	0.01	.990

Note: Analyses included age and sex as covariates.

Discussion

Utilizing a large sample of healthy older adults spanning 60 to 90 years of age, we adopted a comprehensive approach to examine the role of hippocampal redundancy, education, and physical activity in supporting cognition in older adulthood. This is the first study to probe (1) the relationship between hippocampal redundancy and memory through examining hippocampal subregions and various aspects of episodic memory, and (2) the influence of two widely studied protective factors in cognitive aging. We found evidence that posterior, but not anterior, hippocampal redundancy was related to memory performance in older adulthood. Exploratory analyses indicated that this relationship weakens in later older adulthood. However, we did not find evidence that either education or physical activity were associated with hippocampal redundancy, nor did hippocampal redundancy serve a mediating role between those factors and cognition.

In this sample of healthy older adults, we replicate and extend the finding of a positive association between left posterior hippocampal redundancy and memory performance, suggesting a high degree of specificity to cognitive benefits of regional redundancy. The broadest comparison, between cognitive domains, indicated that redundancy was related to memory but not to executive function, providing evidence that cognitive benefits of increased hippocampal redundancy are specific to the hippocampus' primary function (Eichenbaum, 2017), consistent with prior findings (Langella et al., 2021). Within the memory domain, only PSM was associated with hippocampal redundancy. Whereas RAVLT relies on item-level memory, PSM taps into more complex contextual processes. The specific posterior hippocampus-PSM finding may reflect underlying differences in functional connectivity along the long-axis of the hippocampus: posterior, but not anterior, hippocampus connects with a posterior-medial network

which supports memory for contextual events and episodes (Ranganath & Ritchey, 2012; Ritchey, Libby, & Ranganath, 2015). Therefore, functional redundancy of posterior hippocampus may reflect greater connections with such posterior-medial regions, which in turn supports the contextual memory involved in PSM. In both the current study and in Langella et al. (2021), left posterior hippocampal redundancy specifically was related to memory performance in healthy older adults. This lateralization within posterior nodes may reflect the verbal nature of the memory outcome measures in the studies (e.g., word lists, nameable objects). Encoding and retrieval of such verbal information tends to exhibit left-hippocampal lateralization (Frisk & Milner, 1990; Powell et al., 2005); therefore, greater functional redundancy in left hippocampus may be more beneficial for performance on the measured tasks.

Finally, this positive association between redundancy and memory weakened across older adulthood, becoming non-significant in later decades of life. Although the included participants were all considered to be cognitively healthy, high proportions of non-demented older adults exhibit AD neuropathology, particularly in later decades (Price et al., 2009). If the older group is in fact comprised of a higher proportion of adults with significant pathological build up, redundancy may not be protective for adults in more advanced preclinical stages, as it has previously been shown to not confer benefits in early mild cognitive impairment (Langella et al., 2021). Explicitly measuring pathology across this age range will provide further information about the level at which redundancy ceases to offer protection.

Contrary to our hypotheses, education and physical activity, key protective factors in cognitive aging (Norton et al., 2014), did not show any association with hippocampal redundancy. One potential reason for the lack of relationship with education could be the limited range of educational attainment in this sample. The participants were highly educated, with only

three participants not completing at least a high school-level education, and the vast majority completing a college-level degree or higher. This level of education is higher than in many studies finding evidence of its protective nature (Albert et al., 1995; Butler et al., 1996; reviewed in Meng & D'Arcy, 2012). A second explanation could be a true lack of relationship between education and redundancy. Despite prior findings and models supposing education serves as a reserve mechanism (Cabeza et al., 2018; Meng & D'Arcy, 2012), other findings show no relationship between education and hippocampal volume or cognitive decline (Lövdén, Fratiglioni, Glymour, Lindenberger, & Tucker-Drob, 2020; Nyberg et al., 2021). In fact, a recent review suggests education effects may be better reflected by other factors, such as parental socioeconomic status or underlying cognitive ability (Lövdén et al., 2020). Future studies should investigate both greater ranges of educational attainment and potential underlying, explanatory factors.

Similarly, no effects were observed for physical activity, measured through the IPAQ which reflects recent activity over the last week. It is possible a longer-term measure would be more appropriate for measuring effects on brain organization, as prior positive findings of exercise on neural and cognitive measures have examined activity over the course of a decade (Bugg & Head, 2011; Liang et al., 2010) or from pre- and post-interventions spanning several weeks (Erickson et al., 2011; Ji et al., 2018). Likewise, physical activity during midlife is associated with a reduced risk of dementia in later life (Chang et al., 2010; Rovio et al., 2005; Tolppanen et al., 2015). Repeated and regular physical activity is necessary for the underlying mechanisms through which exercise is deemed to be protective (e.g., neurogenesis, synaptogenesis, neurotransmitter production) (El-Sayes, Harasym, Turco, Locke, & Nelson, 2019; Paillard, 2015). However, in our older adult sample, the IPAQ captures only physical

activity engaged in the prior week, a timeframe which is likely missing the longer-term beneficial impact of physical activity and which does not take into account the consistency of physical activity. In other words, it's possible for an individual with a single highly active day to receive the same score as an individual with several moderately active days, though neither score may be reflective of a typical week. Longer-term measures of physical activity may be likely to reflect consistent exercise habits. Indeed, the length of physical activity appears to influence functional brain network measures, such that certain functional changes in older adults were evident after a year-long exercise intervention program but not after six-months (Voss et al., 2010).

This study includes several limitations. Because the sample is cross-sectional, we are unable to know whether redundancy changes precede cognitive change. Longitudinal lifespan studies will be crucial to elucidate the pattern of redundancy across healthy aging. Additionally, participants were deemed to be cognitively healthy based on scores on activities of daily living and the MoCA. Though commonly used in the field, these clinical assessments do not provide information about potential underlying pathology. It is likely that a portion of included participants are harboring various levels of neuropathology or genetic risk for cognitive impairment. Inclusion of these measures in future studies will enable more accurate characterization of healthy aging separate from preclinical aging.

This is the first study to comprehensively examine the relationship between hippocampal redundancy and cognition in healthy aging, along with the role of education and physical activity. We found that left posterior hippocampal redundancy only is beneficial for memory in healthy older adulthood, suggesting heterogeneity in the hippocampus' subregional functional organization as related to supporting healthy memory function in aging. Additionally, benefits

were specific to memory for contextual object sequencing rather than item-level memory. Finally, we found no evidence that education or recent physical activity are associated with hippocampal redundancy, though future studies should examine alternative measures of these constructs as well as additional protective factors in aging. In sum, this study expands on our current knowledge of hippocampal redundancy across healthy older adulthood while providing clear avenues for future research.

CHAPTER 5: INTEGRATIVE DISCUSSION

Summary

Cognitive aging is marked by considerable variability, ranging from preserved cognition to the development of neurodegenerative diseases, including Alzheimer's disease (AD). Therefore, identifying mechanisms which underlie resilience to pathological aging is important in order to support neural and cognitive functioning across older adulthood. This dissertation aimed to present the initial evidence that hippocampal functional redundancy, as defined through resting-state fMRI networks, is a neuroprotective property within the aging brain that contributes to resilience in cognitive aging. To that end, the presented work focused on the primary cognitive domain, episodic memory, and the primary brain region, hippocampus, affected by AD. Study 1 examined hippocampal redundancy across a spectrum of healthy and pathological aging and its relation to cognitive performance (Langella et al., 2021). Study 2 related hippocampal redundancy to underlying AD pathology (i.e., hippocampal atrophy and beta-amyloid, Aß), along with clinical and cognitive outcomes. Finally, Study 3 examined the influence of experiential protective factors, education and physical activity, on hippocampal redundancy and its relation to memory. Throughout these studies, hippocampal redundancy emerged as a mechanism of resilience to pathological aging through its relationships with cognitive, clinical, and pathological measures. However, its role is heterogeneous across hippocampal subregions and stages of cognitive decline. These findings are discussed below, along with their implications and open questions.

Hippocampal Redundancy Supports Resiliency in Aging

The first evidence indicating a neuroprotective role of hippocampal redundancy in aging is the finding that hippocampal redundancy is lower in pathological aging than in healthy aging, measured both by clinical diagnosis and pathological burden. Study 1 reported the initial comparison, finding that posterior hippocampal redundancy is lower in mild cognitive impairment (MCI) than in cognitively normal (CN) older adults but does not differ between early and late MCI stages (Langella et al., 2021). Whole-hippocampal redundancy, examined in Study 2, similarly was higher in healthy aging than in MCI. Further, low hippocampal redundancy in the combined CN and MCI sample was associated with higher Aß and clinical progression to dementia. Together, these results suggest that the onset of pathological aging is accompanied by reductions in hippocampal redundancy, or that individuals with low hippocampal redundancy are more likely to present clinical symptoms. Conversely, these differences were not apparent in hippocampal degree (Study 1; Langella et al., 2021) or local efficiency (Study 2). This distinction between redundancy and other graph measures is consistent with findings in younger adults (Di Lanzo et al., 2012), suggesting that redundancy is capturing a novel aspect of functional network organization.

Also suggestive of hippocampal redundancy's neuroprotective role in aging is the consistent finding across the three studies that higher redundancy is related to better memory performance. However, these effects are most evident in healthy aging. When examined as separate groups, CN, but not early or late MCI, participants showed a mnemonic benefit of posterior hippocampal redundancy in Study 1 (Langella et al., 2021). Study 3, which only included CN participants, also found this positive relationship, but the benefit of redundancy weakened with advancing age, becoming non-significant in later older adulthood. These two

findings suggest that the beneficial cognitive effects may be most evident in adults with low risk of developing AD, since the risk for developing AD increases with age, and a high proportion of individuals in later older adulthood are likely to harbor more advanced stages of underlying pathology (Price et al., 2009). Earlier older adulthood is generally marked by relatively lower levels of pathology, through which hippocampal redundancy appears able to provide protection against memory failure.

Seemingly in contrast to the healthy aging results in Studies 1 and 3, Study 2 found a positive relationship between hippocampal redundancy and memory in a combined CN-MCI sample. However, the combined CN-MCI sample in Study 1 also showed a significant positive redundancy-memory relationship; only when splitting the groups was it apparent the results were specific to CN participants (Langella et al., 2021). These overall positive combined-group findings may reflect a more nuanced relationship, such that the effect weakens across disease progression, that is not detected when comparing categorical groups. Indeed, the progression of AD follows a continuum (Jack et al., 2013; Jack Jr et al., 2018). Employing continuous markers of disease staging (e.g., neurofibrillary tau, Aß, neurodegeneration, clinical rating scales) rather than categorical groups may reveal a progressive weaking in the redundancy-memory relationship similar to the age-redundancy interaction observed in Study 3.

In addition to differing across clinical stages, the redundancy-memory relationship differed between subregions of the hippocampus. In Studies 1 and 3, group differences and relationships with memory were specific to posterior rather than anterior hippocampal redundancy. This is consistent with the wider literature on hippocampal connectivity in memory and aging. Several prominent functional networks are associated with memory processes and posterior hippocampus more so than anterior hippocampus, including the posterior-medial

network (Ranganath & Ritchey, 2012; Ritchey et al., 2015) and the default mode network (Fanselow & Dong, 2010; Kim, 2015; Seitzman et al., 2020). Additionally, hippocampal and default mode network connectivity is altered along the continuum from healthy aging to MCI and AD (as reviewed in Dennis & Thompson, 2014; Hafkemeijer, van der Grond, & Rombouts, 2012; Sheline & Raichle, 2013). Therefore, the primary findings in posterior, rather than anterior, hippocampal redundancy reflect the more general pattern of functional changes across healthy and pathological aging. These anterior-posterior differences also demonstrate the importance of considering other potential sources of heterogeneity within the hippocampus. Effects of redundancy using other hippocampal divisions, such as anatomical subfields, should be investigated. One particular region, *cornu ammonis* region 1, is early affected by AD pathology and volume loss in MCI (Mueller et al., 2010; Padurariu, Ciobica, Mavroudis, Fotiou, & Stavros, 2012) and may demonstrate a similar role in resilience.

Evidence for a Mechanistic Role

To more concretely assess the role of hippocampal redundancy in resilience to pathological aging, Studies 2 and 3 examined whether hippocampal redundancy served a mechanistic role in preserving cognition. Study 2, focusing on pathological markers, found that low hippocampal redundancy mediated the relationship between low hippocampal volume and low memory. Further, this combination of factors related to a higher likelihood of converting to dementia in subsequent years than the combination of high redundancy, volume, and memory. In accordance with one proposed method to establish a reserve-based mechanism (Stern et al., 2019), this study included a measure of brain status (e.g., hippocampal atrophy and Aß burden), clinical and cognitive performance outcomes (e.g., memory and future clinical diagnosis), and the proposed measure of reserve (e.g., hippocampal redundancy). The mediating role of

hippocampal redundancy suggests that it could act as a reserve mechanism. This would be consistent with a recent lifespan study showing that whole-brain redundancy does in fact follow a reserve-type pattern, building across adulthood before declining in older adulthood (Sadiq et al., 2021).

However, Study 3 found no association with two prominent protective factors (education and physical activity) and redundancy, nor did hippocampal redundancy mediate a relationship between either factor and memory performance. These null results may suggest that redundancy is not experience-dependent, though this area warrants more investigation, as a range of environmental factors do influence brain health and resilience broadly (Karatsoreos & McEwen, 2013; Menardi et al., 2021; Tost, Champagne, & Meyer-Lindenberg, 2015). With respect to this study's included measures, the years of educational attainment in our sample was more limited (biased to higher levels of education) than many prior studies indicating a protective effect of education (reviewed in Meng & D'Arcy, 2012; Stern, Albert, Tang, & Tsai, 1999), and the concurrent measure of physical activity may not reflect longer-term levels of activity. Persistent activity, beginning even in middle age, in particular is related to better outcomes (Chang et al., 2010; Rovio et al., 2005; Tolppanen et al., 2015) and to the molecular and cellular changes accompanying the beneficial cognitive and neural effects (El-Sayes et al., 2019; Paillard, 2015). Therefore, the current findings will need to be explored using alternative measures to uncover whether experience can modify redundancy. Future studies should also consider other methods to investigate redundancy's potential role as a reserve mechanism, including the residual method (Reed et al., 2010), in which the variance unexplained by demographic and structural factors (e.g., age, brain atrophy) is related to the proposed mechanism (e.g., redundancy), as well as additional protective factors.

Limitations and Open Questions

The current work describes a neuroprotective role of hippocampal redundancy in aging as defined through resting-state fMRI networks, with the primary findings demonstrating that hippocampal redundancy is an intrinsic property of functional brain networks that supports healthy memory and clinical function. There are many advantages to resting-state data, including the ease of acquisition in patient populations, consistency across research sites, and representation of such intrinsic patterns of functional organization. However, one limitation for cognitive aging science, and pertinent to the findings discussed here, is that cognitive mechanisms are often inferred based on correlations between resting-state connectivity and behavior at a different time point (see Campbell & Schacter, 2017). Correlations between offline behavioral measures and resting-state derived functional connectivity do not provide direct information about hippocampal functional organization during the memory process itself. Although there are many similarities between resting-state and task-based functional networks (Cole, Bassett, Power, Braver, & Petersen, 2014; Kraus et al., 2021; Krienen, Thomas Yeo, & Buckner, 2014), some researchers point to significant differences between rest and task network organization (Davis, Stanley, Moscovitch, & Cabeza, 2017). It is yet to be determined how hippocampal redundancy differs between resting- and task-states and the associated implications for healthy aging. Online investigation of hippocampal redundancy during episodic memory tasks will be a valuable next step in more closely aligning this functional property with specific mnemonic processes.

Finally, it will be important to examine longitudinal changes in hippocampal redundancy as a function of disease progression to more accurately determine whether redundancy is malleable and decreases in response to AD pathology, or if low redundancy is a risk factor itself

in which low-redundancy brains are unable to cope with increasing pathology. Longitudinal studies have consistently demonstrated reconfiguration of functional brain organization in aging (Malagurski, Liem, Oschwald, Mérillat, & Jäncke, 2020b, 2020a; Ousdal et al., 2020; Rakesh, Fernando, & Mansour L., 2020). Therefore, coupled with the cross-sectional finding that redundancy changes across the lifespan (Sadiq et al., 2021), it is plausible that redundancy is not a static trait, and instead can be affected by pathology or environmental factors. The current work suggests that redundancy may be influenced by pathological factors in particular. As discussed previously, though, the effects of physical activity may be more evident using longitudinal designs, particularly beginning in midlife. Because AD pathology begins to aggregate years before the onset of clinical symptoms (Jack et al., 2013), longitudinal studies, even beginning in middle-age, will be central to connecting changes in functional redundancy with pathological and clinical progression.

Conclusion

Despite a theorized protective role of redundancy in the brain (Arkadir et al., 2014; Creasey & Rapoport, 1985; Glassman, 1987), functional redundancy has largely gone unstudied in the context of aging and neurodegenerative diseases. This dissertation provides the first evidence that hippocampal functional redundancy serves as a neuroprotective mechanism in aging. In particular, hippocampal redundancy is associated with better clinical status and outcomes, higher memory performance, and lower levels of pathology. These beneficial effects are most pronounced in healthy or preclinical aging (before the onset of clinical symptoms) and in posterior hippocampus. Future studies should further probe these relationships using longitudinal designs to closely link memory and pathological changes to redundancy, as well as determine to what extent modifiable factors, such as physical activity, can influence redundancy.

Taken together, this dissertation presents hippocampal functional redundancy as a novel marker of resilience to pathological aging.

APPENDIX A: CHAPTER 2 SUPPLEMENTARY MATERIALS

Supplementary Methods

Overall functional connectivity

Overall levels of functional connectivity were calculated for each of the four hippocampal nodes for each subject using (1) all positive correlations and (2) the absolute value of all network correlations, as underlying differences in connectivity may bias patient group comparisons when using proportional thresholding.

Total volume of white matter hyperintensities

Total volume of white matter hyperintensities were available for 114 subjects through ADNI. Volumes were calculated using a Bayesian approach to segment the T1 and fluid attenuation inversion recovery (FLAIR) MR scan sequences (additional protocol information available through ADNI).

Classification of beta-amyloid positivity

Florbetapir PET imaging was available for 81 of the 91 MCI subjects within 1 year of their resting-state scan. Mean florbetapir uptake was calculated for cortical gray matter and normalized using a cerebellar reference region. Subjects with normalized florbetapir uptake equal to or above 1.11 were classified as amyloid-positive, and those below 1.11 were classified as amyloid-negative (C. M. Clark et al., 2011; Joshi et al., 2012) (additional protocol information available through ADNI). Of the 81 MCI participants with available amyloid-beta PET imaging, 50 were amyloid-positive and 31 were amyloid-negative.

Secondary nodal analysis

We performed a secondary analysis on precuneus, anterior cingulate cortex (ACC), frontal, temporal, and parietal cortical nodes. Analyzed nodes were clustered with either the

default mode network or frontoparietal network. Precuneus consisted of six nodes (three from each hemisphere), and ACC was comprised of four nodes (three left hemisphere, one right hemisphere). Both precuneus and ACC were solely comprised of nodes clustering with the default mode network. Frontal (n = 44), temporal (n = 15), and parietal (n = 18) nodes were clustered with default mode and frontoparietal networks. Redundancy was calculated separately for each node, then averaged across all nodes comprising the anatomical region.

Cognitive composite scores

MEM and EF were calculated using an IRT framework (Crane et al., 2012; Gibbons et al., 2012). MEM incorporated RAVLT (Trials 1-5, Interference, Immediate recall, Delay, Recognition), ADAS-Cog (Trials 1-3, Recall, Recognition), Logical Memory (Immediate, Delay), MMSE (word recall). EF was calculated using: Category Fluency (animals, vegetables), WAIS-R Digit Symbol, Digit Span Backwards, Trails A, Trails B, Clock Drawing. Both MEM and EF have a mean of 0 and standard deviation of 1, with positive scores indicating better performance.

Supplementary Tables

Table S2.1 | Hippocampal redundancy omnibus test statistics across densities (df = 2, 126)

	Left Anterior		**Right Anterior**		**Left Posterior**		**Right Posterior**	
Density	*F*	*p*	*F*	*p*	*F*	*p*	*F*	*p*
2.5	1.02	.373	1.82	.162	4.39	.002	2.15	.119
5	1.13	.337	1.43	.254	6.73	.002	4.49	.008
7.5	1.43	.252	1.03	.358	6.22	.001	5.33	.005
10	1.29	.285	1.33	.270	5.66	.003	4.73	.008
12.5	1.45	.239	2.07	.130	5.37	.004	4.89	.007
15	1.72	.186	2.35	.098	5.36	.004	4.12	.018
17.5	1.50	.225	2.40	.094	5.12	.005	4.20	.015
20	1.49	.232	1.93	.152	4.78	.008	5.00	.008
22.5	1.32	.277	2.10	.126	4.70	.010	5.50	.005
25	1.29	.279	2.04	.130	4.27	.014	5.33	.006

Table S2.2 | Left posterior hippocampal redundancy pairwise comparison's test statistics across densities with FDR adjusted *p* values

	CN-eMCI (df = 1, 91)			CN-lMCI (df = 1, 74)			eMCI-lMCI (df = 1, 88)		
Density	*F*	*p*	Adjusted *p*	*F*	*p*	Adjusted *p*	*F*	*p*	Adjusted *p*
2.5	5.40	.003	.008	3.57	.028	.042	0.02	.894	.894
5	8.25	.003	.008	6.32	.008	.012	0.04	.839	.839
7.5	8.56	.001	.004	5.30	.017	.025	0.04	.841	.841
10	7.93	.002	.007	5.14	.022	.032	0.00	.960	.960
12.5	8.24	.003	.009	4.40	.033	.050	0.27	.604	.604
15	8.02	.004	.011	4.90	.027	.040	0.09	.771	.771
17.5	8.29	.003	.008	4.53	.032	.048	0.21	.648	.648
20	7.94	.006	.017	4.30	.040	.060	0.18	.673	.673
22.5	7.52	.006	.018	4.79	.032	.048	0.05	.827	.827
25	6.99	.009	.026	4.47	.036	.054	0.05	.826	.826

Table S2.3 | Right posterior hippocampal redundancy pairwise comparison's test statistics across densities with FDR adjusted *p* values

	CN-eMCI (df = 1, 91)			CN-lMCI (df = 1, 74)			eMCI-lMCI (df = 1, 88)		
Density	*F*	*p*	Adjusted *p*	*F*	*p*	Adjusted *p*	*F*	*p*	Adjusted *p*
5	6.15	.003	.010	3.12	.063	.095	0.55	.466	.466
7.5	8.11	.002	.006	3.84	.043	.065	0.68	.405	.405
10	7.69	.005	.014	3.78	.054	.081	0.54	.469	.469
12.5	7.76	.005	.015	5.04	.027	.041	0.11	.741	.741
15	6.49	.010	.030	4.85	.026	.039	0.02	.885	.885
17.5	6.78	.010	.031	5.08	.023	.035	0.01	.910	.910
20	8.85	.002	.007	5.52	.024	.036	0.07	.792	.792
22.5	9.54	.002	.006	6.82	.011	.016	0.02	.961	.961
25	9.48	.003	.008	6.64	.011	.016	0.01	.935	.935

Table S2.4 | Mean group nodal ratios for posterior hippocampus (HC) and random node (RN) pairs with associated standard error of the mean (SEM) and *p*-value

	CN:eMCI				CN:lMCI				eMCI:lMCI			
Density	HC mean	RN mean	RN SEM	*p*	HC mean	RN mean	RN SEM	*p*	HC mean	RN mean	RN SEM	*p*
2.5	3.19	1.57	.005	.012	2.89	1.74	.006	.050	0.89	1.21	.004	.824
5	2.38	1.28	.003	.001	2.27	1.38	.003	.018	0.95	1.11	.002	.793
7.5	2.06	1.17	.002	< .001	1.86	1.24	.002	.012	0.90	1.08	.001	.907
10	1.72	1.12	.002	.001	1.61	1.16	.002	.011	0.93	1.05	.001	.861
12.5	1.57	1.09	.001	< .001	1.47	1.13	.001	.014	0.94	1.04	.001	.850
15	1.43	1.07	.001	.001	1.40	1.10	.001	.009	0.98	1.03	.001	.748
17.5	1.37	1.06	.001	.001	1.33	1.08	.001	.011	0.97	1.02	.001	.777
20	1.33	1.05	.001	.001	1.29	1.06	.001	.007	0.97	1.02	.001	.793
22.5	1.28	1.04	.001	< .001	1.27	1.05	.001	.004	0.99	1.01	.001	.682
25	1.25	1.03	.001	< .001	1.24	1.04	.001	.003	0.99	1.01	.000	.697

Table S2.5 | Hippocampal redundancy-MMSE regressions across densities

	Left Anterior		Right Anterior		Left Posterior		Right Posterior	
Density	ß	*p*	ß	*p*	ß	*p*	ß	*p*
Avg.	-0.12	.299	0.11	.341	0.06	.567	0.14	.204
2.5	-0.06	.567	0.09	.390	0.03	.805	0.05	.622
5	-0.03	.804	0.10	.358	0.04	.715	0.07	.502
7.5	-0.02	.849	0.08	.465	0.09	.435	0.05	.675
10	-0.04	.741	0.11	.325	0.09	.440	0.05	.615
12.5	-0.03	.785	0.12	.294	0.07	.555	0.07	.511
15	-0.07	.521	0.11	.319	0.07	.527	0.10	.356
17.5	-0.09	.396	0.11	.335	0.06	.601	0.11	.293
20	-0.14	.204	0.12	.285	0.08	.487	0.13	.236
22.5	-0.13	.219	0.09	.423	0.06	.559	0.15	.177
25	-0.12	.296	0.10	.355	0.05	.632	0.16	.142

Table S2.6 | Hippocampal redundancy-MMSE regressions for averaged density, using robust regression (Huber weighting) and Wald test for significance

	ß	***t***	***p***
Left Anterior	-0.13	1.13	.258
Right Anterior	0.12	1.06	.294
Left Posterior	0.07	0.66	.511
Right Posterior	0.13	1.32	.186

Table S2.7 | Cortical redundancy omnibus test statistics across densities (df = 2, 126)

	Precuneus		ACC		Frontal		Temporal		Parietal	
Density	*F*	*p*	*F*	*p*	*F*	*p*	*F*	*p*	*F*	*p*
Avg.	1.12	.337	0.78	.475	0.20	.821	2.34	.097	0.94	.399
2.5	1.85	.160	0.86	.446	0.42	.670	4.08	.002	0.81	.457
5	1.95	.146	1.06	.354	0.45	.642	4.81	.005	0.85	.434
7.5	1.76	.180	1.13	.329	0.33	.722	4.16	.011	0.99	.376
10	1.53	.219	1.03	.360	0.29	.771	3.69	.022	0.93	.400
12.5	1.35	.272	1.00	.364	0.25	.787	3.19	.039	0.83	.449
15	1.36	.260	0.79	.462	0.21	.829	2.86	.054	0.83	.447
17.5	1.24	.293	0.77	.479	0.19	.841	2.66	.074	0.92	.405
20	1.11	.335	0.83	.440	0.18	.840	2.31	.104	0.99	.379
22.5	1.03	.367	0.70	.499	0.18	.837	2.12	.124	0.97	.378
25	0.90	.413	0.73	.489	0.23	.801	2.06	.127	0.88	.421

Table S2.8 | Temporal node redundancy pairwise comparison's test statistics across densities (with significant omnibus) with FDR adjusted *p* values

	CN-eMCI (df = 1, 91)			CN-lMCI (df = 1, 74)			eMCI-lMCI (df = 1, 88)		
Density	*F*	*p*	Adjusted *p*	*F*	*p*	Adjusted *p*	*F*	*p*	Adjusted *p*
2.5	4.39	.009	.013	3.92	.006	.013	0.63	.429	.429
5	5.41	.009	.014	5.10	.008	.014	0.83	.371	.371
7.5	4.60	.030	.045	4.90	.019	.045	0.93	.322	.322
10	3.84	.048	.071	4.73	.026	.071	1.17	.278	.278
12.5	2.79	.101	.152	4.47	.033	.098	1.66	.209	.209

Table S2.9 | Left posterior hippocampal redundancy-memory regressions across densities with standardized beta and *p* values

	Whole group		CN		eMCI		lMCI	
Density	ß	*p*	ß	*p*	ß	*p*	ß	*p*
2.5	0.29	.001	0.38	.017	0.13	.370	-0.14	.439
5	0.32	< .001	0.37	.022	0.12	.380	-0.01	.971
7.5	0.30	.001	0.33	.043	0.17	.230	-0.05	.784
10	0.30	.001	0.33	.041	0.20	.160	-0.04	.832
12.5	0.29	.001	0.36	.025	0.19	.188	-0.12	.495
15	0.29	.001	0.38	.020	0.16	.258	-0.13	.459
17.5	0.27	.002	0.38	.021	0.18	.210	-0.17	.355
20	0.28	.002	0.39	.017	0.19	.179	-0.14	.442
22.5	0.28	.002	0.37	.024	0.22	.133	-0.15	.400
25	0.28	.002	0.37	.028	0.21	.135	-0.14	.442

Table S2.10 | Right posterior hippocampal redundancy-memory regressions across densities with standardized beta and *p* values

	Whole group		CN		eMCI		lMCI	
Density	ß	*p*	ß	*p*	ß	*p*	ß	*p*
2.5	0.05	.608	0.02	.912	0.07	.608	-0.25	.136
5	0.11	.230	-0.05	.784	0.18	.215	-0.12	.482
7.5	0.10	.279	-0.11	.520	0.19	.173	-0.13	.473
10	0.11	.225	-0.11	.523	0.22	.124	-0.11	.537
12.5	0.16	.078	-0.04	.786	0.25	.071	-0.09	.617
15	0.17	.061	-0.03	.871	0.29	.035	-0.12	.492
17.5	0.17	.055	-0.02	.886	0.32	.022	-0.14	.413
20	0.18	.039	0.02	.904	0.29	.038	-0.12	.498
22.5	0.21	.017	0.02	.894	0.33	.016	-0.11	.541
25	0.23	.009	0.09	.600	0.34	.015	-0.10	.582

Table S2.11 | Left posterior hippocampal redundancy-executive function regressions across densities

	Whole group		CN		eMCI		lMCI	
Density	ß	*p*	ß	*p*	ß	*p*	ß	*p*
2.5	0.13	.142	0.21	.197	0.01	.943	-0.27	.123
5	0.12	.187	0.15	.353	0.05	.700	-0.25	.180
7.5	0.10	.267	0.14	.387	0.06	.678	-0.22	.211
10	0.09	.297	0.14	.403	0.09	.529	-0.24	.172
12.5	0.09	.316	0.18	.271	0.06	.657	-0.28	.119
15	0.08	.359	0.17	.321	0.08	.580	-0.28	.116
17.5	0.08	.369	0.19	.252	0.10	.495	-0.30	.088
20	0.07	.435	0.18	.288	0.09	.554	-0.28	.110
22.5	0.08	.387	0.20	.239	0.10	.492	-0.30	.088
25	0.07	.465	0.18	.288	0.09	.544	-0.28	.108

Table S2.12 | Right posterior hippocampal redundancy-executive function regressions across densities

	Whole group		CN		eMCI		lMCI	
Density	ß	*p*	ß	*p*	ß	*p*	ß	*p*
2.5	-0.11	.234	0.02	.924	-0.15	.269	0.36	.031
5	0.02	.854	0.10	.529	-0.07	.644	-0.33	.054
7.5	0.02	.865	0.11	.495	-0.03	.839	-0.31	.066
10	0.02	.831	0.14	.395	0.01	.946	-0.32	.062
12.5	0.03	.714	0.18	.265	-0.00	.995	-0.32	.062
15	0.03	.762	0.12	.454	0.03	.827	-0.27	.119
17.5	0.03	.720	0.12	.466	0.03	.827	-0.23	.185
20	0.03	.748	0.11	.512	0.03	.838	-0.22	.211
22.5	0.04	.650	0.08	.633	0.07	.615	-0.20	.247
25	0.04	.632	0.06	.732	0.07	.638	-0.16	.353

Table S2.13 | Posterior hippocampal redundancy-cognition regressions for averaged density, using robust regression (Huber weighting) and Wald test for significance

	Left Posterior			Right Posterior		
	ß	*t*	*p*	ß	*t*	*p*
Memory						
Whole group	0.19	3.02	.003	0.14	2.27	.025
CN	0.20	2.08	.043	0.04	0.45	.654
eMCI	0.12	1.42	.161	0.19	2.16	.034
lMCI	-0.12	1.36	.187	-0.11	1.19	.246
Executive Function						
Whole group	0.06	0.70	.485	0.04	0.52	.602
CN	0.13	0.82	.410	0.10	0.62	.532
eMCI	0.08	0.62	.532	0.02	0.19	.849
lMCI	-0.31	1.89	.069	-0.19	1.13	.269

Table S2.14 | Hippocampal degree omnibus test statistics across densities (df = 2, 126)

	Left Anterior		Right Anterior		Left Posterior		Right Posterior	
Density	*F*	*p*	*F*	*p*	*F*	*p*	*F*	*p*
2.5	0.21	.820	0.43	.656	1.87	.155	0.42	.663
5	0.01	.994	0.49	.618	1.97	.145	0.72	.497
7.5	0.30	.741	0.38	.680	3.07	.046	1.33	.269
10	0.93	.401	0.68	.513	2.83	.060	1.18	.316
12.5	1.14	.335	0.74	.483	2.53	.083	0.65	.532
15	1.70	.183	0.89	.428	2.70	.073	0.39	.670
17.5	1.32	.268	0.90	.409	2.75	.065	0.55	.576
20	0.93	.403	0.67	.503	2.42	.087	1.00	.375
22.5	0.82	.439	0.78	.462	2.45	.086	1.33	.264
25	1.18	.306	0.85	.429	2.18	.115	1.60	.204

Note: Follow-up tests of left posterior degree at density 7.5 revealed no significant group differences after correcting for multiple comparisons [CN-eMCI: $F(1, 91) = 5.49$, $p = .061$; CN-lMCI: $F(1, 74) = 2.45$, $p = .175$; eMCI-lMCI: $F(1, 88) = 0.25$, $p = .623$].

Table S2.15 | Hippocampal redundancy-white matter hyperintensities regressions for averaged density, using robust regression (Huber weighting) and Wald test for significance

	ß	*t*	*p*
Left Anterior	-0.003	0.03	.977
Right Anterior	0.177	1.65	.100
Left Posterior	0.003	0.04	.964
Right Posterior	0.079	0.92	.357

Table S2.16 | Hippocampal redundancy-global efficiency regressions across densities collapsed across group

	Left Anterior		**Right Anterior**		**Left Posterior**		**Right Posterior**	
Density	ß	*p*	ß	*p*	ß	*p*	ß	*p*
2.5	-0.03	.736	-0.02	.859	0.06	.523	0.14	.123
5	-0.09	.285	-0.08	.369	0.07	.423	0.04	.657
7.5	-0.11	.231	-0.05	.603	0.04	.652	0.11	.205
10	-0.13	.150	-0.11	.234	0.08	.385	0.16	.067
12.5	-0.16	.071	-0.12	.182	0.07	.424	0.11	.195
15	-0.20	.024	-0.12	.192	0.05	.547	0.11	.219
17.5	-0.20	.024	-0.11	.210	0.04	.646	0.05	.542
20	-0.18	.035	-0.08	.383	0.04	.640	0.02	.823
22.5	-0.16	.071	-0.06	.507	0.00	.996	-0.05	.591
25	-0.11	.215	-0.02	.817	-0.03	.768	-0.11	.213

Table S2.17 | Hippocampal redundancy-global efficiency regressions across densities within CN group

	Left Anterior		**Right Anterior**		**Left Posterior**		**Right Posterior**	
Density	ß	*p*	ß	*p*	ß	*p*	ß	*p*
Avg.	-0.25	.127	0.13	.414	-0.10	.530	-0.19	.259
2.5	0.02	.899	0.28	.068	0.03	.835	-0.07	.643
5	0.02	.911	0.17	.282	-0.03	.838	-0.17	.275
7.5	-0.02	.904	0.30	.056	-0.12	.437	-0.12	.433
10	-0.04	.815	0.20	.219	-0.10	.525	-0.08	.617
12.5	-0.14	.391	0.11	.497	-0.10	.509	-0.14	.394
15	-0.22	.196	0.09	.594	-0.13	.418	-0.13	.406
17.5	-0.28	.098	0.10	.530	-0.17	.293	-0.20	.193
20	-0.26	.125	0.14	.373	-0.18	.243	-0.28	.070
22.5	-0.22	.189	0.15	.360	-0.23	.137	-0.39	.011
25	-0.14	.418	0.20	.223	-0.25	.113	-0.43	.004

Table S2.18 | Hippocampal redundancy-global efficiency regressions across densities within eMCI group

	Left Anterior		Right Anterior		Left Posterior		Right Posterior	
Density	ß	*p*	ß	*p*	ß	*p*	ß	*p*
Avg.	-0.11	.431	-0.11	.429	0.32	.019	0.14	.306
2.5	-0.01	.922	-0.23	.102	0.33	.018	0.26	.058
5	-0.10	.496	-0.25	.081	0.41	.003	0.31	.027
7.5	-0.12	.396	-0.21	.132	0.37	.007	0.32	.022
10	-0.18	.211	-0.27	.050	0.32	.020	0.28	.044
12.5	-0.18	.215	-0.28	.046	0.29	.037	0.22	.124
15	-0.20	.168	-0.27	.056	0.25	.068	0.18	.207
17.5	-0.17	.260	-0.26	.067	0.27	.051	0.14	.340
20	-0.15	.296	-0.20	.161	0.30	.034	0.12	.396
22.5	-0.14	.357	-0.18	.219	0.26	.061	0.09	.535
25	-0.06	.671	-0.14	.325	0.26	.060	0.06	.679

Table S2.19 | Hippocampal redundancy-global efficiency regressions across densities within lMCI group

	Left Anterior		Right Anterior		Left Posterior		Right Posterior	
Density	ß	*p*	ß	*p*	ß	*p*	ß	*p*
Avg.	0.17	.328	-0.10	.538	0.05	.763	0.25	.132
2.5	0.16	.402	-0.09	.612	0.04	.808	0.29	.105
5	-0.08	.673	-0.06	.729	0.12	.493	0.26	.142
7.5	0.03	.861	-0.07	.664	0.05	.797	0.23	.190
10	0.07	.697	-0.12	.497	0.06	.747	0.25	.146
12.5	0.14	.416	-0.10	.570	0.05	.777	0.25	.153
15	0.17	.349	-0.08	.660	0.06	.734	0.31	.077
17.5	0.20	.263	-0.08	.643	0.06	.726	0.29	.100
20	0.20	.252	-0.08	.663	0.13	.461	0.30	.085
22.5	0.24	.167	-0.01	.942	0.13	.451	0.28	.106
25	0.23	.190	0.00	.991	0.15	.387	0.26	.138

Table S2.20 | Hippocampal redundancy-global efficiency regressions for averaged density, using robust regression (Huber weighting) and Wald test for significance

	Left Anterior			Right Anterior			Left Posterior			Right Posterior		
	ß	*t*	*p*	ß	*t*	*p*	ß	*t*	*p*	ß	*t*	*p*
Whole group	-0.16	1.89	.064	-0.10	1.17	.256	0.12	1.39	.208	0.07	0.84	.418
CN	-0.28	1.72	.091	0.05	0.33	.755	-0.15	0.95	.346	-0.26	1.62	.112
eMCI	-0.07	0.47	.641	-0.13	0.92	.378	0.32	2.37	.021	0.16	1.19	.233
lMCI	0.14	1.10	.276	-0.12	0.90	.364	-0.06	0.48	.637	0.17	1.30	.202

Supplementary Figures

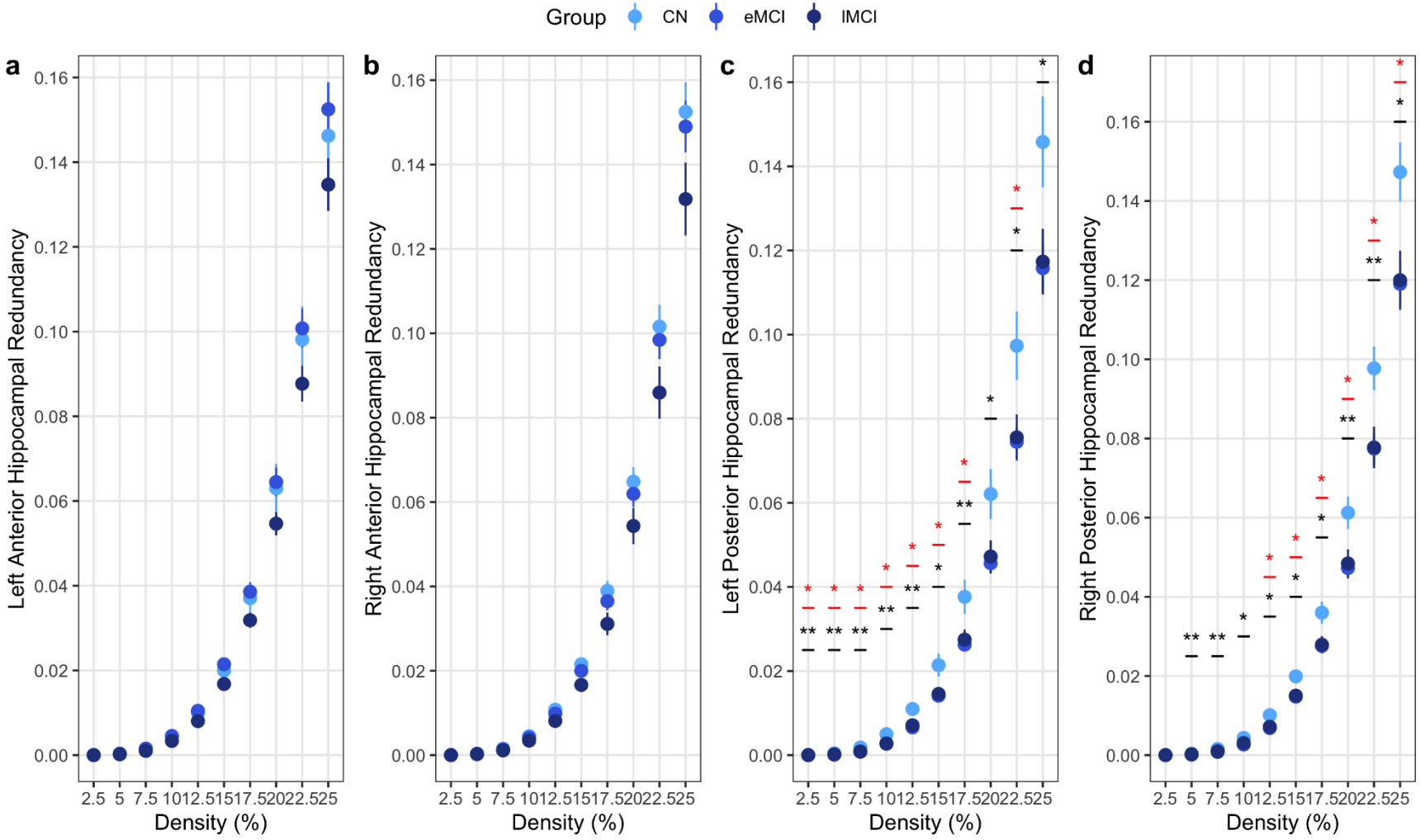

Figure S2.1 | Whole-brain hippocampal redundancy across densities. *$p < .05$, **$p < .01$. CN-eMCI comparison in black, CN-lMCI comparison in red.

Figure S2.2 | CN:eMCI nodal ratios across densities

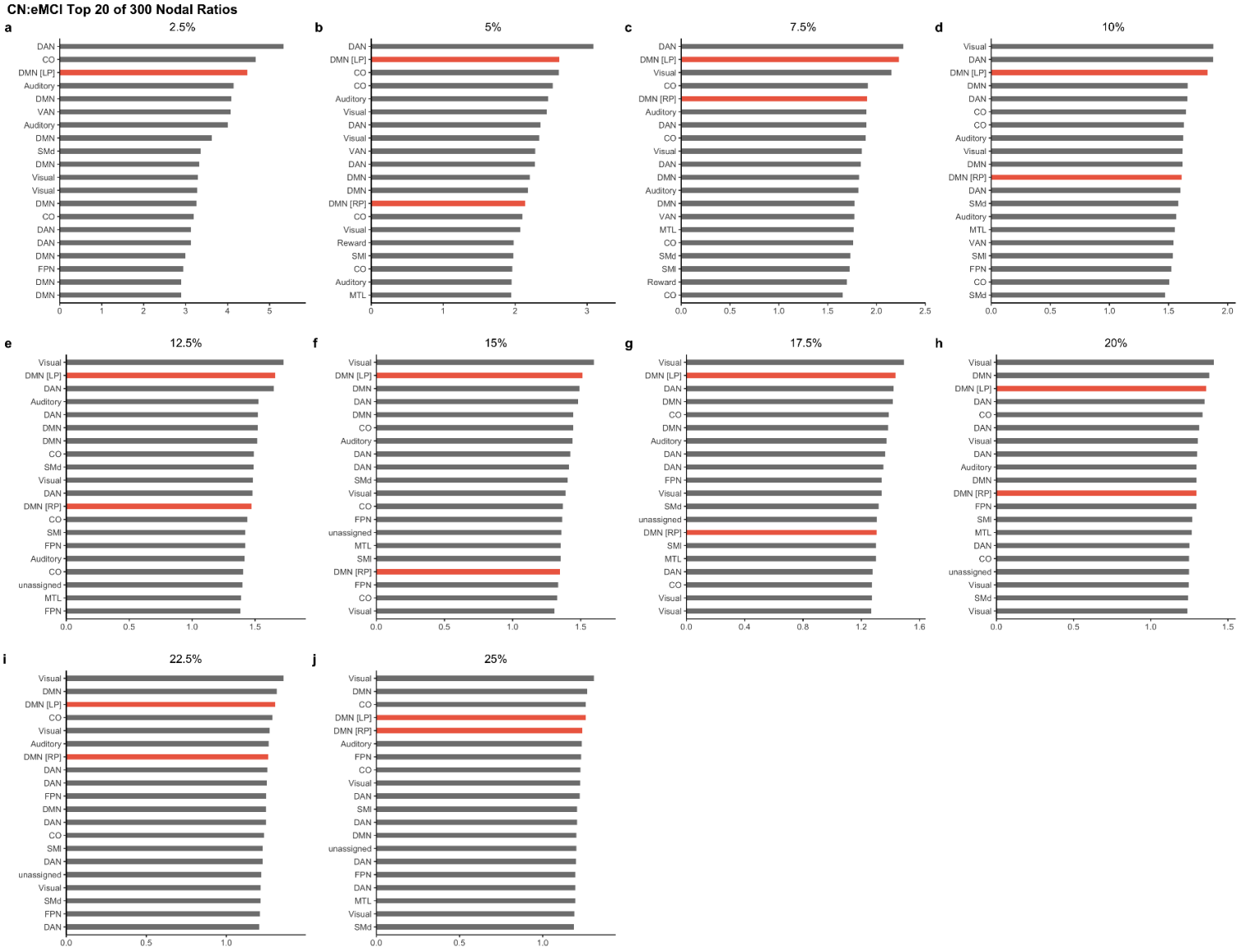

Posterior hippocampal nodes in peach.

Figure S3.3 | CN:lMCI nodal ratios across densities

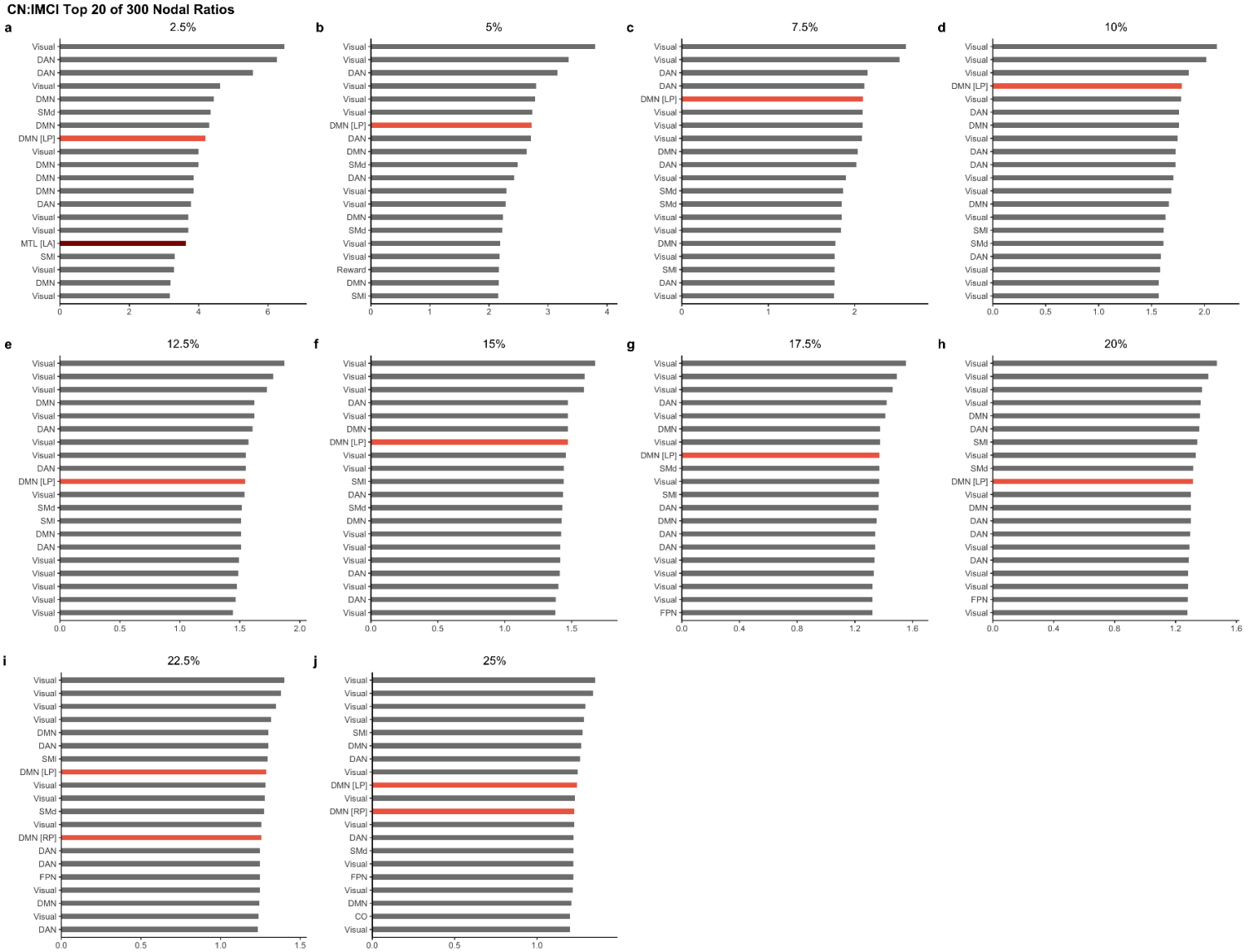

Posterior hippocampal nodes in peach, anterior hippocampal nodes in dark red.

Figure S2.4 | eMCI:lMCI nodal ratios across densities

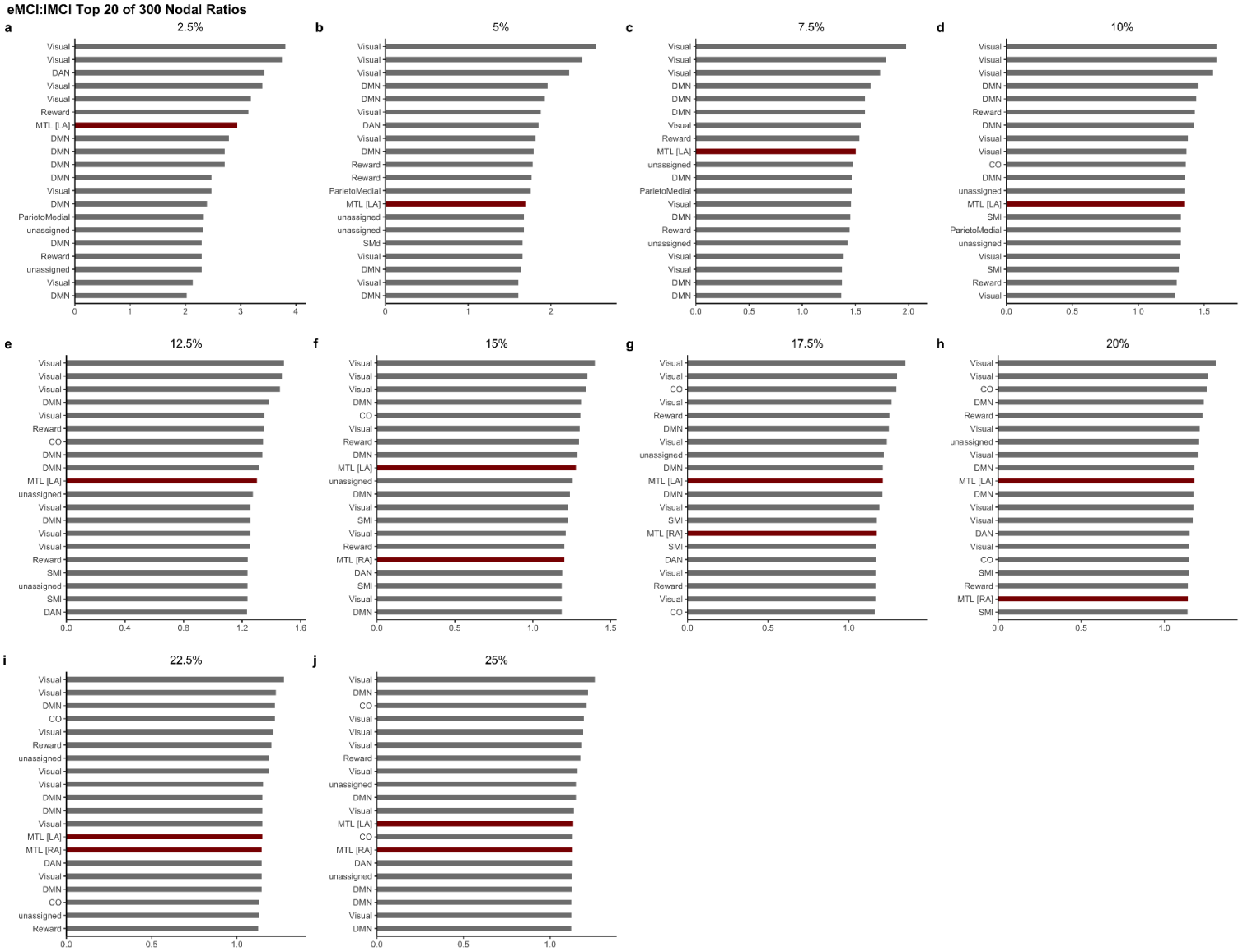

Anterior hippocampal nodes in dark red.

Figure S2.5 | Scatterplots showing hippocampal redundancy-MMSE relationship in MCI subjects

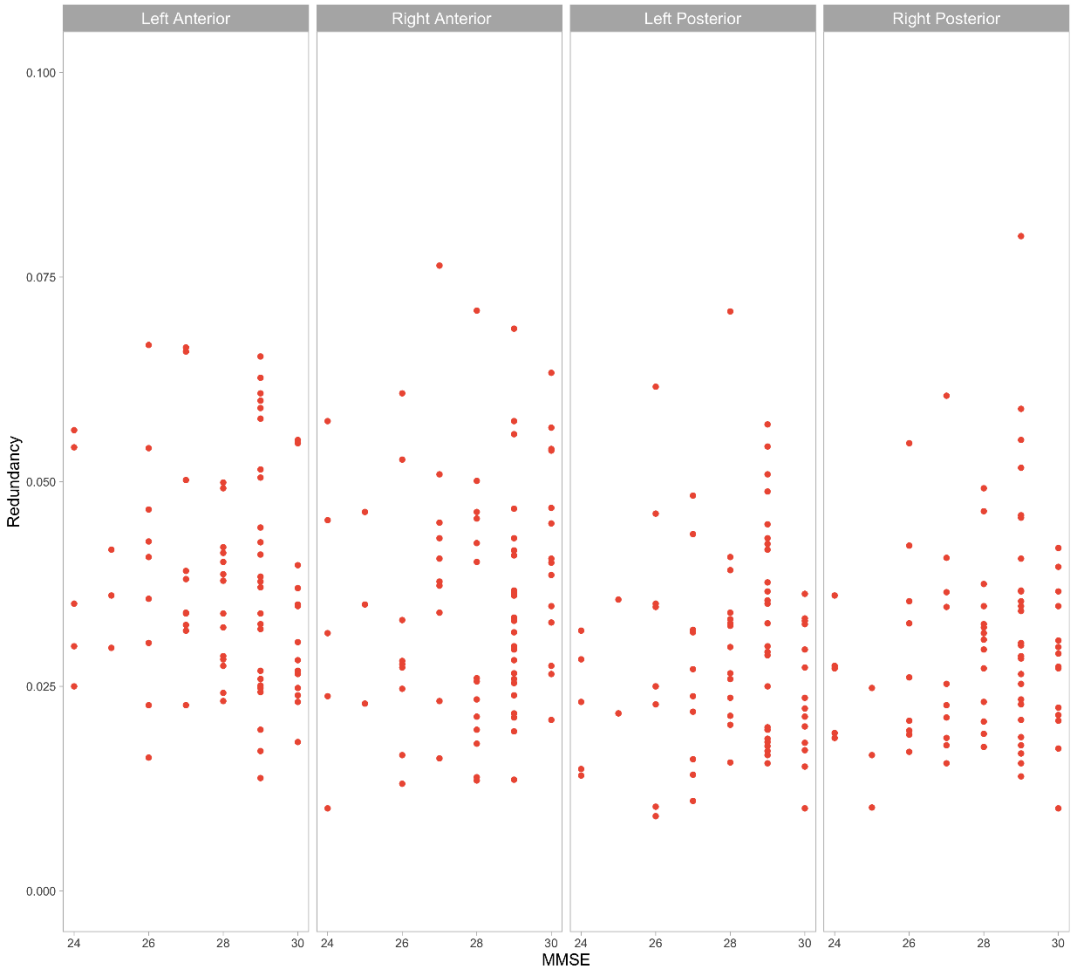

Figure S2.6 | Precuneus and anterior cingulate cortex (ACC) redundancy group difference comparisons

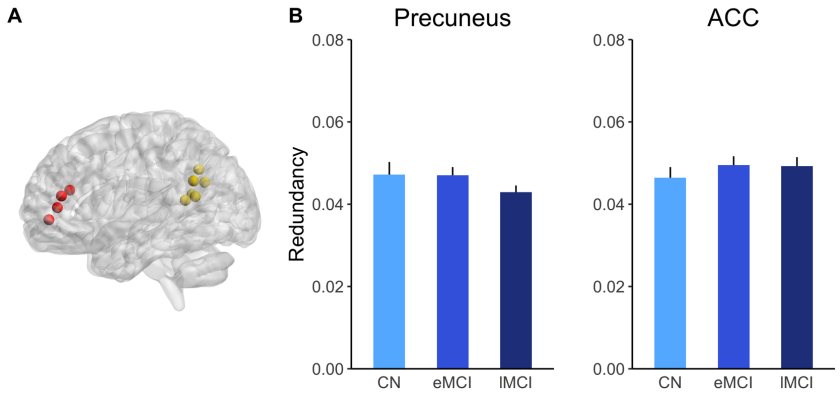

A. Precuneus nodes in yellow, ACC nodes in red. **B.** Group means with standard error bars representing one standard error of the mean.

Figure S2.7 | Within-group scatterplots of hippocampal redundancy-cognition relationships

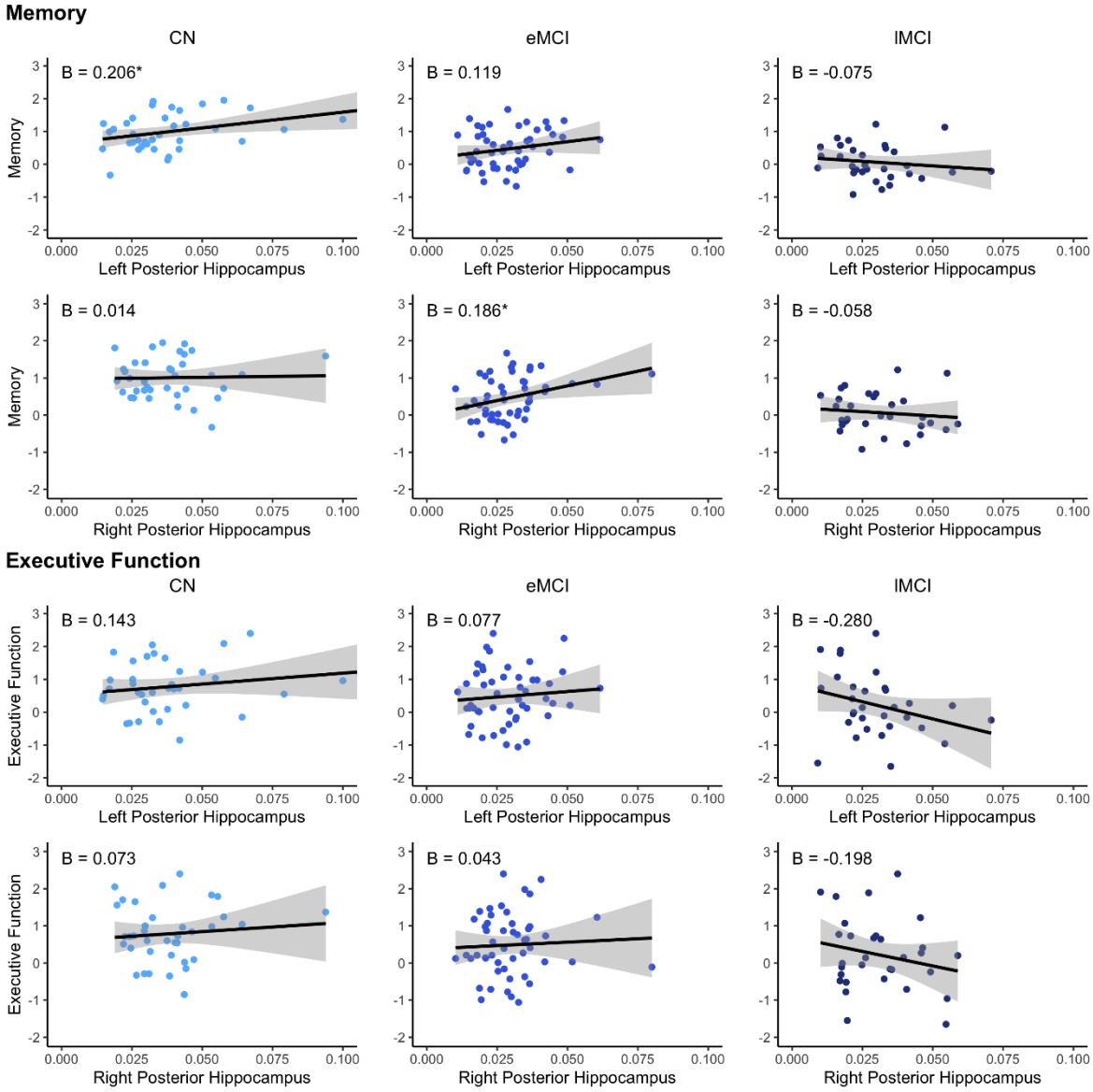

APPENDIX B: CHAPTER 3 SUPPLEMENTARY MATERIALS

Supplementary Methods

Overall functional connectivity

Because underlying group connectivity differences may bias comparisons when using proportional thresholding (van den Heuvel et al., 2017), overall functional connectivity was calculated from the correlation matrix for the hippocampal ROI for each subject using all positive correlations and the absolute value of all network correlations. CN and MCI groups did not differ in hippocampal connectivity, controlling for age, sex, and education [positive correlations: $F(1, 97) = 1.36$, $p = .247$; absolute value: $F(1, 97) = 0.16$, $p = .689$].

White matter hyperintensities

Total volume of white matter hyperintensities, calculated using a Bayesian approach to segment the T1 and fluid attenuation inversion recovery MR scan sequences, were available through ADNI. Full protocol information is available through ADNI. Total volume of white matter hyperintensities was not related to either redundancy (whole-group: ß = 0.06, $p = .561$; MCI only: ß = 0.15, $p = .186$) or local efficiency (whole-group: ß = -0.09, $p = .363$; MCI only: -0.07, $p = .563$).

Cognitive composite scores

The memory composite score was calculated using RAVLT (Trials 1-5, Interference, Immediate recall, Delay, Recognition), ADAS-Cog (Trials 1-3, Recall, Recognition), Logical Memory (Immediate, Delay), and MMSE (word recall) (Crane et al., 2012). The EF composite was calculated using Category Fluency (animals, vegetables), WAIS-R Digit Symbol, Digit Span Backwards, Trails A, Trails B, and Clock Drawing (Gibbons et al., 2012).

Supplementary Tables

Table S3.1 | Test statistics from permutation ANCOVA comparing hippocampal topological network properties between CN and MCI groups across all densities (df = 1, 97)

	Redundancy		Local efficiency	
Density	*F*	*p*	*F*	*p*
2.5	8.00	.007	0.17	.687
5	10.17	.002	0.36	.541
7.5	10.29	.002	0.58	.459
10	8.57	.005	0.04	.845
12.5	8.51	.004	0.01	.923
15	7.77	.004	0.07	.796
17.5	8.03	.007	0.82	.371
20	7.56	.007	0.76	.384
22.5	7.41	.008	0.72	.402
25	6.38	.012	0.72	.396

Table S3.2 | Hippocampal redundancy-local efficiency linear regression output (standardized beta and p-value) across densities in the whole sample and in MCI only

	Whole sample		MCI only	
Density	ß	*p*	ß	*p*
2.5	0.20	.055	0.10	.386
5	0.38	<.001	0.39	.001
7.5	0.52	<.001	0.53	<.001
10	0.45	<.001	0.48	<.001
12.5	0.45	<.001	0.48	<.001
15	0.44	<.001	0.42	<.001
17.5	0.45	<.001	0.41	<.001
20	0.44	<.001	0.40	.001
22.5	0.44	<.001	0.38	.001
25	0.39	<.001	0.32	.006

Table S3.3 | Hippocampal volume-redundancy linear regression output (standardized beta and *p*-value) across densities in the whole sample and in MCI only

	Whole sample		MCI only	
Density	ß	*p*	ß	*p*
2.5	0.24	.043	0.34	.019
5	0.38	.001	0.44	.002
7.5	0.37	.002	0.41	.004
10	0.37	.002	0.41	.004
12.5	0.33	.005	0.38	.007
15	0.29	.015	0.33	.019
17.5	0.26	.028	0.29	.046
20	0.26	.031	0.28	.052
22.5	0.26	.027	0.28	.049
25	0.26	.031	0.27	.056

Table S3.4 | Hippocampal redundancy-memory linear regression output (standardized beta and *p*-value) across densities in the whole sample and in MCI only

	Whole sample		MCI only	
Density	ß	*p*	ß	*p*
2.5	0.26	.005	0.13	.234
5	0.26	.004	0.22	.040
7.5	0.29	.001	0.26	.013
10	0.31	.001	0.29	.005
12.5	0.33	<.001	0.32	.002
15	0.34	<.001	0.33	.002
17.5	0.34	<.001	0.31	.003
20	0.33	<.001	0.30	.005
22.5	0.34	<.001	0.32	.002
25	0.34	<.001	0.31	.003

Table S3.5 | Hippocampal redundancy-executive function linear regression output (standardized beta and *p*-value) across densities in the whole sample and in MCI only

	Whole sample		MCI only	
Density	ß	*p*	ß	*p*
2.5	0.17	.057	0.05	.611
5	0.19	.030	0.09	.376
7.5	0.18	.049	0.09	.356
10	0.18	.046	0.10	.305
12.5	0.18	.049	0.09	.375
15	0.18	.046	0.11	.306
17.5	0.17	.050	0.10	.337
20	0.17	.062	0.10	.346
22.5	0.18	.047	0.12	.255
25	0.17	.064	0.12	.254

Table S3.6 | Hippocampal volume-local efficiency linear regression output (standardized beta and *p*-value) across densities in the whole sample and in MCI only

	Whole sample		MCI only	
Density	ß	*p*	ß	*p*
2.5	0.10	.404	0.15	.303
5	0.23	.055	0.31	.029
7.5	0.17	.152	0.24	.098
10	0.24	.040	0.33	.021
12.5	0.28	.017	0.36	.012
15	0.19	.111	0.30	.033
17.5	0.26	.026	0.35	.014
20	0.25	.034	0.32	.024
22.5	0.23	.050	0.28	.048
25	0.21	.073	0.28	.053

Table S3.7 | Hippocampal local efficiency-memory linear regression output (standardized beta and *p*-value) across densities in the whole sample and in MCI only

	Whole sample		MCI only	
Density	ß	*p*	ß	*p*
2.5	0.08	.395	0.08	.459
5	0.08	.417	-0.01	.941
7.5	0.12	.212	0.09	.385
10	0.08	.390	0.10	.352
12.5	0.04	.640	0.02	.852
15	0.07	.426	0.07	.523
17.5	0.17	.075	0.15	.149
20	0.17	.072	0.17	.117
22.5	0.15	.098	0.17	.104
25	0.16	.084	0.21	.049

Table S3.8 | Hippocampal local efficiency-executive function linear regression output (standardized beta and *p*-value) across densities in the whole sample and in MCI only

	Whole sample		MCI only	
Density	ß	*p*	ß	*p*
2.5	0.01	.901	-0.02	.853
5	0.02	.842	-0.04	.730
7.5	0.04	.652	-0.02	.813
10	0.04	.634	0.01	.902
12.5	0.00	.991	-0.06	.534
15	0.05	.558	0.01	.927
17.5	0.13	.142	0.07	.505
20	0.12	.188	0.06	.552
22.5	0.12	.193	0.04	.669
25	0.12	.172	0.06	.568

Table S3.9 | Mediation output (beta, 95% CI, *p*-value) from hippocampal volume-redundancy-memory model in the whole sample and in MCI only

Whole sample								
	Indirect Effect				Direct Effect			
Density	ß	Lower bound	Upper bound	*p*	ß	Lower bound	Upper bound	*p*
2.5	$8.38x10^{-5}$	$-9.54x10^{-6}$	$1.74x10^{-4}$	.087	$5.80x10^{-4}$	$2.37x10^{-4}$	$9.78x10^{-4}$	.001
5	$1.19x10^{-4}$	$-1.41x10^{-5}$	$2.67x10^{-4}$	.083	$5.45x10^{-4}$	$1.83x10^{-4}$	$9.47x10^{-4}$	.003
7.5	$1.37x10^{-4}$	$1.77x10^{-5}$	$3.11x10^{-4}$	.017	$5.26x10^{-4}$	$1.57x10^{-4}$	$9.21x10^{-4}$	.004
10	$1.49x10^{-4}$	$3.14x10^{-5}$	$3.13x10^{-4}$	.007	$5.14x10^{-4}$	$1.44x10^{-4}$	$9.10x10^{-4}$	.008
12.5	$1.51x10^{-4}$	$3.90x10^{-5}$	$3.11x10^{-4}$	.003	$5.13x10^{-4}$	$1.57x10^{-4}$	$9.02x10^{-4}$	.004
15	$1.40x10^{-4}$	$2.89x10^{-5}$	$2.93x10^{-4}$	.009	$5.23x10^{-4}$	$1.64x10^{-4}$	$9.13x10^{-4}$	.002
17.5	$1.28x10^{-4}$	$2.01x10^{-5}$	$2.73x10^{-4}$	.016	$5.35x10^{-4}$	$1.80x10^{-4}$	$9.30x10^{-4}$	.003
20	$1.21x10^{-4}$	$1.82x10^{-5}$	$2.64x10^{-4}$	.017	$5.42x10^{-4}$	$1.92x10^{-4}$	$9.27x10^{-4}$	.002
22.5	$1.29x10^{-4}$	$2.11x10^{-5}$	$2.71x10^{-4}$	.015	$5.35x10^{-4}$	$1.82x10^{-4}$	$9.14x10^{-4}$	.002
25	$1.25x10^{-4}$	$2.01x10^{-5}$	$2.70x10^{-4}$	.017	$5.38x10^{-4}$	$1.90x10^{-4}$	$9.16x10^{-4}$	.002
MCI only								
	Indirect Effect				Direct Effect			
Density	ß	Lower bound	Upper bound	*p*	ß	Lower bound	Upper bound	*p*
2.5	$1.58x10^{-5}$	$-9.56x10^{-5}$	$1.49x10^{-4}$	.732	$6.26x10^{-4}$	$2.90x10^{-4}$	$1.00x10^{-3}$	<.001
5	$6.69x10^{-5}$	$-6.69x10^{-5}$	$2.79x10^{-4}$	.312	$5.75x10^{-4}$	$1.94x10^{-4}$	$9.53x10^{-4}$	.003
7.5	$9.82x10^{-5}$	$-2.09x10^{-5}$	$3.17x10^{-4}$	.129	$5.44x10^{-4}$	$1.61x10^{-4}$	$9.30x10^{-4}$	.008
10	$1.19x10^{-4}$	$-4.91x10^{-6}$	$3.27x10^{-4}$	.064	$5.23x10^{-4}$	$1.50x10^{-4}$	$9.09x10^{-4}$	.007
12.5	$1.34x10^{-4}$	$9.57x10^{-6}$	$3.46x10^{-4}$	.025	$5.08x10^{-4}$	$1.40x10^{-4}$	$8.90x10^{-4}$	.007
15	$1.24x10^{-4}$	$9.09x10^{-6}$	$3.25x10^{-4}$	.027	$5.18x10^{-4}$	$1.43x10^{-4}$	$9.06x10^{-4}$	.007
17.5	$1.04x10^{-4}$	$6.10x10^{-7}$	$2.90x10^{-4}$	.047	$5.38x10^{-4}$	$1.67x10^{-4}$	$9.24x10^{-4}$	.004
20	$9.39x10^{-5}$	$-9.79x10^{-7}$	$2.76x10^{-4}$	.058	$5.48x10^{-4}$	$1.77x10^{-4}$	$9.39x10^{-4}$	.002
22.5	$1.04x10^{-4}$	$9.59x10^{-7}$	$2.86x10^{-4}$	.047	$5.38x10^{-4}$	$1.76x10^{-4}$	$9.29x10^{-4}$	.003
25	$1.01x10^{-4}$	$-3.88x10^{-7}$	$2.79x10^{-4}$	.053	$5.41x10^{-4}$	$1.81x10^{-4}$	$9.26x10^{-4}$	.003

Table S3.10 | Mediation output (beta, 95% CI, *p*-value) from hippocampal volume-redundancy-executive function model in the whole sample and in MCI only

Whole sample								
	Indirect Effect				Direct Effect			
Density	ß	Lower bound	Upper bound	*p*	ß	Lower bound	Upper bound	*p*
2.5	$8.45x10^{-5}$	$-4.11x10^{-5}$	$2.13x10^{-4}$	.183	$3.30x10^{-4}$	$-1.09x10^{-4}$	$8.18x10^{-4}$	.139
5	$1.50x10^{-4}$	$-1.51x10^{-5}$	$3.39x10^{-4}$	.079	$2.64x10^{-4}$	$-1.98x10^{-4}$	$7.86x10^{-4}$	.265
7.5	$1.28x10^{-4}$	$-2.54x10^{-5}$	$3.29x10^{-4}$	.107	$2.87x10^{-4}$	$-1.97x10^{-4}$	$7.87x10^{-4}$	.241
10	$1.30x10^{-4}$	$-1.92x10^{-5}$	$3.35x10^{-4}$	.088	$2.85x10^{-4}$	$-2.11x10^{-4}$	$7.88x10^{-4}$	.254
12.5	$1.15x10^{-4}$	$-1.79x10^{-5}$	$3.15x10^{-4}$	.100	$3.00x10^{-4}$	$-1.85x10^{-4}$	$7.94x10^{-4}$	.225
15	$1.05x10^{-4}$	$-1.38x10^{-5}$	$2.99x10^{-4}$	.097	$3.09x10^{-4}$	$-1.61x10^{-4}$	$7.88x10^{-4}$	.199
17.5	$9.37x10^{-5}$	$-1.62x10^{-5}$	$2.68x10^{-4}$	.111	$3.21x10^{-4}$	$-1.50x10^{-4}$	$8.07x10^{-4}$	.176
20	$8.71x10^{-5}$	$-1.97x10^{-5}$	$2.60x10^{-4}$	.139	$3.28x10^{-4}$	$-1.38x10^{-4}$	$8.11x10^{-4}$	.160
22.5	$9.63x10^{-5}$	$-1.69x10^{-5}$	$2.75x10^{-4}$	.111	$3.18x10^{-4}$	$-1.56x10^{-4}$	$8.04x10^{-4}$	.180
25	$8.66x10^{-5}$	$-2.31x10^{-5}$	$2.61x10^{-4}$	.145	$3.28x10^{-4}$	$-1.30x10^{-4}$	$8.08x10^{-4}$	.158
MCI only								
	Indirect Effect				Direct Effect			
Density	ß	Lower bound	Upper bound	*p*	ß	Lower bound	Upper bound	*p*
2.5	$1.81x10^{-5}$	$-2.14x10^{-4}$	$1.71x10^{-4}$	.887	$2.97x10^{-4}$	$-2.31x10^{-4}$	$8.78x10^{-4}$	.262
5	$5.92x10^{-5}$	$-1.67x10^{-4}$	$2.86x10^{-4}$	.565	$2.56x10^{-4}$	$-3.03x10^{-4}$	$8.37x10^{-4}$	.371
7.5	$6.14x10^{-5}$	$-1.21x10^{-4}$	$3.08x10^{-4}$	.527	$2.53x10^{-4}$	$-3.40x10^{-4}$	$8.09x10^{-4}$	.382
10	$7.18x10^{-5}$	$-9.98x10^{-5}$	$3.42x10^{-4}$	.451	$2.43x10^{-4}$	$-3.37x10^{-4}$	$7.78x10^{-4}$	.390
12.5	$5.51x10^{-5}$	$-1.16x10^{-4}$	$3.25x10^{-4}$	.561	$2.60x10^{-4}$	$-3.25x10^{-4}$	$8.12x10^{-4}$	.371
15	$6.26x10^{-5}$	$-7.84x10^{-5}$	$3.12x10^{-4}$	.432	$2.52x10^{-4}$	$-3.12x10^{-4}$	$7.78x10^{-4}$	.393
17.5	$5.09x10^{-5}$	$-7.65x10^{-5}$	$2.75x10^{-4}$	.483	$2.64x10^{-4}$	$-2.87x10^{-4}$	$7.77x10^{-4}$	.341
20	$4.87x10^{-5}$	$-7.99x10^{-5}$	$2.85x10^{-4}$	.502	$2.66x10^{-4}$	$-2.83x10^{-4}$	$7.80x10^{-4}$	.338
22.5	$6.29x10^{-5}$	$-6.66x10^{-5}$	$3.12x10^{-4}$	.395	$2.52x10^{-4}$	$-2.98x10^{-4}$	$7.74x10^{-4}$	.369
25	$6.16x10^{-5}$	$-6.49x10^{-5}$	$3.07x10^{-4}$	.403	$2.53x10^{-4}$	$-2.93x10^{-4}$	$7.72x10^{-4}$	.339

Table S3.11 | Mediation output (beta, 95% CI, *p*-value) from hippocampal volume-local efficiency-memory model in the whole sample and in MCI only

Whole sample								
	Indirect Effect				Direct Effect			
Density	ß	Lower bound	Upper bound	*p*	ß	Lower bound	Upper bound	*p*
2.5	$9.28x10^{-6}$	$-3.68x10^{-5}$	$7.82x10^{-5}$	.739	$6.54x10^{-4}$	$3.01x10^{-4}$	$1.04x10^{-3}$	<.001
5	$5.89x10^{-6}$	$-8.55x10^{-5}$	$9.49x10^{-5}$	.895	$6.58x10^{-4}$	$3.03x10^{-4}$	$1.05x10^{-3}$	<.001
7.5	$2.15x10^{-5}$	$-2.81x10^{-5}$	$1.27x10^{-4}$	.448	$6.42x10^{-4}$	$2.86x10^{-4}$	$1.02x10^{-3}$	<.001
10	$6.45x10^{-6}$	$-8.15x10^{-5}$	$1.15x10^{-4}$	.884	$6.57x10^{-4}$	$3.15x10^{-4}$	$1.04x10^{-3}$	<.001
12.5	$-1.71x10^{-5}$	$-1.29x10^{-4}$	$7.14x10^{-5}$	.677	$6.80x10^{-4}$	$3.33x10^{-4}$	$1.06x10^{-3}$	<.001
15	$7.88x10^{-6}$	$-5.61x10^{-5}$	$8.11x10^{-5}$	.773	$6.56x10^{-4}$	$3.05x10^{-4}$	$1.04x10^{-3}$	<.001
17.5	$4.60x10^{-5}$	$-3.36x10^{-5}$	$1.36x10^{-4}$	.238	$6.17x10^{-4}$	$2.70x10^{-4}$	$1.01x10^{-3}$	.001
20	$4.59x10^{-5}$	$-2.83x10^{-5}$	$1.41x10^{-4}$	.213	$6.17x10^{-4}$	$2.71x10^{-4}$	$1.00x10^{-3}$	<.001
22.5	$3.87x10^{-5}$	$-3.65x10^{-5}$	$1.31x10^{-4}$	.312	$6.25x10^{-4}$	$2.90x10^{-4}$	$1.02x10^{-3}$	.001
25	$3.98x10^{-5}$	$-2.76x10^{-5}$	$1.35x10^{-4}$	.263	$6.24x10^{-4}$	$2.75x10^{-4}$	$1.01x10^{-3}$	.001
MCI only								
	Indirect Effect				Direct Effect			
Density	ß	Lower bound	Upper bound	*p*	ß	Lower bound	Upper bound	*p*
2.5	$8.08x10^{-6}$	$-5.55x10^{-5}$	$8.55x10^{-5}$	.846	$6.34x10^{-4}$	$2.99x10^{-4}$	$1.02x10^{-3}$	<.001
5	$-4.94x10^{-5}$	$-2.21x10^{-4}$	$3.43x10^{-5}$	.280	$6.91x10^{-4}$	$3.47x10^{-4}$	$1.11x10^{-3}$	<.001
7.5	$8.63x10^{-6}$	$-7.89x10^{-5}$	$1.05x10^{-4}$	.845	$6.33x10^{-4}$	$2.89x10^{-4}$	$1.03x10^{-3}$	<.001
10	$1.81x10^{-6}$	$-1.29x10^{-4}$	$1.31x10^{-4}$	.982	$6.40x10^{-4}$	$2.92x10^{-4}$	$1.03x10^{-3}$	<.001
12.5	$-4.87x10^{-5}$	$-2.13x10^{-4}$	$4.85x10^{-5}$	.350	$6.91x10^{-4}$	$3.61x10^{-4}$	$1.08x10^{-3}$	<.001
15	$-9.91x10^{-6}$	$-1.08x10^{-4}$	$6.66x10^{-5}$	.822	$6.52x10^{-4}$	$3.21x10^{-4}$	$1.03x10^{-3}$	<.001
17.5	$2.94x10^{-5}$	$-6.74x10^{-5}$	$1.26x10^{-4}$	.507	$6.12x10^{-4}$	$2.68x10^{-4}$	$1.00x10^{-3}$	<.001
20	$3.76x10^{-5}$	$-5.53x10^{-5}$	$1.46x10^{-4}$	.394	$6.04x10^{-4}$	$2.69x10^{-4}$	$9.85x10^{-4}$	.001
22.5	$4.05x10^{-5}$	$-3.94x10^{-5}$	$1.48x10^{-4}$	.320	$6.01x10^{-4}$	$2.59x10^{-4}$	$9.93x10^{-4}$	.001
25	$5.57x10^{-5}$	$-1.73x10^{-5}$	$1.75x10^{-4}$	.150	$5.86x10^{-4}$	$2.49x10^{-4}$	$9.74x10^{-4}$	.001

Table S3.12 | Mediation output (beta, 95% CI, *p*-value) from hippocampal volume-local efficiency-executive function model in the whole sample and in MCI only

Whole sample								
	Indirect Effect				Direct Effect			
Density	ß	Lower bound	Upper bound	*p*	ß	Lower bound	Upper bound	*p*
2.5	-2.89×10^{-7}	-5.50×10^{-5}	8.98×10^{-5}	.918	4.15×10^{-4}	-3.52×10^{-5}	8.77×10^{-4}	.072
5	-5.87×10^{-6}	-1.26×10^{-4}	1.12×10^{-4}	.897	4.21×10^{-4}	-3.79×10^{-5}	8.97×10^{-4}	.071
7.5	8.14×10^{-6}	-8.40×10^{-5}	1.10×10^{-4}	.854	4.07×10^{-4}	-4.34×10^{-5}	8.94×10^{-4}	.080
10	7.75×10^{-6}	-1.02×10^{-4}	1.49×10^{-4}	.854	4.07×10^{-4}	-7.52×10^{-5}	8.97×10^{-4}	.097
12.5	-2.43×10^{-5}	-1.69×10^{-4}	1.25×10^{-4}	.717	4.39×10^{-4}	-4.76×10^{-5}	9.15×10^{-4}	.076
15	1.37×10^{-5}	-8.16×10^{-5}	1.34×10^{-4}	.727	4.01×10^{-4}	-5.69×10^{-5}	8.97×10^{-4}	.087
17.5	6.60×10^{-5}	-4.42×10^{-5}	2.15×10^{-4}	.250	3.49×10^{-4}	-1.27×10^{-4}	8.51×10^{-4}	.148
20	5.51×10^{-5}	-5.25×10^{-5}	2.12×10^{-4}	.326	3.60×10^{-4}	-1.12×10^{-4}	8.38×10^{-4}	.129
22.5	5.13×10^{-5}	-4.73×10^{-5}	1.90×10^{-4}	.321	3.63×10^{-4}	-1.11×10^{-4}	8.53×10^{-4}	.125
25	5.09×10^{-5}	-4.58×10^{-5}	1.73×10^{-4}	.289	3.64×10^{-4}	-9.58×10^{-5}	8.57×10^{-4}	.125
MCI only								
	Indirect Effect				Direct Effect			
Density	ß	Lower bound	Upper bound	*p*	ß	Lower bound	Upper bound	*p*
2.5	-1.16×10^{-5}	-1.12×10^{-4}	1.06×10^{-4}	.834	3.26×10^{-4}	-1.97×10^{-4}	8.35×10^{-4}	.208
5	-4.99×10^{-5}	-2.55×10^{-4}	1.38×10^{-4}	.554	3.65×10^{-4}	-1.95×10^{-4}	8.97×10^{-4}	.194
7.5	-2.67×10^{-5}	-1.88×10^{-4}	1.03×10^{-4}	.666	3.42×10^{-4}	-2.11×10^{-4}	9.03×10^{-4}	.221
10	-1.45×10^{-5}	-1.61×10^{-4}	2.07×10^{-4}	.900	3.29×10^{-4}	-2.61×10^{-4}	8.82×10^{-4}	.268
12.5	-8.75×10^{-5}	-2.74×10^{-4}	1.33×10^{-4}	.378	4.02×10^{-4}	-1.81×10^{-4}	9.38×10^{-4}	.180
15	-1.40×10^{-5}	-1.71×10^{-4}	1.86×10^{-4}	.877	3.29×10^{-4}	-2.45×10^{-4}	8.71×10^{-4}	.259
17.5	3.22×10^{-5}	-1.44×10^{-4}	2.36×10^{-4}	.703	2.83×10^{-4}	-3.19×10^{-4}	8.81×10^{-4}	.339
20	2.53×10^{-5}	-1.28×10^{-4}	2.30×10^{-4}	.734	2.90×10^{-4}	-2.91×10^{-4}	8.45×10^{-4}	.310
22.5	1.25×10^{-5}	-1.28×10^{-4}	1.91×10^{-4}	.846	3.02×10^{-4}	-2.63×10^{-4}	8.39×10^{-4}	.280
25	2.26×10^{-5}	-1.25×10^{-4}	1.90×10^{-4}	.727	2.92×10^{-4}	-2.60×10^{-4}	8.38×10^{-4}	.292

Table S3.13 | Mediation output (beta, 95% CI, *p*-value) from hippocampal volume-redundancy-memory model moderated by Aß burden in the whole sample

Aß Positive								
	Indirect Effect				Direct Effect			
Density	ß	Lower bound	Upper bound	*p*	ß	Lower bound	Upper bound	*p*
2.5	$8.27x10^{-5}$	$-4.43x10^{-5}$	$2.05x10^{-4}$	.211	$8.53x10^{-4}$	$4.50x10^{-4}$	$1.36x10^{-3}$	<.001
5	$1.14x10^{-4}$	$-1.76x10^{-5}$	$2.80x10^{-4}$	.098	$8.22x10^{-4}$	$4.16x10^{-4}$	$1.31x10^{-3}$	<.001
7.5	$1.43x10^{-4}$	$6.12x10^{-7}$	$3.52x10^{-4}$	.048	$7.93x10^{-4}$	$3.85x10^{-4}$	$1.27x10^{-3}$	<.001
10	$1.61x10^{-4}$	$1.57x10^{-5}$	$3.72x10^{-4}$	.020	$7.75x10^{-4}$	$3.55x10^{-4}$	$1.25x10^{-3}$	.001
12.5	$1.61x10^{-4}$	$1.30x10^{-5}$	$3.71x10^{-4}$	.029	$7.75x10^{-4}$	$3.53x10^{-4}$	$1.24x10^{-3}$	<.001
15	$1.53x10^{-4}$	$-2.96x10^{-6}$	$3.62x10^{-4}$	.055	$7.83x10^{-4}$	$3.72x10^{-4}$	$1.24x10^{-3}$	<.001
17.5	$1.38x10^{-4}$	$-9.87x10^{-6}$	$3.31x10^{-4}$	.073	$7.98x10^{-4}$	$3.96x10^{-4}$	$1.27x10^{-3}$	<.001
20	$1.25x10^{-4}$	$-1.27x10^{-5}$	$3.17x10^{-4}$	.078	$8.12x10^{-4}$	$4.11x10^{-4}$	$1.28x10^{-3}$	<.001
22.5	$1.39x10^{-4}$	$-3.76x10^{-6}$	$3.26x10^{-4}$	.057	$7.97x10^{-4}$	$3.97x10^{-4}$	$1.27x10^{-3}$	<.001
25	$1.43x10^{-4}$	$-5.42x10^{-8}$	$3.36x10^{-4}$	.050	$7.93x10^{-4}$	$3.91x10^{-4}$	$1.26x10^{-3}$	<.001
Aß Negative								
	Indirect Effect				Direct Effect			
Density	ß	Lower bound	Upper bound	*p*	ß	Lower bound	Upper bound	*p*
2.5	$7.49x10^{-5}$	$-2.23x10^{-5}$	$1.97x10^{-4}$	.129	$1.71x10^{-4}$	$-3.14x10^{-4}$	$7.41x10^{-4}$	.500
5	$1.07x10^{-4}$	$-1.30x10^{-5}$	$2.68x10^{-4}$	.079	$1.39x10^{-4}$	$-3.57x10^{-4}$	$7.02x10^{-4}$	.590
7.5	$1.23x10^{-4}$	$1.44x10^{-5}$	$2.90x10^{-4}$	.024	$1.23x10^{-4}$	$-3.72x10^{-4}$	$6.68x10^{-4}$	.628
10	$1.31x10^{-4}$	$2.01x10^{-5}$	$3.00x10^{-4}$	.014	$1.15x10^{-4}$	$-3.94x10^{-4}$	$6.47x10^{-4}$	.690
12.5	$1.30x10^{-4}$	$1.60x10^{-5}$	$3.01x10^{-4}$	.021	$1.16x10^{-4}$	$-3.76x10^{-4}$	$6.57x10^{-4}$	.677
15	$1.27x10^{-4}$	$1.39x10^{-5}$	$2.93x10^{-4}$	.028	$1.19x10^{-4}$	$-3.73x10^{-4}$	$6.65x10^{-4}$	.652
17.5	$1.14x10^{-4}$	$-4.08x10^{-6}$	$2.85x10^{-4}$	.059	$1.32x10^{-4}$	$-3.57x10^{-4}$	$6.85x10^{-4}$	.601
20	$1.18x10^{-4}$	$-1.44x10^{-6}$	$2.97x10^{-4}$	.053	$1.28x10^{-4}$	$-3.69x10^{-4}$	$6.83x10^{-4}$	.606
22.5	$1.21x10^{-4}$	$-1.04x10^{-6}$	$2.92x10^{-4}$	.052	$1.25x10^{-4}$	$-3.52x10^{-4}$	$6.79x10^{-4}$	.625
25	$1.11x10^{-4}$	$-1.52x10^{-5}$	$2.88x10^{-4}$	.081	$1.35x10^{-4}$	$-3.56x10^{-4}$	$6.77x10^{-4}$	.603

Table S3.14 | Mediation output (beta, 95% CI, *p*-value) from hippocampal volume-redundancy-memory model moderated by Aß burden in MCI only

Aß Positive								
	Indirect Effect				Direct Effect			
Density	ß	Lower bound	Upper bound	*p*	ß	Lower bound	Upper bound	*p*
2.5	$9.78x10^{-6}$	$-1.06x10^{-4}$	$1.49x10^{-4}$	.812	$9.50x10^{-4}$	$5.78x10^{-4}$	$1.40x10^{-3}$	<.001
5	$6.81x10^{-5}$	$-6.39x10^{-5}$	$2.96x10^{-4}$	.325	$8.91x10^{-4}$	$5.14x10^{-4}$	$1.33x10^{-3}$	<.001
7.5	$1.15x10^{-4}$	$-2.30x10^{-5}$	$3.89x10^{-4}$	.136	$8.44x10^{-4}$	$4.57x10^{-4}$	$1.27x10^{-3}$	<.001
10	$1.43x10^{-4}$	$-3.42x10^{-6}$	$4.01x10^{-4}$	.061	$8.17x10^{-4}$	$4.13x10^{-4}$	$1.24x10^{-3}$	<.001
12.5	$1.65x10^{-4}$	$5.31x10^{-6}$	$4.35x10^{-4}$	.034	$7.94x10^{-4}$	$3.76x10^{-4}$	$1.21x10^{-3}$	.001
15	$1.64x10^{-4}$	$6.34x10^{-6}$	$4.38x10^{-4}$	.034	$7.96x10^{-4}$	$3.90x10^{-4}$	$1.20x10^{-3}$	<.001
17.5	$1.43x10^{-4}$	$1.83x10^{-6}$	$3.90x10^{-4}$	.044	$8.16x10^{-4}$	$4.07x10^{-4}$	$1.25x10^{-3}$	<.001
20	$1.26x10^{-4}$	$-1.68x10^{-6}$	$3.58x10^{-4}$	.059	$8.34x10^{-4}$	$4.32x10^{-4}$	$1.26x10^{-3}$	<.001
22.5	$1.45x10^{-4}$	$6.01x10^{-6}$	$3.88x10^{-4}$	.033	$8.14x10^{-4}$	$4.15x10^{-4}$	$1.25x10^{-3}$	<.001
25	$1.42x10^{-4}$	$4.70x10^{-6}$	$3.78x10^{-4}$	.033	$8.18x10^{-4}$	$4.07x10^{-4}$	$1.25x10^{-3}$	.001
Aß Negative								
	Indirect Effect				Direct Effect			
Density	ß	Lower bound	Upper bound	*p*	ß	Lower bound	Upper bound	*p*
2.5	$5.46x10^{-6}$	$-1.05x10^{-4}$	$1.30x10^{-4}$	.880	$1.25x10^{-4}$	$-4.17x10^{-4}$	$7.58x10^{-4}$	.646
5	$4.23x10^{-5}$	$-6.29x10^{-5}$	$2.12x10^{-4}$	.356	$8.77x10^{-5}$	$-4.72x10^{-4}$	$7.25x10^{-4}$	.765
7.5	$6.12x10^{-5}$	$-2.25x10^{-5}$	$1.94x10^{-4}$	.149	$6.88x10^{-5}$	$-4.70x10^{-4}$	$6.97x10^{-4}$	.807
10	$6.92x10^{-5}$	$-1.85x10^{-5}$	$2.03x10^{-4}$	.130	$6.08x10^{-5}$	$-4.73x10^{-4}$	$7.00x10^{-4}$	.818
12.5	$7.15x10^{-5}$	$-2.16x10^{-5}$	$2.02x10^{-4}$	.125	$5.85x10^{-5}$	$-4.68x10^{-4}$	$6.75x10^{-4}$	.835
15	$6.41x10^{-5}$	$-3.64x10^{-5}$	$1.92x10^{-4}$	.176	$6.60x10^{-5}$	$-4.65x10^{-4}$	$6.93x10^{-4}$	.811
17.5	$3.45x10^{-5}$	$-7.59x10^{-5}$	$1.55x10^{-4}$	.463	$9.55x10^{-5}$	$-4.25x10^{-4}$	$7.34x10^{-4}$	.732
20	$3.70x10^{-5}$	$-5.91x10^{-5}$	$1.63x10^{-4}$	.394	$9.30x10^{-5}$	$-4.42x10^{-4}$	$7.19x10^{-4}$	.724
22.5	$3.75x10^{-5}$	$-6.38x10^{-5}$	$1.60x10^{-4}$	.409	$9.26x10^{-5}$	$-4.42x10^{-4}$	$7.01x10^{-4}$	.737
25	$3.32x10^{-5}$	$-7.31x10^{-5}$	$1.55x10^{-4}$	.436	$9.68x10^{-5}$	$-4.33x10^{-4}$	$7.20x10^{-4}$	.710

Table S3.15 | Insular volume-insular redundancy linear regression output (standardized beta and *p*-value) across densities in the whole sample and in MCI only

	Whole sample		MCI only	
Density	ß	*p*	ß	*p*
2.5	-0.01	.926	-0.03	.819
5	0.02	.845	0.01	.951
7.5	0.03	.764	0.01	.907
10	0.05	.614	0.03	.798
12.5	0.08	.466	0.06	.608
15	0.09	.402	0.08	.528
17.5	0.10	.330	0.09	.476
20	0.11	.311	0.10	.431
22.5	0.12	.271	0.11	.372
25	0.11	.296	0.10	.389

Table S3.16 | Memory-insular redundancy linear regression output (standardized beta and *p*-value) across densities in the whole sample and in MCI only

	Whole sample		MCI only	
Density	ß	*p*	ß	*p*
2.5	0.06	.353	-0.003	.967
5	0.06	.314	0.03	.688
7.5	0.04	.528	-0.002	.973
10	0.04	.509	-0.001	.994
12.5	0.03	.586	-0.004	.955
15	0.04	.516	0.01	.922
17.5	0.05	.426	0.01	.880
20	0.05	.405	0.02	.808
22.5	0.06	.369	0.01	.852
25	0.06	.362	0.02	.800

Table S3.17 | Mediation output (beta, 95% CI, *p*-value) from Insular volume-insular redundancy-memory model in the whole sample and in MCI only

Whole sample								
	Indirect Effect				Direct Effect			
Density	ß	Lower bound	Upper bound	*p*	ß	Lower bound	Upper bound	*p*
2.5	-1.26×10^{-6}	-3.17×10^{-5}	2.62×10^{-5}	.903	2.10×10^{-4}	-4.69×10^{-5}	4.67×10^{-4}	.103
5	2.77×10^{-6}	-3.11×10^{-5}	3.17×10^{-5}	.920	2.06×10^{-4}	-4.63×10^{-5}	4.70×10^{-4}	.103
7.5	2.55×10^{-6}	-2.83×10^{-5}	2.70×10^{-5}	.928	2.06×10^{-4}	-4.94×10^{-5}	4.63×10^{-4}	.106
10	4.28×10^{-6}	-2.98×10^{-5}	3.37×10^{-5}	.871	2.05×10^{-4}	-5.00×10^{-5}	4.63×10^{-4}	.111
12.5	4.62×10^{-6}	-3.17×10^{-5}	3.79×10^{-5}	.883	2.04×10^{-4}	-4.23×10^{-5}	4.70×10^{-4}	.110
15	6.39×10^{-6}	-3.22×10^{-5}	4.29×10^{-5}	.792	2.02×10^{-4}	-4.63×10^{-5}	4.58×10^{-4}	.105
17.5	9.23×10^{-6}	-2.81×10^{-5}	5.16×10^{-5}	.678	2.00×10^{-4}	-5.72×10^{-5}	4.71×10^{-4}	.115
20	1.01×10^{-5}	-2.69×10^{-5}	5.49×10^{-5}	.645	1.99×10^{-4}	-6.08×10^{-5}	4.61×10^{-4}	.125
22.5	1.18×10^{-5}	-2.78×10^{-5}	5.75×10^{-5}	.590	1.97×10^{-4}	-5.74×10^{-5}	4.58×10^{-4}	.119
25	1.15×10^{-5}	-2.38×10^{-5}	5.92×10^{-5}	.585	1.97×10^{-4}	-5.35×10^{-5}	4.62×10^{-4}	.119
MCI only								
	Indirect Effect				Direct Effect			
Density	ß	Lower bound	Upper bound	*p*	ß	Lower bound	Upper bound	*p*
2.5	6.13×10^{-8}	-3.15×10^{-5}	2.37×10^{-5}	.942	1.24×10^{-4}	-1.37×10^{-4}	3.69×10^{-4}	.302
5	4.06×10^{-7}	-3.57×10^{-5}	2.39×10^{-5}	.887	1.24×10^{-4}	-1.38×10^{-4}	3.63×10^{-4}	.316
7.5	-9.09×10^{-8}	-3.29×10^{-5}	2.11×10^{-5}	.869	1.24×10^{-4}	-1.32×10^{-4}	3.61×10^{-4}	.319
10	-1.52×10^{-7}	-4.02×10^{-5}	2.37×10^{-5}	.875	1.24×10^{-4}	-1.38×10^{-4}	3.57×10^{-4}	.306
12.5	-9.51×10^{-7}	-4.79×10^{-5}	2.76×10^{-5}	.863	1.25×10^{-4}	-1.30×10^{-4}	3.65×10^{-4}	.305
15	3.09×10^{-7}	-4.74×10^{-5}	3.45×10^{-5}	.925	1.24×10^{-4}	-1.33×10^{-4}	3.59×10^{-4}	.316
17.5	8.90×10^{-7}	-4.61×10^{-5}	3.83×10^{-5}	.983	1.23×10^{-4}	-1.35×10^{-4}	3.69×10^{-4}	.314
20	2.08×10^{-6}	-4.34×10^{-5}	4.68×10^{-5}	.970	1.22×10^{-4}	-1.36×10^{-4}	3.63×10^{-4}	.312
22.5	1.36×10^{-6}	-4.77×10^{-5}	4.61×10^{-5}	.987	1.23×10^{-4}	-1.37×10^{-4}	3.60×10^{-4}	.320
25	2.32×10^{-6}	-4.08×10^{-5}	5.00×10^{-5}	.932	1.22×10^{-4}	-1.39×10^{-4}	3.62×10^{-4}	.324

APPENDIX C: CHAPTER 4 SUPPLEMENTARY MATERIALS

Supplementary Tables

Table S4.1 | Regression output for hippocampal redundancy participant motion parameters across densities

	Left Anterior		Right Anterior		Left Posterior		Right Posterior	
Density	ß	*p*	ß	*p*	ß	*p*	ß	*p*
Average Motion								
Avg.	0.01	.939	-0.05	.471	-0.07	.320	0.08	.263
2.5	0.04	.528	0.02	.453	-0.05	.469	-0.01	.839
5	0.01	.849	0.02	.730	-0.05	.509	-0.03	.646
7.5	-0.05	.465	0.02	.995	-0.03	.624	0.03	.634
10	-0.04	.540	0.02	.787	-0.06	.365	0.06	.418
12.5	-0.01	.888	-0.06	.419	-0.06	.346	0.09	.181
15	-0.01	.916	-0.04	.537	-0.08	.247	0.08	.239
17.5	-0.01	.873	-0.03	.702	-0.07	.297	0.09	.200
20	-0.01	.919	-0.04	.572	-0.06	.358	0.08	.232
22.5	0.01	.925	-0.06	.388	-0.06	.344	0.07	.290
25	0.02	.741	-0.05	.431	-0.06	.355	0.07	.338
Invalid Scans								
Avg.	0.07	.310	-0.03	.638	0.04	.526	0.07	.325
2.5	0.02	.777	0.08	.752	-0.03	.618	0.02	.768
5	0.06	.384	0.08	.953	0.01	.918	<0.01	.969
7.5	0.04	.517	0.08	.973	0.01	.877	0.02	.780
10	0.07	.309	0.08	.884	-0.01	.922	0.02	.745
12.5	0.09	.176	-0.04	.563	-0.01	.887	0.08	.254
15	0.06	.357	-0.03	.656	<0.01	.977	0.08	.259
17.5	0.02	.817	0.00	.964	0.04	.543	0.07	.300
20	0.06	.363	-0.03	.642	0.06	.391	0.08	.266
22.5	0.07	.296	-0.03	.614	0.06	.370	0.06	.380
25	0.08	.236	-0.04	.574	0.04	.585	0.06	.376

Note: ß = standardized beta

Table S4.2 | Hippocampal redundancy-learning regressions across densities

	Left Anterior		Right Anterior		Left Posterior		Right Posterior	
Density	ß	*p*	ß	*p*	ß	*p*	ß	*p*
2.5	0.01	.913	<0.01	.980	0.07	.236	0.02	.705
5	0.02	.738	0.02	.730	0.11	.082	-0.04	.512
7.5	0.01	.909	<0.01	.952	0.08	.182	-0.02	.751
10	-0.02	.715	-0.04	.521	0.09	.174	<0.01	.972
12.5	-0.01	.842	-0.03	.689	0.09	.172	<0.01	.990
15	0.01	.821	-0.03	.620	0.08	.222	-0.02	.701
17.5	0.01	.821	-0.04	.553	0.08	.202	-0.03	.640
20	0.03	.587	-0.04	.537	0.07	.284	-0.03	.617
22.5	0.03	.633	-0.03	.632	0.06	.314	-0.03	.605
25	0.03	.614	-0.05	.462	0.05	.465	-0.04	.541

Note: Analyses included age and sex as covariates. ß = standardized beta

Table S4.3 | Hippocampal redundancy-immediate recall regressions across densities

	Left Anterior		Right Anterior		Left Posterior		Right Posterior	
Density	ß	*p*	ß	*p*	ß	*p*	ß	*p*
2.5	0.04	.526	-0.06	.360	0.04	.564	<0.01	.970
5	0.07	.318	-0.07	.263	0.09	.182	-0.03	.591
7.5	0.01	.902	-0.08	.199	0.04	.554	-0.01	.867
10	-0.02	.753	-0.11	.091	0.04	.537	<0.01	.959
12.5	-0.01	.898	-0.08	.206	0.05	.477	0.01	.918
15	<0.01	.968	-0.10	.133	0.06	.369	0.01	.910
17.5	-0.03	.695	-0.10	.117	0.08	.201	0.01	.845
20	-0.02	.817	-0.11	.111	0.08	.216	0.04	.503
22.5	-0.02	.767	-0.09	.156	0.08	.228	0.04	.537
25	-0.02	.800	-0.11	.098	0.08	.241	0.03	.671

Note: Analyses included age and sex as covariates. ß = standardized beta

Table S4.4 | Hippocampal redundancy-picture sequence memory regressions across densities

	Left Anterior		Right Anterior		Left Posterior		Right Posterior	
Density	ß	*p*	ß	*p*	ß	*p*	ß	*p*
2.5	0.05	.494	-0.03	.767	0.03	.608	<0.01	.966
5	0.08	.283	0.01	.899	0.13	.057	<0.01	.975
7.5	0.09	.227	0.02	.764	0.12	.086	0.04	.547
10	0.08	.253	<0.01	.961	0.12	.089	0.01	.862
12.5	0.10	.165	-0.01	.848	0.14	.039	0.06	.417
15	0.08	.236	-0.02	.751	0.17	.015	0.02	.789
17.5	0.10	.143	-0.02	.789	0.20	.004	0.02	.727
20	0.13	.082	-0.03	.722	0.19	.006	0.03	.619
22.5	0.12	.088	-0.04	.589	0.17	.017	0.04	.598
25	0.11	.137	-0.08	.286	0.15	.028	0.03	.644

Note: Analyses included age and sex as covariates. ß = standardized beta

Table S4.5 | Hippocampal redundancy-TMT-B regressions across densities

	Left Anterior		Right Anterior		Left Posterior		Right Posterior	
Density	ß	*p*	ß	*p*	ß	*p*	ß	*p*
2.5	0.04	.554	-0.02	.725	-0.02	.809	0.06	.385
5	-0.08	.238	-0.03	.699	-0.05	.487	0.10	.132
7.5	-0.14	.037	-0.04	.545	<0.01	.991	0.08	.244
10	-0.14	.029	-0.04	.556	0.03	.698	0.05	.452
12.5	-0.12	.075	-0.02	.788	0.02	.796	0.02	.791
15	-0.08	.225	0.01	.922	-0.02	.715	0.02	.783
17.5	-0.06	.353	<0.01	.964	-0.05	.468	-0.02	.735
20	-0.09	.181	<0.01	.963	-0.05	.436	-0.03	.695
22.5	-0.06	.347	0.01	.909	-0.05	.479	-0.07	.325
25	-0.02	.779	0.01	.919	-0.03	.626	-0.07	.277

Note: Analyses included age and sex as covariates. ß = standardized beta

Table S4.6 | Hippocampal redundancy-cognition regressions for averaged density, using robust regression (Huber weighting) and Wald test for significance

	Left Anterior			Right Anterior			Left Posterior			Right Posterior		
	ß	*t*	*p*	ß	*t*	*p*	ß	*t*	*p*	ß	*t*	*p*
Learning	0.02	0.36	.717	-0.05	0.81	.745	0.05	0.71	.196	-0.05	0.76	.451
Recall	-0.02	0.32	.422	-0.12	1.81	.072	0.07	0.98	.321	0.03	0.40	.672
PSM	0.09	1.30	.485	-0.07	1.00	.324	0.17	2.34	.020	0.03	0.44	.547
TMT-B	-0.03	0.75	.445	0.02	0.42	.694	-0.03	0.59	.659	-0.04	0.83	.421

Note: Analyses included age and sex as covariates. ß = standardized beta

Table S4.7 | Left posterior hippocampal redundancy and age interaction regression output in predicting cognitive performance across densities

	Learning		Recall		PSM		TMT-B	
Density	ß	*p*	ß	*p*	ß	*p*	ß	*p*
2.5	-0.05	.502	-0.11	.193	-0.13	.131	-0.02	.806
5	-0.01	.816	-0.09	.164	-0.14	.050	-0.04	.514
7.5	-0.01	.831	-0.10	.123	-0.16	.033	-0.07	.283
10	<0.01	.971	-0.07	.260	-0.14	.053	-0.03	.675
12.5	<-0.01	.942	-0.10	.154	-0.15	.051	-0.02	.744
15	-0.02	.811	-0.10	.119	-0.17	.026	0.03	.702
17.5	-0.04	.531	-0.13	.043	-0.18	.016	-0.01	.916
20	-0.05	.440	-0.13	.042	-0.17	.026	-0.03	.663
22.5	-0.07	.264	-0.14	.029	-0.18	.014	-0.01	.843
25	-0.08	.205	-0.14	.034	-0.22	.004	0.01	.874

Note: Analyses included sex as a covariate. ß = standardized beta

Table S4.8 | Hippocampal redundancy-education and hippocampal redundancy-physical activity regressions for averaged density, using robust regression (Huber weighting) and Wald test for significance

	Left Anterior			Right Anterior			Left Posterior			Right Posterior		
	ß	*t*	*p*	ß	*t*	*p*	ß	*t*	*p*	ß	*t*	*p*
Education	-0.01	0.08	.937	-0.003	0.04	.968	0.08	1.17	.241	0.05	0.74	.463
Physical Activity	0.04	0.55	.582	0.003	0.04	.964	-0.08	1.18	.236	-0.06	0.94	.347
Phys. Act (Log)	0.02	0.32	.749	-0.07	0.95	.350	-0.03	0.36	.721	-0.06	0.84	.406

Note: Analyses included age and sex as covariates. ß = standardized beta

Table S4.9 | Education-hippocampal redundancy regressions across densities

	Left Anterior		Right Anterior		Left Posterior		Right Posterior	
Density	ß	*p*	ß	*p*	ß	*p*	ß	*p*
2.5	-0.17	.020	-0.03	.684	0.08	.277	-0.08	.270
5	-0.14	.056	-0.05	.498	0.11	.108	-0.06	.379
7.5	-0.09	.215	-0.03	.713	0.10	.164	-0.02	.797
10	-0.05	.521	-0.03	.709	0.10	.152	0.01	.861
12.5	-0.04	.540	<0.01	.991	0.09	.219	0.04	.602
15	-0.04	.615	0.01	.916	0.12	.080	0.08	.265
17.5	-0.05	.522	-0.01	.895	0.11	.131	0.05	.456
20	-0.02	.744	-0.04	.593	0.09	.190	0.03	.625
22.5	-0.02	.809	-0.02	.758	0.07	.347	0.01	.853
25	-0.01	.846	-0.05	.470	0.08	.286	0.06	.367

Note: Analyses included age and sex as covariates. ß = standardized beta

Table S4.10 | Physical activity-hippocampal redundancy regressions across densities

	Left Anterior		Right Anterior		Left Posterior		Right Posterior	
Density	ß	*p*	ß	*p*	ß	*p*	ß	*p*
2.5	0.04	.573	-0.05	.440	-0.03	.698	0.01	.923
5	0.04	.520	-0.12	.093	-0.03	.705	-0.01	.862
7.5	0.03	.619	-0.14	.044	-0.04	.558	-0.07	.345
10	0.04	.526	-0.13	.059	-0.01	.853	-0.06	.380
12.5	0.03	.699	-0.13	.056	-0.04	.608	-0.04	.573
15	0.02	.821	-0.10	.144	-0.03	.662	-0.07	.335
17.5	0.01	.851	-0.09	.172	-0.02	.774	-0.06	.360
20	-0.01	.920	-0.09	.182	<0.01	.993	-0.04	.581
22.5	<0.01	.981	-0.08	.218	-0.02	.766	-0.04	.595
25	<0.01	.966	-0.06	.356	-0.03	.710	-0.05	.439

Note: Analyses included age and sex as covariates. Physical activity log-transformed. ß = standardized beta

Table S4.11 | Multiple mediation indirect effects of education on learning through redundancy across densities

	Left Anterior		Right Anterior		Left Posterior		Right Posterior		Joint	
Density	ß	*p*	ß	*p*	ß	*p*	ß	*p*	ß	*p*
2.5	-0.01	.796	0.01	.810	0.02	.619	<-0.01	.941	0.01	.854
5	-0.02	.649	<0.01	.878	0.04	.442	0.01	.737	0.04	.605
7.5	<-0.01	.912	<0.01	.879	0.03	.550	<0.01	.927	0.03	.625
10	<0.01	.868	<0.01	.911	0.03	.498	<0.01	.897	0.04	.534
12.5	<0.01	.922	<-0.01	.980	0.02	.575	<0.01	.931	0.03	.664
15	<-0.01	.954	<-0.01	.900	0.03	.545	-0.01	.818	0.02	.812
17.5	<-0.01	.919	<-0.01	.939	0.03	.566	-0.01	.828	0.02	.812
20	<-0.01	.990	<0.01	.959	0.02	.619	-0.01	.843	0.02	.795
22.5	<0.01	.976	<-0.01	.962	0.01	.681	<-0.01	.896	0.01	.860
25	<-0.01	.995	<0.01	.897	0.01	.732	-0.01	.699	<0.01	.960

Note: Analyses included age and sex as covariates.

Table S4.12 | Multiple mediation indirect effects of education on recall through redundancy across densities

	Left Anterior		Right Anterior		Left Posterior		Right Posterior		Joint	
Density	ß	*p*	ß	*p*	ß	*p*	ß	*p*	ß	*p*
2.5	-0.01	.358	<0.01	.817	0.01	.605	<-0.01	.811	<-0.01	.850
5	-0.02	.358	0.01	.751	0.01	.413	<0.01	.805	0.01	.819
7.5	<-0.01	.718	<0.01	.978	0.01	.598	<0.01	.977	<0.01	.867
10	<0.01	.988	<0.01	.925	0.01	.648	<-0.01	.948	0.01	.794
12.5	<-0.01	.954	<-0.01	.825	<0.01	.658	<-0.01	.949	<0.01	.985
15	<-0.01	.938	-0.01	.755	0.01	.541	<-0.01	.903	<0.01	.968
17.5	<-0.01	.985	<-0.01	.888	0.01	.456	<-0.01	.930	0.01	.767
20	<-0.01	.962	<0.01	.976	0.01	.497	<0.01	.973	0.01	.700
22.5	<-0.01	.972	<-0.01	.889	0.01	.562	<0.01	.996	<0.01	.838
25	<-0.01	.960	<0.01	.901	0.01	.547	<0.01	.950	0.01	.681

Note: Analyses included age and sex as covariates.

Table S4.13 | Multiple mediation indirect effects of education on PSM through redundancy across densities

	Left Anterior		Right Anterior		Left Posterior		Right Posterior		Joint	
Density	ß	*p*	ß	*p*	ß	*p*	ß	*p*	ß	*p*
2.5	-0.04	.584	0.01	.902	0.01	.790	-0.01	.904	-0.03	.795
5	-0.04	.594	<0.01	.971	0.07	.408	<0.01	.947	0.04	.795
7.5	-0.02	.794	<-0.01	.935	0.05	.501	0.01	.864	0.04	.775
10	0.01	.919	<-0.01	.984	0.05	.547	<-0.01	.970	0.05	.707
12.5	<0.01	.993	-0.01	.912	0.04	.651	0.02	.742	0.05	.717
15	<0.01	.993	-0.01	.882	0.08	.435	0.01	.924	0.07	.634
17.5	-0.01	.934	-0.01	.938	0.08	.459	0.01	.912	0.08	.647
20	0.01	.918	<-0.01	.969	0.09	.404	<0.01	.945	0.09	.572
22.5	0.01	.907	-0.01	.878	0.04	.606	<0.01	.994	0.04	.788
25	<0.01	.979	0.01	.899	0.06	.502	<0.01	.993	0.07	.664

Note: Analyses included age and sex as covariates.

Table S4.14 | Multiple mediation indirect effects of education on TMT-B through redundancy across densities

	Left Anterior		Right Anterior		Left Posterior		Right Posterior		Joint	
Density	ß	*p*	ß	*p*	ß	*p*	ß	*p*	ß	*p*
2.5	-0.07	.709	-0.01	.915	0.03	.819	-0.04	.803	-0.09	.783
5	0.23	.345	-0.02	.877	-0.02	.871	-0.09	.724	0.11	.772
7.5	0.23	.472	-0.02	.881	0.07	.680	-0.01	.970	0.27	.524
10	0.08	.776	-0.01	.947	0.09	.596	0.05	.830	0.21	.587
12.5	0.07	.768	-0.01	.946	0.05	.709	0.04	.806	0.16	.628
15	0.03	.875	0.02	.859	-0.01	.955	0.07	.725	0.11	.707
17.5	0.03	.838	0.02	.886	-0.04	.718	0.01	.952	0.01	.957
20	0.01	.963	0.01	.943	-0.04	.744	0.01	.960	-0.01	.965
22.5	0.01	.972	0.02	.871	-0.02	.812	<0.01	.997	<0.01	.988
25	0.01	.925	0.01	.941	-0.02	.821	-0.06	.795	-0.06	.829

Note: Analyses included age and sex as covariates.

Table S4.15 | Multiple mediation indirect effects of physical activity on learning through redundancy across densities

	Left Anterior		Right Anterior		Left Posterior		Right Posterior		Joint	
Density	ß	*p*	ß	*p*	ß	*p*	ß	*p*	ß	*p*
2.5	-0.01	.832	0.01	.890	-0.03	.593	-0.01	.771	-0.05	.639
5	0.01	.835	-0.01	.881	-0.02	.795	-0.01	.895	-0.03	.850
7.5	<-0.01	.999	0.01	.904	-0.01	.857	<-0.01	.966	<-0.01	.983
10	-0.01	.791	0.06	.555	0.01	.904	-0.02	.794	0.04	.787
12.5	<-0.01	.954	0.04	.645	-0.01	.909	-0.01	.829	0.02	.884
15	0.01	.809	0.04	.624	-0.01	.918	0.01	.924	0.05	.708
17.5	0.01	.819	0.05	.594	-0.01	.910	0.01	.838	0.06	.663
20	<0.01	.919	0.05	.605	<0.01	.962	0.01	.864	0.07	.624
22.5	<0.01	.941	0.04	.646	-0.01	.885	0.01	.807	0.04	.734
25	0.01	.906	0.03	.712	-0.01	.853	0.03	.706	0.05	.703

Note: Analyses included age and sex as covariates.

Table S4.16 | Multiple mediation indirect effects of physical activity on recall through redundancy across densities

	Left Anterior		Right Anterior		Left Posterior		Right Posterior		Joint	
Density	ß	*p*	ß	*p*	ß	*p*	ß	*p*	ß	*p*
2.5	<0.01	.930	0.01	.649	-0.01	.713	<-0.01	.819	<0.01	.971
5	0.02	.571	0.03	.408	-0.01	.782	<-0.01	.865	0.04	.475
7.5	<0.01	.830	0.04	.359	<-0.01	.957	<-0.01	.910	0.04	.455
10	<0.01	.944	0.04	.352	<0.01	.878	<-0.01	.875	0.04	.441
12.5	<0.01	.830	0.04	.386	<-0.01	.980	<-0.01	.872	0.04	.477
15	0.01	.738	0.03	.508	<-0.01	.942	<-0.01	.876	0.03	.599
17.5	<0.01	.886	0.03	.526	<-0.01	.932	<-0.01	.851	0.02	.693
20	<0.01	.881	0.03	.512	<0.01	.919	-0.01	.722	0.03	.635
22.5	<0.01	.920	0.02	.558	<-0.01	.883	-0.01	.718	0.01	.827
25	<0.01	.886	0.02	.687	-0.01	.821	-0.01	.827	0.01	.912

Note: Analyses included age and sex as covariates.

Table S4.17 | Multiple mediation indirect effects of physical activity on PSM through redundancy across densities

	Left Anterior		Right Anterior		Left Posterior		Right Posterior		Joint	
Density	ß	*p*	ß	*p*	ß	*p*	ß	*p*	ß	*p*
2.5	-0.08	.634	0.01	.908	-0.01	.815	0.01	.829	-0.06	.766
5	-0.02	.893	0.01	.935	-0.07	.604	0.01	.937	-0.07	.803
7.5	-0.02	.853	<0.01	.988	-0.06	.624	-0.03	.780	-0.12	.692
10	0.01	.951	0.05	.743	-0.02	.905	-0.01	.931	0.04	.887
12.5	0.01	.965	0.09	.547	-0.04	.826	<0.01	.978	0.06	.818
15	<-0.01	.982	0.07	.609	-0.05	.820	<-0.01	.970	0.02	.945
17.5	-0.01	.953	0.08	.596	-0.02	.954	-0.01	.923	0.05	.873
20	-0.06	.683	0.07	.637	0.04	.860	<-0.01	.982	0.06	.860
22.5	-0.06	.670	0.08	.577	-0.01	.943	<-0.01	.995	0.01	.971
25	-0.05	.709	0.09	.613	<0.01	.996	<0.01	.946	0.04	.877

Note: Analyses included age and sex as covariates.

Table S4.18 | Multiple mediation indirect effects of physical activity on TMT-B through redundancy across densities

	Left Anterior		Right Anterior		Left Posterior		Right Posterior		Joint	
Density	ß	*p*	ß	*p*	ß	*p*	ß	*p*	ß	*p*
2.5	0.10	.735	0.11	.636	0.02	.906	0.07	.779	0.30	.529
5	-0.21	.600	0.07	.841	0.06	.745	0.04	.921	-0.04	.955
7.5	-0.24	.680	0.19	.637	<-0.01	.998	-0.18	.670	-0.24	.775
10	-0.32	.581	0.14	.701	<0.01	.991	-0.13	.708	-0.31	.694
12.5	-0.18	.725	0.02	.952	-0.02	.926	-0.04	.900	-0.22	.760
15	-0.08	.836	-0.10	.726	0.04	.852	-0.07	.833	-0.21	.733
17.5	-0.06	.861	-0.10	.721	0.06	.823	0.03	.927	-0.07	.901
20	0.02	.968	-0.12	.710	0.02	.949	0.02	.948	-0.07	.915
22.5	0.01	.962	-0.10	.729	0.05	.829	0.08	.826	0.04	.947
25	0.01	.958	-0.04	.871	0.05	.812	0.12	.783	0.13	.815

Note: Analyses included age and sex as covariates.

REFERENCES

2020 Alzheimer's disease facts and figures. (2020). *Alzheimer's and Dementia*, *16*(3), 391–460. https://doi.org/10.1002/alz.12068

Achard, S., & Bullmore, E. (2007). Efficiency and Cost of Economical Brain Functional Networks. *PLOS Computational Biology*, *3*(2), e17. Retrieved from https://doi.org/10.1371/journal.pcbi.0030017

Aisen, P. S., Petersen, R. C., Donohue, M., Gamst, A., Raman, R., Thomas, R. G., … Initiative, A. D. N. (2010). Clinical core of the Alzheimer's Disease Neuroimaing Initiative: Progress and plans. *Alzheimer's & Dementia*, *6*(3), 239–246. https://doi.org/10.1016/j.jalz.2010.03.006.

Aisen, P. S., Petersen, R. C., Donohue, M., & Weiner, M. W. (2015). Alzheimer's Disease Neuroimaging Initiative 2 Clinical Core: Progress and plans. *Alzheimer's and Dementia*, *11*(7), 734–739. https://doi.org/10.1016/j.jalz.2015.05.005

Aittokallio, T., & Schwikowski, B. (2006). Graph-based methods for analysing networks in cell biology. *Briefings in Bioinformatics*, *7*(3), 243–255. https://doi.org/10.1093/bib/bbl022

Albert, M. S., Jones, K., Savage, C. R., Berkman, L., & et al. (1995). Predictors of cognitive change in older persons: MacArthur studies of successful aging. *Psychology and Aging*, *10*(4), 578–589. https://doi.org/10.1037//0882-7974.10.4.578

Apostolova, L. G., Green, A. E., Babakchanian, S., Hwang, K. S., Chou, Y.-Y., Toga, A. W., & Thompson, P. M. (2012). Hippocampal atrophy and ventricular enlargement in normal aging, mild cognitive impairment (MCI), and Alzheimer Disease. *Alzheimer Disease and Associated Disorders*, *26*(1), 17–27. https://doi.org/10.1097/WAD.0b013e3182163b62

Arkadir, D., Bergman, H., & Fahn, S. (2014). Redundant dopaminergic activity may enable compensatory axonal sprouting in Parkinson disease. *Neurology*, *82*(12), 1093–1098. https://doi.org/10.1212/WNL.0000000000000243

Arnaiz, E., & Almkvist, O. (2003). Neuropsychological features of mild cognitive impairment and preclinical alzheimer's disease. *Acta Neurologica Scandinavica*, *107*, 34–41.

Avena-Koenigsberger, A., Misic, B., & Sporns, O. (2018). Communication dynamics in complex brain networks. *Nature Reviews Neuroscience*, *19*(1), 17–33. https://doi.org/10.1038/nrn.2017.149

Badhwar, A. P., Tam, A., Dansereau, C., Orban, P., Hoffstaedter, F., & Bellec, P. (2017). Resting-state network dysfunction in Alzheimer's disease: A systematic review and meta-analysis. *Alzheimer's and Dementia: Diagnosis, Assessment and Disease Monitoring*, *8*, 73–85. https://doi.org/10.1016/j.dadm.2017.03.007

Barnes, J., Bartlett, J. W., van de Pol, L. A., Loy, C. T., Scahill, R. I., Frost, C., … Fox, N. C. (2009). A meta-analysis of hippocampal atrophy rates in Alzheimer's disease. *Neurobiology*

of Aging, *30*(11), 1711–1723. https://doi.org/10.1016/j.neurobiolaging.2008.01.010

Bassett, D. S., & Sporns, O. (2017). Network neuroscience. *Nature Neuroscience*, *20*(3), 353–364. https://doi.org/10.1038/nn.4502

Bennett, D. A., Schneider, J. A., Arvanitakis, Z., Kelly, J. F., Aggarwal, N. T., Shah, R. C., & Wilson, R. S. (2006). Neuropathology of older persons without cognitive impairment from two community-based studies. *Neurology*, *66*(12), 1837–1844. https://doi.org/10.1212/01.wnl.0000219668.47116.e6

Billinton, R., & Allan, R. N. (1992). *Reliability Evaluation of Engineering Systems*. *Springer*. Boston. https://doi.org/https:/doi.org/10.1007/978-1-4899-0685-4

Binnewijzend, M. A. A., Schoonheim, M. M., Sanz-Arigita, E., Wink, A. M., van der Flier, W. M., Tolboom, N., … Barkhof, F. (2012). Resting-state fMRI changes in Alzheimer's disease and mild cognitive impairment. *Neurobiology of Aging*, *33*(9), 2018–2028. https://doi.org/10.1016/j.neurobiolaging.2011.07.003

Blessing, E. M., Beissner, F., Schumann, A., Brünner, F., & Bär, K. J. (2016). A data-driven approach to mapping cortical and subcortical intrinsic functional connectivity along the longitudinal hippocampal axis. *Human Brain Mapping*, *37*(2), 462–476. https://doi.org/10.1002/hbm.23042

Braak, H., & Braak, E. (1991). Neuropathological stageing of Alzheimer-related changes. *Acta Neurologica*, *82*, 239–259.

Buckner, R. L., Andrews-Hanna, J. R., & Schacter, D. L. (2008). The brain's default network: Anatomy, function, and relevance to disease. *Annals of the New York Academy of Sciences*, *1124*, 1–38. https://doi.org/10.1196/annals.1440.011

Bugg, J. M., & Head, D. (2011). Exercise moderates age-related atrophy of the medial temporal lobe. *Neurobiology of Aging*, *32*(3), 506–514. https://doi.org/10.1016/j.neurobiolaging.2009.03.008

Bullmore, E., & Sporns, O. (2009). Complex brain networks: Graph theoretical analysis of structural and functional systems. *Nature Reviews Neuroscience*, *10*(3), 186–198. https://doi.org/10.1038/nrn2575

Butler, S. M., Ashford, J. W., & Snowdon, D. A. (1996). Age, Education, and Changes in the Mini-Mental State Exam Scores of Older Women: Findings from the Nun Study. *Journal of the American Geriatrics Society*, *44*(6), 675–681. https://doi.org/https://doi.org/10.1111/j.1532-5415.1996.tb01831.x

Cabeza, R., Albert, M., Belleville, S., Craik, F. I. M., Duarte, A., Grady, C. L., … Rajah, M. N. (2018). Maintenance, reserve and compensation: The cognitive neuroscience of healthy ageing. *Nature Reviews Neuroscience*, *19*(11), 701–710. https://doi.org/10.1038/s41583-018-0068-2

Cabral, J. C. C., Veleda, G. W., Mazzoleni, M., Colares, E. P., Neiva-Silva, L., & Neves, V. T. das. (2016). Stress and Cognitive Reserve as independent factors of neuropsychological performance in healthy elderly. *Ciencia e Saude Coletiva*, *21*(11), 3499–3508. https://doi.org/10.1590/1413-812320152111.17452015

Campbell, K. L., & Schacter, D. L. (2017). Ageing and the resting state: is cognition obsolete? *Language, Cognition and Neuroscience*, *32*(6), 661–668. https://doi.org/10.1080/23273798.2016.1227858

Cao, M., Wang, J.-H., Dai, Z.-J., Cao, X.-Y., Jiang, L.-L., Fan, F.-M., … He, Y. (2014). Topological organization of the human brain functional connectome across the lifespan. *Developmental Cognitive Neuroscience*, *7*, 76–93. https://doi.org/https://doi.org/10.1016/j.dcn.2013.11.004

Chang, M., Jonsson, P. V, Snaedal, J., Bjornsson, S., Saczynski, J. S., Aspelund, T., … Launer, L. J. (2010). The Effect of Midlife Physical Activity on Cognitive Function Among Older Adults: AGES—Reykjavik Study. *The Journals of Gerontology: Series A*, *65A*(12), 1369–1374. https://doi.org/10.1093/gerona/glq152

Christensen, H., Korten, A. E., Jorm, A. F., Henderson, A. S., Jacomb, P. A., Rodgers, B., & Mackinnon, A. J. (1997). Education and decline in cognitive performance: Compensatory but not protective. *International Journal of Geriatric Psychiatry*, *12*(3), 323–330. https://doi.org/https://doi.org/10.1002/(SICI)1099-1166(199703)12:3<323::AID-GPS492>3.0.CO;2-N

Clark, C. M., Schneider, J. A., Bedell, B. J., Beach, T. G., Bilker, W. B., Mintun, M. A., … Skovronsky, D. M. (2011). Use of florbetapir-PET for imaging β-amyloid pathology. *JAMA - Journal of the American Medical Association*, *305*(3), 275–283. https://doi.org/10.1001/jama.2010.2008

Clark, R. E., & Squire, L. R. (2013). Similarity in form and function of the hippocampus in rodents, monkeys, and humans. *Proceedings of the National Academy of Sciences of the United States of America*, *110*(SUPPL2), 10365–10370. https://doi.org/10.1073/pnas.1301225110

Cole, M. W., Bassett, D. S., Power, J. D., Braver, T. S., & Petersen, S. E. (2014). Intrinsic and Task-Evoked Network Architectures of the Human Brain. *Neuron*, *83*(1), 238–251. https://doi.org/https://doi.org/10.1016/j.neuron.2014.05.014

Crane, P. K., Carle, A., Gibbons, L. E., Insel, P., Mackin, R. S., Gross, A., … Initiative, for the A. D. N. (2012). Development and assessment of a composite score for memory in the Alzheimer's Disease Neuroimaging Initiative (ADNI). *Brain Imaging and Behavior*, *6*(4), 502–516. https://doi.org/10.1007/s11682-012-9186-z

Creasey, H., & Rapoport, S. I. (1985). The aging human brain. *Annals of Neurology*, *17*(1), 2–10. https://doi.org/10.1002/ana.410170103

Daugherty, A. M., Bender, A. R., Raz, N., & Ofen, N. (2016). Age Differences in Hippocampal

Subfield Volumes from Childhood to Late Adulthood. *Hippocampus*, *26*(2), 220–228. https://doi.org/doi:10.1002/hipo.22517.

Davis, S. W., Stanley, M. L., Moscovitch, M., & Cabeza, R. (2017). Resting-state networks do not determine cognitive function networks: a commentary on Campbell and Schacter (2016). *Language, Cognition and Neuroscience*, *32*(6), 669–673. https://doi.org/doi:10.1080/23273798.2016.1252847

de Godoy, L. L., Alves, C. A. P. F., Saavedra, J. S. M., Studart-Neto, A., Nitrini, R., da Costa Leite, C., & Bisdas, S. (2020). Understanding brain resilience in superagers: a systematic review. *Neuroradiology*. https://doi.org/10.1007/s00234-020-02562-1

De Vico Fallani, F., Toppi, J., Di Lanzo, C., Vecchiato, G., Astolfi, L., Borghini, G., … Babiloni, F. (2012). Redundancy in functional brain connectivity from eeg recordings. *International Journal of Bifurcation and Chaos*, *22*(7). https://doi.org/doi.org/10.1142/S0218127412501581

Delli Pizzi, S., Punzi, M., & Sensi, S. L. (2019). Functional signature of conversion of patients with mild cognitive impairment. *Neurobiology of Aging*, *74*, 21–37. https://doi.org/10.1016/j.neurobiolaging.2018.10.004

Dennis, E. L., & Thompson, P. M. (2014). Functional Brain Connectivity using fMRI in Aging and Alzheimer's Disease. *Neuropsychology Review*, *24*(1), 49–62. https://doi.org/10.1007/s11065-014-9249-6

Di Lanzo, C., Marzetti, L., Zappasodi, F., De Vico Fallani, F., & Pizzella, V. (2012). Redundancy as a graph-based index of frequency specific MEG functional connectivity. *Computational and Mathematical Methods in Medicine*, *2012*, 1–9. https://doi.org/10.1155/2012/207305

Dickerson, B. C., Salat, D. H., Greve, D. N., Chua, E. F., Rand-Giovannetti, E., Rentz, D. M., … Sperling, R. A. (2005). Increased hippocampal activation in mild cognitive impairment compared to normal aging and AD. *Neurology*, *65*(3), 404–411. https://doi.org/10.1212/01.wnl.0000171450.97464.49

Driscoll, I., Resnick, S. M., Troncoso, J. C., An, Y., O'Brien, R., & Zonderman, A. B. (2006). Impact of Alzheimer's pathology on cognitive trajectories in nondemented elderly. *Annals of Neurology*, *60*(6), 688–695. https://doi.org/10.1002/ana.21031

Driscoll, I., & Troncoso, J. (2011). Asymptomatic Alzheimer's disease: A prodrome or a state of resilience? *Current Alzheimer Research*, *8*(4), 330–335. https://doi.org/10.2174/1567211212225942050

Dunn, C. J., Duffy, S. L., Hickie, I. B., Lagopoulos, J., Lewis, S. J. G., Naismith, S. L., & Shine, J. M. (2014). Deficits in episodic memory retrieval reveal impaired default mode network connectivity in amnestic mild cognitive impairment. *NeuroImage: Clinical*, *4*, 473–480. https://doi.org/10.1016/j.nicl.2014.02.010

Eichenbaum, H. (2017). On the Integration of Space, Time, and Memory. *Neuron*, *95*(5), 1007–1018. https://doi.org/10.1016/j.neuron.2017.06.036

El-Sayes, J., Harasym, D., Turco, C. V., Locke, M. B., & Nelson, A. J. (2019). Exercise-Induced Neuroplasticity: A Mechanistic Model and Prospects for Promoting Plasticity. *Neuroscientist*, *25*(1), 65–85. https://doi.org/10.1177/1073858418771538

Erickson, K. I., Voss, M. W., Prakash, R. S., Basak, C., Szabo, A., Chaddock, L., … Kramer, A. F. (2011). Exercise training increases size of hippocampus and improves memory. *Proceedings of the National Academy of Sciences of the United States of America*, *108*(7), 3017–3022. https://doi.org/10.1073/pnas.1015950108

Escandon, A., Al-Hammadi, N., & Galvin, J. E. (2010). Effect of cognitive fluctuation on neuropsychological performance in aging and dementia. *Neurology*, *74*(3), 210–217. https://doi.org/10.1212/WNL.0b013e3181ca017d

Fanselow, M. S., & Dong, H.-W. (2010). Are the dorsal and ventral hippocampus functionally distinct structures? *Neuron*, *65*(1), 7–19. https://doi.org/10.1016/j.neuron.2009.11.031.

Fischl, B. (2012). FreeSurfer. *NeuroImage*, *62*, 774–781.

Fjell, A. M., McEvoy, L., Holland, D., Dale, A. M., & Walhovd, K. B. (2014). What is normal in normal aging? Effects of Aging, Amyloid and Alzheimer's Disease on the Cerebral Cortex and the Hippocampus. *Progress in Neurobiology*, *117*, 20–40. https://doi.org/doi:10.1016/j.pneurobio.2014.02.004

Frankó, E., & Joly, O. (2013). Evaluating Alzheimer's Disease Progression Using Rate of Regional Hippocampal Atrophy. *PLOS ONE*, *8*(8), 1–11. https://doi.org/10.1371/journal.pone.0071354

Frisk, V., & Milner, B. (1990). The role of the left hippocampal region in the acquisition and retention of story content. *Neuropsychologia*, *28*(4), 349–359. https://doi.org/https://doi.org/10.1016/0028-3932(90)90061-R

Frossard, J., & Renaud, O. (2019). permuco: Permutation Tests for Regression, (Repeated Measures) ANOVA/ANCOVA and Comparison of Signals. Retrieved from https://cran.r-project.org/package=permuco

Gallagher, M., & Koh, M. T. (2011). Episodic memory on the path to Alzheimer's disease. *Current Opinion in Neurobiology*, *21*(6), 929–934. https://doi.org/10.1016/j.conb.2011.10.021

Geerligs, L., Renken, R. J., Saliasi, E., Maurits, N. M., & Lorist, M. M. (2015). A Brain-Wide Study of Age-Related Changes in Functional Connectivity. *Cerebral Cortex*, *25*(7), 1987–1999. https://doi.org/10.1093/cercor/bhu012

Gibbons, L. E., Carle, A. C., Mackin, R. S., Harvey, D., Mukherjee, S., Insel, P., … Initiative, for the A. D. N. (2012). A composite score for executive functioning, validated in

Alzheimer's Disease Neuroimaging Initiative (ADNI) participants with baseline mild cognitive impairment. *Brain Imaging and Behavior*, *6*(4), 517–527. https://doi.org/10.1007/s11682-012-9176-1

Giogkaraki, E., Michaelides, M. P., & Constantinidou, F. (2013). The role of cognitive reserve in cognitive aging: Results from the neurocognitive study on aging. *Journal of Clinical & Experimental Neuropsychology*, *35*(10), 1024–1035. Retrieved from http://10.0.4.56/13803395.2013.847906

Glasser, M. F., Sotiropoulos, S. N., Wilson, J. A., Coalson, T. S., Fischl, B., Andersson, J. L., … Jenkinson, M. (2013). The minimal preprocessing pipelines for the Human Connectome Project. *NeuroImage*, *80*, 105–124. https://doi.org/10.1016/j.neuroimage.2013.04.127

Glassman, R. B. (1987). An hypothesis about redundancy and reliability in the brains of higher species: Analogies with genes, internal organs, and engineering systems. *Neuroscience and Biobehavioral Reviews*, *11*(3), 275–285. https://doi.org/10.1016/S0149-7634(87)80014-3

Golomb, J., de Leon, M. J., Kluger, A., George, A. E., Tarshish, C., & Ferris, S. H. (1993). Hippocampal atrophy in aging: An association with recent memory impairment. *JAMA Neurology*, *50*, 967–973.

Grundman, M., Sencakova, D., Jack, C. R., Petersen, R. C., Kim, H. T., Schultz, A., … Thal, L. J. (2002). Brain MRI hippocampal volume and prediction of clinical status in a mild cognitive impairment trial. *Journal of Molecular Neuroscience*, *19*(1–2), 23–27. https://doi.org/10.1007/s12031-002-0006-6

Hafkemeijer, A., van der Grond, J., & Rombouts, S. A. R. B. (2012). Imaging the default mode network in aging and dementia. *Biochimica et Biophysica Acta - Molecular Basis of Disease*, *1822*(3), 431–441. https://doi.org/10.1016/j.bbadis.2011.07.008

Harms, M. P., Somerville, L. H., Ances, B. M., Andersson, J., Barch, D. M., Bastiani, M., … Yacoub, E. (2018). Extending the Human Connectome Project across ages: Imaging protocols for the Lifespan Development and Aging projects. *NeuroImage*, *183*, 972–984. https://doi.org/10.1016/j.neuroimage.2018.09.060

Harris, J. A., Devidze, N., Verret, L., Ho, K., Halabisky, B., Thwin, M. T., … Mucke, L. (2010). Transsynaptic progression of amyloid-b-induced neuronal dysfunction within the entorhinal-hippocampal network. *Neuron*, *68*(3), 428–441. https://doi.org/10.1016/j.neuron.2010.10.020

Huang, K.-L., Hsiao, I.-T., Kuo, H.-C., Hsieh, C.-J., Hsieh, Y.-C., Wu, Y.-M., … Huang, C.-C. (2019). Correlation between visual association memory test and structural changes in patients with Alzheimer's disease and amnestic mild cognitive impairment. *Journal of the Formosan Medical Association*, *118*(9), 1325–1332. https://doi.org/https://doi.org/10.1016/j.jfma.2018.12.001

Jack, C. R., Knopman, D. S., Jagust, W. J., Petersen, R. C., Weiner, M. W., Aisen, P. S., … Trojanowski, J. Q. (2013). Tracking pathophysiological processes in Alzheimer's disease:

An updated hypothetical model of dynamic biomarkers. *The Lancet Neurology*, *12*(2), 207–216. https://doi.org/10.1016/S1474-4422(12)70291-0

Jack, C. R., Petersen, R. C., Xu, Y., O'Brien, P. C., Smith, G. E., Ivnik, R. J., … Kokmen, E. (2000). Rates of hippocampal atrophy correlate with change in clinical status in aging and AD. *Neurology*, *55*(4), 484–489. https://doi.org/10.1212/wnl.55.4.484

Jack Jr, C. R., Bennett, D. A., Blennow, K., Carrillo, M. C., Dunn, B., Budd Haeberlein, S., … Dement Author manuscript, A. (2018). NIA-AA Research Framework: Toward a biological definition of Alzheimer's disease. *Alzheimers Dement*, *14*(4), 535–562. https://doi.org/10.1016/j.jalz.2018.02.018.NIA-AA

Ji, L., Pearlson, G. D., Zhang, X., Steffens, D. C., Ji, X., Guo, H., & Wang, L. (2018). Physical exercise increases involvement of motor networks as a compensatory mechanism during a cognitively challenging task. *International Journal of Geriatric Psychiatry*, *33*(8), 1153–1159. https://doi.org/10.1002/gps.4909

Joshi, A. D., Pontecorvo, M. J., Clark, C. M., Carpenter, A. P., Jennings, D. L., Sadowsky, C. H., … Skovronsky, D. M. (2012). Performance characteristics of amyloid PET with florbetapir F 18 in patients with Alzheimer's disease and cognitively normal subjects. *Journal of Nuclear Medicine*, *53*(3), 378–384. https://doi.org/10.2967/jnumed.111.090340

Karatsoreos, I. N., & McEwen, B. S. (2013). Resilience and vulnerability: a neurobiological perspective. *F1000prime Reports*, *5*, 13. https://doi.org/10.12703/P5-13

Kassambara, A., Kosinski, M., Biecek, P., & Fabian, S. (2020). survminer: Drawing survival curves using "ggplot2."

Katzman, R., Terry, R., DeTeresa, R., Brown, T., Davies, P., Fuld, P., … Peck, A. (1988). Clinical, pathological, and neurochemical changes in dementia: A subgroup with preserved mental status and numerous neocortical plaques. *Annals of Neurology*, *23*(2), 138–144. https://doi.org/10.1002/ana.410230206

Kim, H. (2015). Encoding and retrieval along the long axis of the hippocampus and their relationships with dorsal attention and default mode networks: The HERNET model. *Hippocampus*, *25*(4), 500–510. https://doi.org/10.1002/hipo.22387

Koch, W., Teipel, S., Mueller, S., Benninghoff, J., Wagner, M., Bokde, A. L. W., … Meindl, T. (2012). Diagnostic power of default mode network resting state fMRI in the detection of Alzheimer's disease. *Neurobiology of Aging*, *33*(3), 466–478. https://doi.org/10.1016/j.neurobiolaging.2010.04.013

Koen, J. D., & Yonelinas, A. P. (2014). The effects of healthy aging, amnestic mild cognitive impairment, and Alzheimer's disease on recollection and familiarity: A meta-analytic review. *Neuropsychology Review*, *24*(3), 332–354. https://doi.org/10.1007/s11065-014-9266-5

Kraus, B. T., Perez, D., Ladwig, Z., Seitzman, B. A., Dworetsky, A., Petersen, S. E., & Gratton,

C. (2021). Network variants are similar between task and rest states. *NeuroImage*, *229*, 117743. https://doi.org/https://doi.org/10.1016/j.neuroimage.2021.117743

Krienen, F. M., Thomas Yeo, B. T., & Buckner, R. L. (2014). Reconfigurable task-dependent functional coupling modes cluster around a core functional architecture. *Philosophical Transactions of the Royal Society B: Biological Sciences*, *369*(1653). https://doi.org/10.1098/rstb.2013.0526

Langella, S., Sadiq, M. U., Mucha, P. J., Giovanello, K. S., & Dayan, E. (2021). Lower functional hippocampal redundancy in mild cognitive impairment. *Translational Psychiatry*, *11*(61). https://doi.org/10.1038/s41398-020-01166-w

Latora, V., & Marchiori, M. (2001). Efficient behavior of small-world networks. *Physical Review Letters*, *87*(19), 198701. https://doi.org/10.1103/PhysRevLett.87.198701

Leal, S. L., & Yassa, M. A. (2015). Neurocognitive Aging and the Hippocampus across Species. *Trends in Neurosciences*, *38*(12), 800–812. https://doi.org/10.1016/j.tins.2015.10.003

Leistritz, L., Weiss, T., Bär, K.-J., De VicoFallani, F., Babiloni, F., Witte, H., & Lehmann, T. (2013). Network Redundancy Analysis of Effective Brain Networks; a Comparison of Healthy Controls and Patients with Major Depression. *PLOS ONE*, *8*(4), e60956. Retrieved from https://doi.org/10.1371/journal.pone.0060956

Liang, K. Y., Mintun, M. A., Fagan, A. M., Goate, A. M., Bugg, J. M., Holtzman, D. M., … Head, D. (2010). Exercise and Alzheimer's disease biomarkers in cognitively normal older adults. *Annals of Neurology*, *68*(3), 311–318. https://doi.org/https://doi.org/10.1002/ana.22096

Long, J. A. (2019). interactions: Comprehensive, User-Friendly Toolkit for Probing Interactions. Retrieved from https://cran.r-project.org/package=interactions

Lövdén, M., Fratiglioni, L., Glymour, M. M., Lindenberger, U., & Tucker-Drob, E. M. (2020). Education and Cognitive Functioning Across the Life Span. *Psychological Science in the Public Interest : A Journal of the American Psychological Society*, *21*(1), 6–41. https://doi.org/10.1177/1529100620920576

Ma, C.-L., Ma, X.-T., Wang, J.-J., Liu, H., Chen, Y.-F., & Yang, Y. (2017). Physical exercise induces hippocampal neurogenesis and prevents cognitive decline. *Behavioural Brain Research*, *317*, 332–339. https://doi.org/https://doi.org/10.1016/j.bbr.2016.09.067

Maechler, M. (2020). Utilities from "Seminar fuer Statistik" ETH Zurich. Retrieved from http://cran.r-project.org/web/packages/sfsmic

Malagurski, B., Liem, F., Oschwald, J., Mérillat, S., & Jäncke, L. (2020a). Functional dedifferentiation of associative resting state networks in older adults – A longitudinal study. *NeuroImage*, *214*, 116680. https://doi.org/https://doi.org/10.1016/j.neuroimage.2020.116680

Malagurski, B., Liem, F., Oschwald, J., Mérillat, S., & Jäncke, L. (2020b). Longitudinal functional brain network reconfiguration in healthy aging. *Human Brain Mapping*, *41*(17), 4829–4845. https://doi.org/10.1002/hbm.25161

Malek-Ahmadi, M., Powell, J. J., Belden, C. M., Oconnor, K., Evans, L., Coon, D. W., & Nieri, W. (2015). Age-and education-adjusted normative data for the Montreal Cognitive Assessment (MoCA) in older adults age 70-99. *Aging, Neuropsychology, and Cognition*, *22*(6), 755–761. https://doi.org/10.1080/13825585.2015.1041449

Menardi, A., Reineberg, A. E., Vallesi, A., Friedman, N. P., Banich, M. T., & Santarnecchi, E. (2021). Heritability of brain resilience to perturbation in humans. *NeuroImage*, *235*(December 2020), 118013. https://doi.org/10.1016/j.neuroimage.2021.118013

Meng, X., & D'Arcy, C. (2012). Education and dementia in the context of the cognitive reserve hypothesis: a systematic review with meta-analyses and qualitative analyses. *PloS One*, *7*(6), e38268. https://doi.org/10.1371/journal.pone.0038268

Miller, S. L., Fenstermacher, E., Bates, J., Blacker, D., Sperling, R. A., & Dickerson, B. C. (2008). Hippocampal activation in adults with mild cognitive impairment predicts subsequent cognitive decline. *Journal of Neurology, Neurosurgery and Psychiatry*, *79*(6), 630–635. https://doi.org/10.1136/jnnp.2007.124149

Mohan, A., Roberto, A. J., Mohan, A., Lorenzo, A., Jones, K., Carney, M. J., … Lapidus, K. A. B. (2016). The significance of the Default Mode Network (DMN) in neurological and neuropsychiatric disorders: A review. *Yale Journal of Biology and Medicine*, *89*(1), 49–57.

Montine, T. J., Cholerton, B. A., Corrada, M. M., Edland, S. D., Flanagan, M. E., Hemmy, L. S., … White, L. R. (2019). Concepts for brain aging: Resistance, resilience, reserve, and compensation. *Alzheimer's Research and Therapy*, *11*. https://doi.org/https://doi.org/10.1186/s13195-019-0479-y

Morra, J. H., Tu, Z., Apostolova, L. G., Green, A. E., Avedissian, C., Madsen, S. K., … Initiative, A. D. N. (2009). Automated mapping of hippocampal atrophy in 1-year repeat MRI data from 490 subjects with Alzheimer's disease, mild cognitive impairment, and elderly controls. *NeuroImage*, *45*(1 Suppl), S3–S15. https://doi.org/10.1016/j.neuroimage.2008.10.043

Mueller, S. G., Schuff, N., Yaffe, K., Madison, C., Miller, B., & Weiner, M. W. (2010). Hippocampal atrophy patterns in mild cognitive impairment and alzheimer's disease. *Human Brain Mapping*, *31*(9), 1339–1347. https://doi.org/10.1002/hbm.20934

Nathan, P. J., Lim, Y. Y., Abbott, R., Galluzzi, S., Marizzoni, M., Babiloni, C., … Frisoni, G. B. (2017). Association between CSF biomarkers, hippocampal volume and cognitive function in patients with amnestic mild cognitive impairment (MCI). *Neurobiology of Aging*, *53*, 1–10. https://doi.org/10.1016/j.neurobiolaging.2017.01.013

Navlakha, S., He, X., Faloutsos, C., & Bar-Joseph, Z. (2014). Topological properties of robust biological and computational networks. *Journal of the Royal Society, Interface / the Royal*

Society, *11*, 20140283. https://doi.org/10.1098/rsif.2014.0283

Nelson, P. T., Alafuzoff, I., Bigio, E. H., Bouras, C., Braak, H., Cairns, N. J., … Beach, T. G. (2012). Correlation of Alzheimer disease neuropathologic changes with cognitive status: A review of the literature. *Journal of Neuropathology & Experimental Neurology*, *71*(5), 362–381.

Nguyen, A. T., Xu, J., Luu, D. K., Zhao, Q., & Yang, Z. (2019). Advancing System Performance with Redundancy: From Biological to Artificial Designs. *Neural Computation*, *31*, 555–573. https://doi.org/10.1162/neco_a_01166

Nichols, E., Szoeke, C. E. I., Vollset, S. E., Abbasi, N., Abd-Allah, F., Abdela, J., … Murray, C. J. L. (2019). Global, regional, and national burden of Alzheimer's disease and other dementias, 1990–2016: A systematic analysis for the Global Burden of Disease Study 2016. *The Lancet Neurology*, *18*(1), 88–106. https://doi.org/10.1016/S1474-4422(18)30403-4

Norton, S., Matthews, F. E., Barnes, D. E., Yaffe, K., & Brayne, C. (2014). Potential for primary prevention of Alzheimer's disease: an analysis of population-based data. *The Lancet Neurology*, *13*(8), 788–794. https://doi.org/10.1016/S1474-4422(14)70136-X

Nyberg, L., Magnussen, F., Lundquist, A., Baaré, W., Bartrés-Faz, D., Bertram, L., … Fjell, A. M. (2021). Educational attainment does not influence brain aging. *Proceedings of the National Academy of Sciences*, *118*(18), e2101644118. https://doi.org/10.1073/pnas.2101644118

O'Brien, J. L., O'Keefe, K. M., LaViolette, P. S., DeLuca, A. N., Blacker, D., Dickerson, B. C., & Sperling, R. A. (2010). Longitudinal fMRI in elderly reveals loss of hippocampal activation with clinical decline. *Neurology*, *74*(24), 1969–1976. https://doi.org/10.1212/WNL.0b013e3181e3966e

O'Shea, A., Cohen, R., Porges, E., Nissim, N., & Woods, A. (2016). Cognitive Aging and the Hippocampus in Older Adults. *Frontiers in Aging Neuroscience*, *8*, 298. https://doi.org/10.3389/fnagi.2016.00298

Olson, A. K., Eadie, B. D., Ernst, C., & Christie, B. R. (2006). Environmental enrichment and voluntary exercise massively increase neurogenesis in the adult hippocampus via dissociable pathways. *Hippocampus*, *16*(3), 250–260. https://doi.org/10.1002/hipo.20157

Ousdal, O. T., Kaufmann, T., Kolskår, K., Vik, A., Wehling, E., Lundervold, A. J., … Westlye, L. T. (2020). Longitudinal stability of the brain functional connectome is associated with episodic memory performance in aging. *Human Brain Mapping*, *41*(3), 697–709. https://doi.org/10.1002/hbm.24833

Padurariu, M., Ciobica, A., Mavroudis, I., Fotiou, D., & Stavros, B. (2012). Hippocampal neuronal loss in the CA1 and CA3 areas of AD patients. *Psychiatria Danubina*, *24*(2), 7.

Paillard, T. (2015). Preventive effects of regular physical exercise against cognitive decline and the risk of dementia with age advancement. *Sports Medicine - Open*, *1*(1), 20.

https://doi.org/10.1186/s40798-015-0016-x

Peng, G.-P., Feng, Z., He, F.-P., Chen, Z.-Q., Liu, X.-Y., Liu, P., & Luo, B.-Y. (2015). Correlation of Hippocampal Volume and Cognitive Performances in Patients with Either Mild Cognitive Impairment or Alzheimer's disease. *CNS Neuroscience & Therapeutics*, *21*(1), 15–22. https://doi.org/https://doi.org/10.1111/cns.12317

Petersen, R. C., Lopez, O., Armstrong, M. J., Getchius, T. S. D., Ganguli, M., Gloss, D., … Rae-Grant, A. (2018). Practice guideline update summary: Mild cognitive impairment report of theguideline development, dissemination, and implementation. *Neurology*, *90*(3), 126–135. https://doi.org/10.1212/WNL.0000000000004826

Piras, F., Cherubini, A., Caltagirone, C., & Spalletta, G. (2011). Education mediates microstructural changes in bilateral hippocampus. *Human Brain Mapping*, *32*(2), 282–289. https://doi.org/10.1002/hbm.21018

Pitkow, X., & Angelaki, D. E. (2017). Inference in the brain: Statistics flowing in redundant population codes. *Neuron*, *94*(5), 943–953. https://doi.org/10.1016/j.neuron.2017.05.028

Poppenk, J., Evensmoen, H. R., Moscovitch, M., & Nadel, L. (2013). Long-axis specialization of the human hippocampus. *Trends in Cognitive Sciences*, *17*(5), 230–240. https://doi.org/10.1016/j.tics.2013.03.005

Powell, H. W. R., Koepp, M. J., Symms, M. R., Boulby, P. A., Salek-Haddadi, A., Thompson, P. J., … Richardson, M. P. (2005). Material-specific lateralization of memory encoding in the medial temporal lobe: Blocked versus event-related design. *NeuroImage*, *27*(1), 231–239. https://doi.org/https://doi.org/10.1016/j.neuroimage.2005.04.033

Price, J. L., Mckeel, D. W., Buckles, V. D., Roe, C. M., Xiong, C., Grundman, M., … Morris, J. C. (2009). Neuropathology of nondemented aging : Presumptive evidence for preclinical Alzheimer disease, *30*, 1026–1036. https://doi.org/10.1016/j.neurobiolaging.2009.04.002

Price, J. L., & Morris, J. C. (1999). Tangles and plaques in nondemented aging and ?preclinical? Alzheimer's disease. *Annals of Neurology*, *45*(3), 358–368. https://doi.org/10.1002/1531-8249(199903)45:3<358::AID-ANA12>3.0.CO;2-X

Rakesh, D., Fernando, K. B., & Mansour L., S. (2020). Functional dedifferentiation of the brain during healthy aging. *Journal of Neurophysiology*, *123*(4), 1279–1282. https://doi.org/10.1152/jn.00039.2020

Ranganath, C., & Ritchey, M. (2012). Two cortical systems for memory- guided behaviour. *Nature Reviews Neuroscience*, *13*(10), 713–726. https://doi.org/10.1038/nrn3338

Rashid, M. H., Zahid, M. F., Zain, S., Kabir, A., & Hassan, S. U. (2020). The Neuroprotective Effects of Exercise on Cognitive Decline: A Preventive Approach to Alzheimer Disease. *Cureus*, *12*(2), e6958–e6958. https://doi.org/10.7759/cureus.6958

Raz, N., Lindenberger, U., Rodrigue, K. M., Kennedy, K. M., Head, D., Williamson, A., …

Acker, J. D. (2005). Regional Brain Changes in Aging Healthy Adults: General Trends, Individual Differences and Modifiers. *Cerebral Cortex*, *15*(11), 1676–1689. https://doi.org/10.1093/cercor/bhi044

Reas, E. T., Laughlin, G. A., Bergstrom, J., Kritz-Silverstein, D., Richard, E. L., Barrett-Connor, E., & McEvoy, L. K. (2019). Lifetime physical activity and late-life cognitive function: the Rancho Bernardo study. *Age and Ageing*, *48*(2), 241–246. https://doi.org/10.1093/ageing/afy188

Reed, B. R., Mungas, D., Farias, S. T., Harvey, D., Beckett, L., Widaman, K., … DeCarli, C. (2010). Measuring cognitive reserve based on the decomposition of episodic memory variance. *Brain*, *133*(8), 2196–2209. https://doi.org/10.1093/brain/awq154

Ripley, B. (2020). Robust Fitting of Linear Models. Retrieved from https://cran.r-project.org/package=rlm

Ritchey, M., Libby, L. A., & Ranganath, C. (2015). *Cortico-hippocampal systems involved in memory and cognition: The PMAT framework*. *Progress in Brain Research* (1st ed., Vol. 219). Elsevier B.V. https://doi.org/10.1016/bs.pbr.2015.04.001

Rovio, S., Kåreholt, I., Helkala, E.-L., Viitanen, M., Winblad, B., Tuomilehto, J., … Kivipelto, M. (2005). Leisure-time physical activity at midlife and the risk of dementia and Alzheimer's disease. *The Lancet Neurology*, *4*(11), 705–711. https://doi.org/https://doi.org/10.1016/S1474-4422(05)70198-8

Rubinov, M., & Sporns, O. (2010). Complex network measures of brain connectivity: Uses and interpretations. *NeuroImage*, *52*(3), 1059–1069. https://doi.org/10.1016/j.neuroimage.2009.10.003

Sadiq, M. U., Langella, S., Giovanello, K. S., Mucha, P. J., & Dayan, E. (2021). Accrual of functional redundancy along the lifespan and its effects on cognition. *NeuroImage*, *229*, 117737. https://doi.org/10.1016/j.neuroimage.2021.117737

Salthouse, T. A. (2010). Influence of age on practice effects in longitudinal neurocognitive change. *Neuropsychology*, *24*(5), 563–572. https://doi.org/10.1037/a0019026

Schönheit, B., Zarski, R., & Ohm, T. G. (2004). Spatial and temporal relationships between plaques and tangles in Alzheimer-pathology. *Neurobiology of Aging*, *25*(6), 697–711. https://doi.org/10.1016/j.neurobiolaging.2003.09.009

Seitzman, B. A., Gratton, C., Marek, S., Raut, R. V., Dosenbach, N. U. F., Schlaggar, B. L., … Greene, D. J. (2020). A set of functionally-defined brain regions with improved representation of the subcortex and cerebellum. *NeuroImage*, *206*. https://doi.org/https://doi.org/10.1016/j.neuroimage.2019.116290

Sheline, Y. I., & Raichle, M. E. (2013). Resting State Functional Connectivity in Preclinical Alzheimer's Disease: A Review. *Biological Psychiatry*, *74*(5), 340–347. https://doi.org/10.1016/j.biopsych.2012.11.028.Resting

Sheng, C., Xia, M., Yu, H., Huang, Y., Lu, Y., Liu, F., … Han, Y. (2017). Abnormal global functional network connectivity and its relationship to medial temporal atrophy in patients with amnestic mild cognitive impairment. *PLoS ONE*, *12*(6), 1–16. https://doi.org/10.1371/journal.pone.0179823

Shohamy, D., & Turk-Browne, N. B. (2013). Mechanisms for widespread hippocampal involvement in cognition. *Journal of Experimental Psychology: General*, *142*(4), 1159–1170. https://doi.org/10.1037/a0034461

Sluimer, J. D., van der Flier, W. M., Karas, G. B., van Schijndel, R., Barnes, J., Boyes, R. G., … Barkhof, F. (2009). Accelerating regional atrophy rates in the progression from normal aging to Alzheimer's disease. *European Radiology*, *19*(12), 2826. https://doi.org/10.1007/s00330-009-1512-5

Sohn, W. S., Yoo, K., Na, D. L., & Jeong, Y. (2014). Progressive Changes in Hippocampal Resting-state Connectivity Across Cognitive Impairment: A Cross-sectional Study From Normal to Alzheimer Disease. *Alzheimer Disease & Associated Disorders*, *28*(3). Retrieved from https://journals.lww.com/alzheimerjournal/Fulltext/2014/07000/Progressive_Changes_in_Hippocampal_Resting_state.6.aspx

Stern, Y. (2006). Cognitive Reserve and Alzheimer Disease. *Alzheimer Disease & Associated Disorders*, *20*. Retrieved from https://journals.lww.com/alzheimerjournal/Fulltext/2006/07001/Cognitive_Reserve_and_Alzheimer_Disease.10.aspx

Stern, Y., Albert, S., Tang, M. X., & Tsai, W. Y. (1999). Rate of memory decline in AD is related to education and occupation: Cognitive reserve? *Neurology*, *53*(9), 1942–1947. https://doi.org/10.1212/wnl.53.9.1942

Stern, Y., Barnes, C. A., Grady, C., Jones, R. N., & Raz, N. (2019). Brain reserve, cognitive reserve, compensation, and maintenance: Operationalization, validity, and mechanisms of cognitive resilience. *Neurobiology of Aging*, *83*, 124–129. https://doi.org/10.1016/j.neurobiolaging.2019.03.022

Strange, B. A., Witter, M. P., Lein, E. S., & Moser, E. I. (2014). Functional organization of the hippocampal longitudinal axis. *Nature Reviews Neuroscience*, *15*(10), 655–669. https://doi.org/10.1038/nrn3785

Su, F., Shu, H., Ye, Q., Xie, C., Yuan, B., Zhang, Z., & Bai, F. (2017). Integration of Multilocus Genetic Risk into the Default Mode Network Longitudinal Trajectory during the Alzheimer's Disease Process. *Journal of Alzheimer's Disease*, *56*(2), 491–507. https://doi.org/10.3233/JAD-160787

Therneau, T. (2020). A package for survival analysis in R.

Tingley, D., Yamamoto, T., Hirose, K., Keele, L., & Imai, K. (2014). mediation: R package for causal mediation analysis. *Journal of Statistical Software*, *59*(5), 1–38.

Tolppanen, A.-M., Solomon, A., Kulmala, J., Kåreholt, I., Ngandu, T., Rusanen, M., … Kivipelto, M. (2015). Leisure-time physical activity from mid- to late life, body mass index, and risk of dementia. *Alzheimer's & Dementia*, *11*(4), 434-443.e6. https://doi.org/https://doi.org/10.1016/j.jalz.2014.01.008

Tononi, G., Sporns, O., & Edelman, G. M. (1999). Measures of degeneracy and redundancy in biological networks. *Proceedings of the National Academy of Sciences of the United States of America*, *96*(6), 3257–3262. https://doi.org/10.1073/pnas.96.6.3257

Torchiano, M. (2020). Efficient Effect Size Computation. Retrieved from https://cran.r-project.org/web/packages/effsize/

Tost, H., Champagne, F. A., & Meyer-Lindenberg, A. (2015). Environmental influence in the brain, human welfare and mental health. *Nature Neuroscience*, *18*(10), 1421–1431. https://doi.org/10.1038/nn.4108

van den Heuvel, M. P., de Lange, S. C., Zalesky, A., Seguin, C., Yeo, B. T. T., & Schmidt, R. (2017). Proportional thresholding in resting-state fMRI functional connectivity networks and consequences for patient-control connectome studies: Issues and recommendations. *NeuroImage*, *152*(February), 437–449. https://doi.org/10.1016/j.neuroimage.2017.02.005

Voss, M., Prakash, R., Erickson, K., Basak, C., Chaddock, L., Kim, J., … Kramer, A. (2010). Plasticity of Brain Networks in a Randomized Intervention Trial of Exercise Training in Older Adults . *Frontiers in Aging Neuroscience* . Retrieved from https://www.frontiersin.org/article/10.3389/fnagi.2010.00032

Wang, Y., Risacher, S. L., West, J. D., McDonald, B. C., MaGee, T. R., Farlow, M. R., … Saykin, A. J. (2013). Altered Default Mode Network Connectivity in Older Adults with Cognitive Complaints and Amnestic Mild Cognitive Impairment. *Journal of Alzheimer's Disease*, *35*(4), 751–760. https://doi.org/doi:10.3233/JAD-130080

Wang, Z., Liang, P., Jia, X., Qi, Z., Yu, L., Yang, Y., … Li, K. (2011). Baseline and longitudinal patterns of hippocampal connectivity in mild cognitive impairment: Evidence from resting state fMRI. *Journal of the Neurological Sciences*, *309*(1–2), 79–85. https://doi.org/10.1016/j.jns.2011.07.017

Wenger, E., & Lövdén, M. (2016). The Learning Hippocampus: Education and Experience-Dependent Plasticity. *Mind, Brain, and Education*, *10*(3), 171–183. https://doi.org/10.1111/mbe.12112

Whitfield-Gabrieli, S., & Nieto-Castanon, A. (2012). Conn: A functional connectivity toolbox for correlated and anticorrelated brain networks. *Brain Connectivity*, *2*(3), 125–141. https://doi.org/10.1089/brain.2012.0073

Wilson, R. S., Wang, T., Yu, L., Bennett, D. A., & Boyle, P. A. (2020). Normative Cognitive Decline in Old Age. *Annals of Neurology*, *87*(6), 816–829. https://doi.org/10.1002/ana.25711

Yan, H., Zhang, Y., Chen, H., Wang, Y., & Liu, Y. (2013). Altered effective connectivity of the default mode network in resting-state amnestic type mild cognitive impairment. *Journal of the International Neuropsychological Society*, *19*(4), 400–409. https://doi.org/10.1017/S1355617712001580

Yankner, B. A., Lu, T., & Loerch, P. (2008). The Aging Brain. *Annual Review of Pathology: Mechanisms of Disease*, *3*, 41–66. https://doi.org/10.1146/annurev.pathmechdis.2.010506.092044

Yu, Q., & Li, B. (2020). mma: Multiple Mediation Analysis.